Volume 43 Number 1/2 December 1986

PHILIPS TECHNICAL REVIEW

Accordion imager

PHILAN

Nickel-hydride cell

Dielectric resonators

PHILIPS

Philips Technical Review (ISSN 0031-7926) is published by Philips Research Laboratories, Eindhoven, the Netherlands, and deals with the investigations, processes and products of the laboratories and other establishments that form part of or are associated with the Philips group of companies. In the articles the associated technical problems are treated along with their physical or chemical background. The Review covers a wide range of subjects, each article being intended not only for the specialist in the subject but also for the non-specialist reader with a general technical or scientific training.

The Review appears in English and Dutch editions; both are identical in contents. There are twelve numbers per volume, each of about 32 pages. An index is included with each volume and indexes covering ten volumes are published (the latest one was included in Volume 40, 1982).

PHILIPS TECHNICAL REVIEW

Volume 43, No. 1/2, Dec. 1986

Contents

PHILIPS

PHILIPS TECHNICAL REVIEW

Volume 43, No. 1/2, Dec. 1986

The accordion imager, a new solid-state image sensor

A. J. P. Theuwissen and C. H. L. Weijtens

No image sensor can compete with the human eye. Even if a charge distribution could be produced in a solid-state image sensor with the same accuracy as an image is formed on the retina, the information could not be transferred in the same way. Each photosensitive element in the eye has its own channel for transferring the image information to the brain. A simulation of this system would require far too many connections. The information originating from all the individual image elements in solid-state image sensors is ultimately transferred through a single channel. The idea for the transfer of the image information in the 'accordion imager' described below was first put forward in the early eighties at Philips Research Laboratories.

Introduction

A solid-state image sensor seems to be an attractive alternative to the conventional television camera tube. In a camera tube an electron beam scans the charge distribution produced on a photoconductor by incident light. In most solid-state sensors the charge distribution is not scanned; the charge is transferred directly.

Major applications of such image sensors are to be found in monitoring and surveillance equipment, electronic cameras and even in toys. Because of the interesting applications in the consumer market it is important to keep the price of the imager low. Since the price is directly related to the size of the sensor, the sensor should be as small as possible without loss of resolution.

A solid-state image sensor has a number of advantages compared with a camera tube: it can be made in IC technology, its weight is low, it requires little power and it is small and robust. Image-lag or 'comet' effects can be avoided and the image area is not damaged if the light beam is too bright. The image quality, however, is not that of a camera tube. For a comparable image quality, a solid-state sensor should have a certain minimum number of picture elements (pixels). But this must not require any change in the critical dimensions (and hence a new technology) or make the chip too expensive. In the current state of the technology the chip will only compare with other image sensors if its area is less than 40 mm^2.

A solid-state image sensor is simply a silicon chip. It consists of two parts, an image section and a storage section. In the image section incident light generates electrons, which are collected in potential wells at defined positions on the surface (the pixels). This results in a distribution of charge packets that corresponds to an image. The size of a charge packet corresponds to the quantity of light that arrives at a pixel. After charge has been accumulated during a specific period (the 'integration period') this charge distribution is transferred in its entirety [1] to the storage section, which is shielded from light. The transfer has to be very fast to ensure that the charge packets in transit are not significantly affected by incident light. Nor, of

Dr Ir A. J. P. Theuwissen and Drs C. H. L. Weijtens are with Philips Research Laboratories, Eindhoven.

[1] The charge distribution corresponding to an image is transferred in its entirety to the storage section situated below the image section. Sensors of this type are therefore called frame-transfer (FT) devices.

course, must there be any interaction between the charge packets. The potential wells in the silicon are produced by applying voltages to a number of electrodes positioned on the surface, perpendicular to linear channels of n-type silicon.

From the storage section the charge packets are transferred row by row (line by line) to the output register. Further processing for television pictures can then take place in the usual way.

The resolution of the sensor is determined by the number of pixels per unit area. The dimensions of a pixel are fixed by the width of one n-channel and by the number and dimensions of the electrodes that are necessary to produce the potential wells. In a four-phase image sensor a pixel comprises four electrodes (see *fig. 1*).

Fig. 2 shows a cross-section through part of a four-phase image sensor, which is essentially a shift register of the CCD type (charge-coupled device) [2]. A substrate of p-type silicon contains narrow channels of n-type material. Above this there is an insulating layer of silicon oxide, and on top of that layer there are the electrodes, consisting of polycrystalline silicon. Light passing through the electrodes and the insulating layer generates electrons in the silicon. In addition to electrons positive charge carriers are also generated, and these are conducted to earth. The potential wells in which the electrons are collected are created by applying a positive voltage to electrodes *2*, *3* and *4* and a negative voltage to electrodes *1*. The first signal (marked t_0) represents this situation, which remains unchanged for the full integration period of 20 ms. Then the charge distribution is transferred to the storage section. In the image sensor shown in fig. 2 this transfer is effected by generating a peristaltic 'potential movement' controlled by a clock signal. This propels the charge packets towards the storage section.

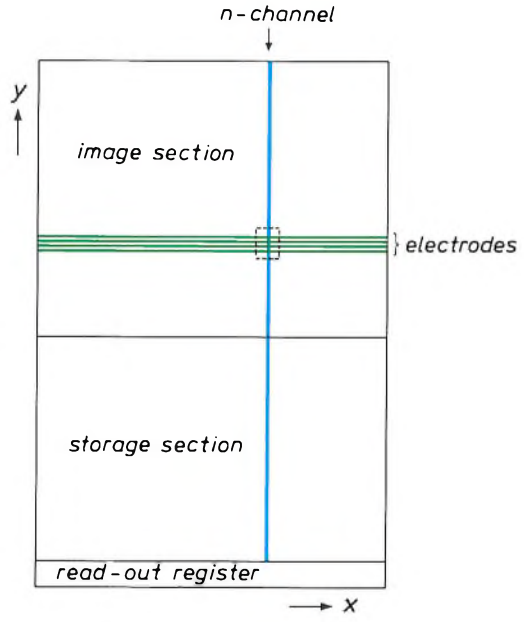

Fig. 1. Diagram representing a solid-state image sensor. From top to bottom, the sensor consists of three sections: an image section, a storage section and a read-out register. In the image and storage sections the n-channels are vertical (y-direction). For clarity only one n-channel is indicated. The electrodes run horizontally across the channels (x-direction). The figure shows only four electrodes for the image section. The dotted rectangle indicates a picture element (a pixel) in a four-phase image sensor. Each pixel contains a charge packet at the end of an integration period. After an integration period has been completed, all the charge packets are transferred to the storage section simultaneously. The storage section contains as many pixels as the image section. From the storage section the charge packets are moved towards the read-out register a row at a time. Each row of charge packets contains information that corresponds to a line in a television picture.

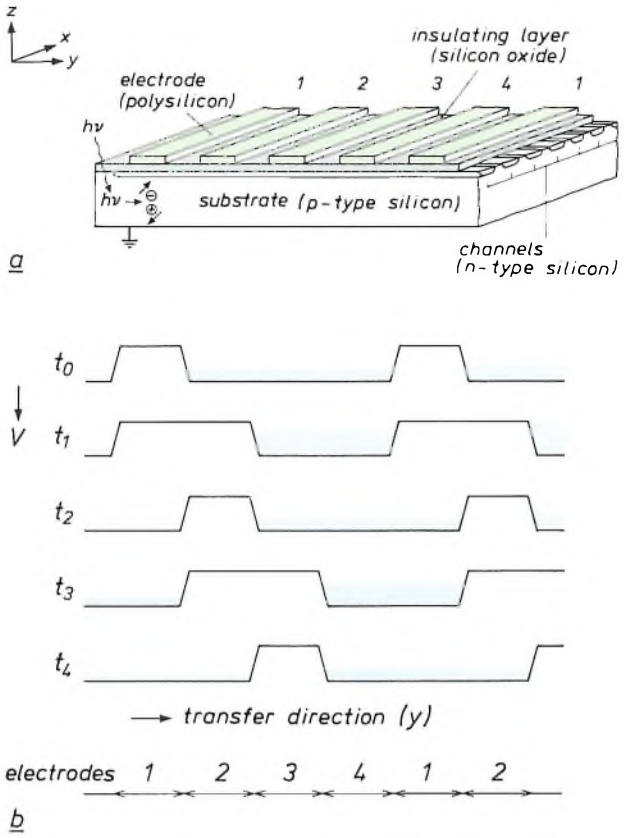

Fig. 2. *a*) Diagram of part of a four-phase solid-state image sensor. A p-type silicon substrate contains narrow channels of n-type silicon (in the y-direction). The surface of the substrate is covered with a layer of silicon oxide, and on top of that layer are the polysilicon electrodes (in the x-direction). The silicon oxide is necessary to prevent conduction between the substrate and the electrodes and between the electrodes themselves. Light passing through the transparent electrodes and the silicon oxide releases electrons and holes in the silicon ($h\nu \rightarrow +$ and $-$). The holes are conducted to earth and the electrons are collected in potential wells in the n-channels which are produced by applying voltages to the electrodes. *b*) Potential (V) in the silicon at consecutive times. The first signal represents the situation during an integration period. The electrons are collected in the potential well beneath the electrodes *2*, *3* and *4*. From the moment t_1 the changes in the voltages on the electrodes cause a peristaltic transfer of the charge packets. The blue colouring indicates the contents of a potential well. All the charge packets are transferred simultaneously.

The peristaltic 'potential movement' can in principle be produced with only three electrodes. We use four electrodes to obtain the usual interlacing for television pictures. During successive integration periods the voltage patterns on the electrodes are shifted symmetrically with respect to each other by an integer number of electrodes. In the field duration following the transfer in fig. 2, electrode *3* acts as a barrier electrode and the voltage on electrodes *1*, *2* and *4* produces the potential wells.

For the *collection* of the charge packets during the integration period two electrodes per pixel are sufficient. The peristaltic charge *transfer* can only take place if a pixel consists of more than two electrodes. In fig. 2 there are four. Because of these extra electrodes a row of pixels occupies a relatively large area on the chip. This has detrimental consequences for the resolution in the vertical direction (y), which is determined by the number of pixels per unit length. For this reason we wanted to make a sensor with smaller pixels. The obvious way of doing this is to make the electrodes narrower. However, this would require an entirely new technology for producing the sensors. Another way of making the pixels smaller is to reduce the number of electrodes in each row. This does not greatly affect the production process, but it does of course change the transfer mechanism. The way in which this problem has been solved in our new 'accordion imager' is treated in this article, which describes the operation of the sensor, its design and its characteristics.

The 'accordion' operation

The new 'accordion imager' [3] is a solid-state image sensor with only two electrodes per pixel, which serve alternately as integration and barrier electrodes in successive integration periods. The storage section also consists of elements with only two electrodes. Charge transfer takes place as follows. After an integration period the potential wells and barriers are doubled in width one at a time. This process starts at the interface between the image and storage sections of the sensor. The charge distribution is stretched like an accordion. When the lower edge of the storage section is reached the potential wells and barriers are reduced to a width of one electrode, one at a time. The charge distribution is now 'squeezed together' like an accordion. The result of this stretching and squeezing is that the entire charge distribution is moved from the image section to the storage section. The transfer from the storage section to the output register can be made in the same way.

It is clear that in this method of transfer the voltages on the electrodes will change in a more complex way than in the four-phase sensor. The benefits, however, are considerable: with the same technology as used for producing a four-phase sensor an equally large sensor can be made that has twice as many pixels, or a smaller sensor with the same number of pixels. The accordion imager has the same number of pixels as the four-phase sensor but occupies a smaller chip area.

The detailed action for the charge transfer in the accordion imager is illustrated in fig. 3 and fig. 4. At time t_0 (*fig. 3*) the sensor is in one of the two states in which charge is accumulated during a period of 20 ms, the integration period. At time t_1 the first charge packet (*a*) is stretched. At time t_2 it is pushed further towards the output. The other charge packets (*b*, *c*, ...) stay in position. At time t_3 the second charge packet (*b*) starts to move, and so on. This change from a static two-phase system to a dynamic four-phase system continues until every charge packet has been spread over two electrodes. The separation between each two charge packets has a width of two elec-

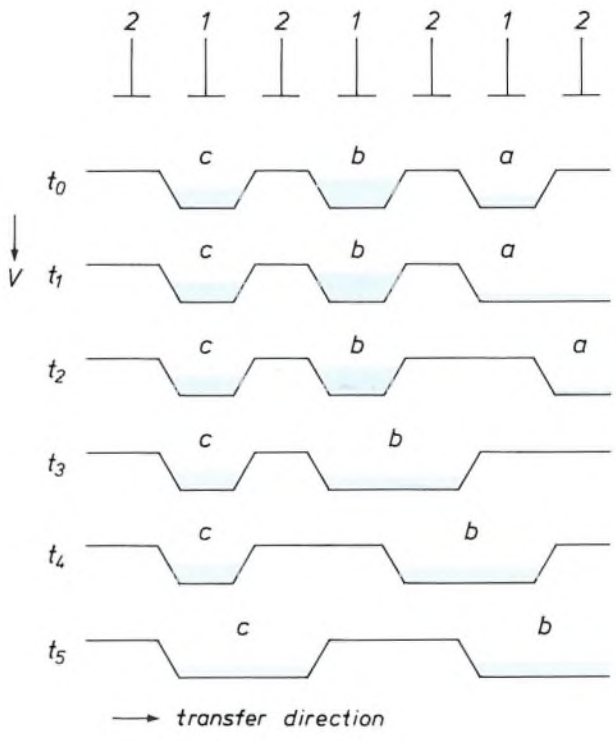

Fig. 3. Principle of the 'accordion' mechanism. The starting point is a two-phase system, in which charge is collected beneath the electrodes *1* during the integration period and the electrodes *2* form a barrier between the different charge packets. A four-phase system is built from this, a step at a time. The state at time t_0 occurs at the end of an integration period, t_1 to t_5 indicate the successive stages in 'stretching the accordion'. It can clearly be seen that charge packet *a* is transferred first, followed by charge packet *b*, and so on to the output of the sensor.

[2] F. L. J. Sangster and K. Teer, Bucket-brigade electronics — new possibilities for delay, time-axis conversion, and scanning, IEEE J. SC-4, 131-136, 1969.

[3] The ideas on which this work is based were put forward by A. J. J. Boudewijns, now with the Consumer Electronics Division, Philips NPB, formerly with Philips Research Laboratories, and M. G. Collet and L. J. M. Esser of these laboratories.

trodes. At this moment the first packet has arrived at the first part of the storage section and the accordion starts to close up. The potential wells and barriers are gradually made one electrode wide.

The entire process of stretching and squeezing the 'accordion' is illustrated in *fig. 4* for a sensor in which the image and storage sections each have eight electrodes. Note that at the end of the cycle the sensor is in the appropriate state for collecting charge beneath the electrodes that were barrier electrodes in the previous integration period; this provides the interlacing.

In the accordion imager the charge transfer takes place over two times 588 electrodes (image and storage). This takes 0.5 ms, which is sufficiently short compared with the integration period of 20 ms. The application of the voltages to the electrodes is obviously more complicated than in the four-phase sensor. The voltage change is no longer the same for electrodes with the same number, as it was in the four-phase sensor. In the following section we shall show how the required voltage pattern on the electrodes is produced.

The accordion imager

Principle

So far we have considered the consequences of the changing voltages on the electrodes for the charge transfer. Let us now see how these voltage changes are produced.

The image sensor is controlled by two shift registers, one for the image section and one for the storage section. These shift registers consist of cells, each with a clock input. The output of each cell is connected to an electrode of the sensor and to the input of the next cell. At the input of the first cell the signal can be either *IM* (for the image section of the sensor) or *ST* (for the storage section of the sensor). The clock signals ϕ_1, which controls the clock inputs of the odd cells in each shift register, and ϕ_2, which controls the clock inputs of the even cells, make this input signal shift step by step through the register, with signal inversion after each cell. This process produces the required voltage pattern on the electrodes. The signal at the input of the first cell of the shift register (*IM* or *ST*) causes the stretching and squeezing of the accordion. The way in which this is done is illustrated in *fig. 5* for a small part of the sensor (8 electrodes of the image section and 8 electrodes of the storage section with the associated shift registers).

At the moment when the clock associated with a cell generates a pulse, the output of the cell takes on a value opposite to the value at the input. The input signals *IM* and *ST*, as shown in fig. 5*a*, produce the potential profile shown in fig. 5*b* on the electrodes $A_I, B_I \ldots$. As long as the input signal *IM* is changing, the potential wells and barriers are two electrodes wide and the charge packets are transferred. The variation of the potential wells and barriers with time can be seen in fig. 5 from the values of the outputs $A_I, B_I, \ldots$ at consecutive times. We see that the required potential pattern is produced at the numbered times, and that it corresponds to the state of the sensor as illustrated in fig. 4.

As soon as the input signal *IM* (or *ST*) becomes constant, the voltages on the electrodes of the image section (or storage section) also become constant, after a short delay. Gradually the accordion is squeezed shut, and the process continues until the potential distribution consists of wells and barriers, each with a width of only one electrode. This potential distribution remains unchanged as long as the signal *IM* remains constant. By keeping the input signal *IM* high in one integration period and low in the other, the electrodes function alternately as barrier and integration electrodes (see fig. 4 and fig. 5).

Correct operation of the sensor requires a number of synchronization signals — in addition to the clock signals ϕ_1 and ϕ_2 and the control signals *IM* and *ST*. These synchronization signals indicate the start and finish of the stretching of the two 'accordions' (the image and storage sections). They can be determined by counting the number of clock pulses, for example. Some of them can also be derived from the state of the shift register [4]. The first synchronization signal indicates the start of the stretching of the charge distribution in the image section and coincides with the end of the integration period. This signal must of course be supplied from outside the chip [5]. The end of the stretching process is reached when the potential of the final electrode of the image section, electrode H_I in the example given in figures 4 and 5, changes for the first time. The arrows in fig. 5 indicate the states from which the synchronization signals are derived. At this time, t_8, the accordion of the storage section starts to close up. There must then be no further change in the signal *ST*.

When the charge distribution in the storage section has completely closed up, signal *IM* is kept constant. The potential distribution in the image section also closes up. The time at which this must start to happen is reached when there is no further change in the potentials of the last two electrodes in the storage section (t_{15}).

[4] A. J. P. Theuwissen, C. H. L. Weijtens and J. N. G. Cox, The accordion imager: more than just a CCD-sensor, Proc. Electronic Imaging 85, Boston 1985, pp. 87-90.

[5] J. N. G. Cox contributed to the design and construction of the special electronic units required here.

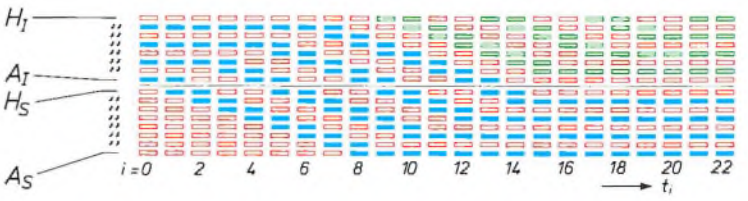

Fig. 4. A complete cycle of the stretching and squeezing of the 'accordion' of an image sensor consisting of 16 electrodes. A_I to H_I indicate the electrodes of the image section, A_S to H_S the electrodes of the storage section. A blue rectangle corresponds to an integration electrode that has a row of charge packets beneath it. A red rectangle corresponds to a barrier electrode, and a green rectangle to an electrode that has no charge beneath it yet, but is at a positive potential. The first column gives the potential distribution at t_0, i.e. at the time when a complete integration period has just finished. Beneath the electrodes A_I, C_I, E_I and G_I there are rows of charge packets (*a*, *b*, *c* and *d*). At t_1 the first row of charge packets starts to move, at t_3 the second, and so on. At time t_8 the first row of charge packets has arrived at the lower edge of the storage section, and the 'accordion' of the storage section can then be squeezed shut. At t_9 the first row of charge packets is again one electrode wide. We note that from t_9 the electrodes of the image section that no longer take part in the transfer of the current charge distribution take up a new potential distribution, which will collect charge during the next integration period. After the complete charge distribution has arrived in the storage section, a clock signal must be sent to provide the potential distribution in the image section with the required one-electrode-wide wells and barriers. From t_{21} charge can be collected beneath the electrodes (B_I, D_I, F_I and H_I). After completion of this integration period A_I, C_I, E_I and G_I are again used to collect the electrons, so that the complete cycle of stretching and squeezing starts again.

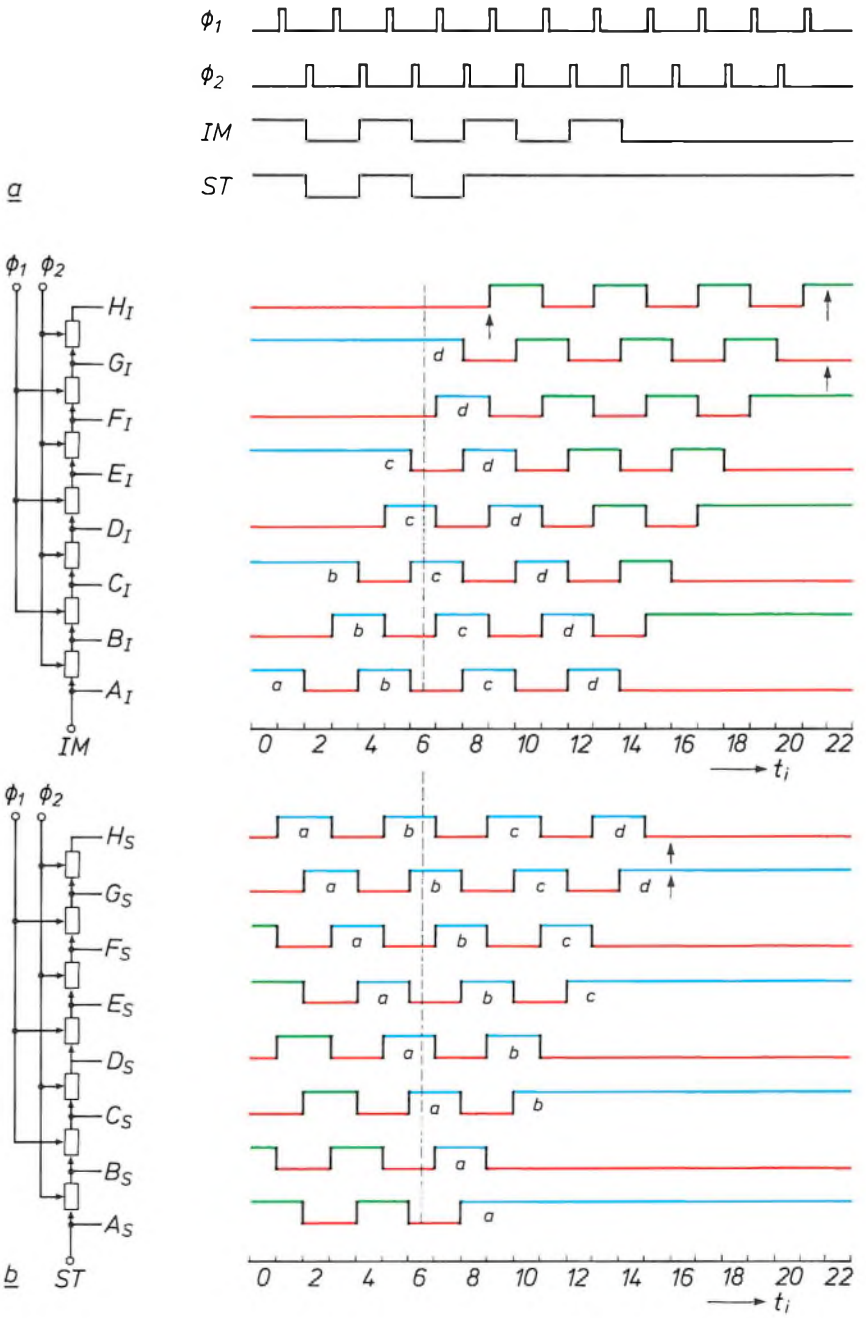

Fig. 5. *a*) Control signals for the transfer of the charge distribution from image section to storage section in the 16-electrode image sensor shown in fig. 4. *IM* and *ST* are the input signals of the 7-cell shift registers (shown as rectangles). These registers produce the potential profile shown in *b* on the electrodes A_S to H_I. The clock signals ϕ_1 and ϕ_2 are necessary for 'clocking' the input signal through the shift register. This potential profile causes the row of charge packets (whose position is indicated by *a*, *b*, *c*, ...) to be transferred from the image section to the storage section. The numbers below the time axis and the designations of the electrodes correspond to those given in fig. 4. At time t_6, for example (see dashed line), the potential pattern on the electrodes corresponds to the pattern in fig. 4 for t_6. The arrows indicate the points in the potential pattern from which the synchronization signals can be determined (see text). After the transfer the functions (separation and integration) of the electrodes in the image section are exchanged.

The final synchronization signal, which indicates that the accordion of the image section is squeezed fully shut, is derived from the states of the two final electrodes of the image section. For the sensor to function correctly it is not necessary to 'know' when the 'accordion' is squeezed shut again. However, to keep the dissipation low, the clocks are stopped at that time (t_{22}).

During the next integration period the charge distribution from the storage section is read out line by line (not shown in fig. 5). This is also done with the 'accordion' action. We should note that after this transfer the 'accordion' of the storage section is squeezed shut. This implies that at time t_0 the potential distribution on the electrodes of the storage section consists of wells and barriers two electrodes wide. At the end of this integration period a new charge distribution has been produced in the image section. At this moment the clocks are started again, and then the signals *IM* and *ST* are triggered by external pulses.

Practical design

The two shift registers for the control of the electrodes of the image and storage sections of the accordion imager have to be fabricated on the same chip as the CCD. The same design rules apply to the produc-

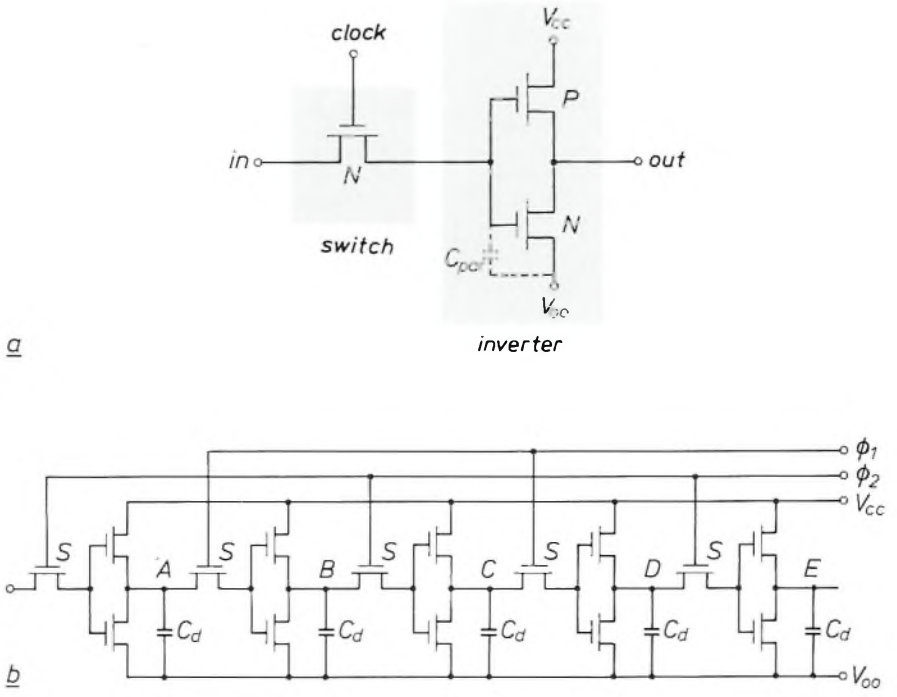

Fig. 6. *a*) Schematic diagram of a cell of the digital shift register that effects the transfer of the charge distribution. A cell consists of a combination of MOS transistors. The first NMOS transistor feeds the input signal along the register 'in phase with' the clock, which therefore acts as a switch. The output of this switch is connected to the gates of an NMOS transistor and a PMOS transistor. The source of the NMOS transistor is connected to a low voltage (V_{00}) and the source of the PMOS transistor is connected to a high (V_{cc}) voltage. This means that the drain electrodes, which are interconnected, are at a high voltage when the output of the switch — the value of the gate voltage — is low, or at a low voltage when the output of the switch is high. The final part of the cell acts as an inverter. The dashed capacitor C_{par} represents the parasitic capacitance of the connections. *b*) A row of these cells forms the shift register. The switches *S* are connected alternately to the clock signals ϕ_1 and ϕ_2. The output of each cell (A_1, B_1, ...) is connected to the input of the next one and to a CCD electrode (shown here as a capacitance C_d). The parasitic capacitances are not shown.

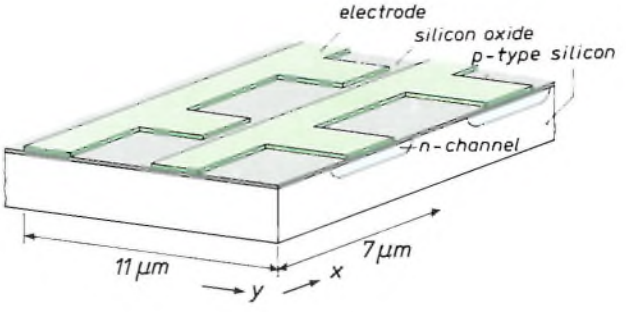

Fig. 7. Diagram showing the arrangement of the CCD electrodes and n-channels in the image section of the accordion imager. The electrodes are shaped in such a way that they do not cover the entire surface but leave some of the p-type material and a part of the n-channels accessible to incident light. This increases the blue sensitivity of the sensor. The polysilicon electrodes absorb light strongly in the blue wavelength range.

tion of the CCD and the shift registers. This means that the shift registers have to be fabricated in the 3.5-μm technology normally used for the CCDs. Moreover, the cells of the shift register should require as little energy as possible and occupy the smallest possible chip area. The simplest arrangement that delivers the required signal and also meets the above requirements is a combination of three MOS transistors per cell: two n-type and one p-type (see *fig. 6a*). The output signal from such a cell becomes the inverse of the input as soon as the clock gives a pulse. While the clock remains inactive (although the input may change) the output remains constant because of the stray capacitance of the inverter gate.

A shift register consists of 587 cells (the number of CCD electrodes less one). The inputs of the switches of these cells are connected alternately to one of the two clock signals. These two clock signals must not overlap in time. Otherwise, the shift register would behave like a row of unsynchronized inverters while both clocks were active.

Each CCD electrode is controlled by a cell of the shift register. The shift register obviously ought to be placed next to the electrodes on the chip, but this is not so easy.

The minimum dimensions of a photosensitive element of the image sensor are 7 μm in the horizontal direction and 11 μm in the vertical direction [6] (see *fig. 7*). The electrodes, which are made of polysilicon, are shaped in such a way that some of the p-type material and a part of the n-channels are accessible to incident light. This improves the sensitivity of the sensor to blue light (polysilicon is almost opaque to blue light). In the storage section of the sensor it is not necessary to leave a part of the silicon surface uncovered by the electrodes. The area of the part of the channel beneath the electrode must be the same as in the image section if it is to have the same charge storage capacity. This means that the dimension in the *y*-direction of a pixel in the storage section can be smaller than in the image section. This vertical dimension is 9 μm. In *fig. 8* it can indeed be seen that the storage section of the sensor is smaller than the image section.

It is obvious that a shift-register cell cannot be located next to every horizontal electrode: a cell consists of a number of p-n junctions and therefore has a vertical dimension several times the minimum width of 3.5 μm. For this reason a few of these cells (four) are placed side by side and on opposite sides of the CCD. The distribution of the available chip area among the different components can be seen in *Table I*.

The synchronization signals that mark the start and finish of the stretching and closing of the 'accordions' (see previous subsection) can be determined by means of a small on-chip electronic circuit consisting of about 20 gates. This circuit determines the logical state of the final two electrodes of the image and storage sections. The clock signals and input signals are started or stopped depending on this state.

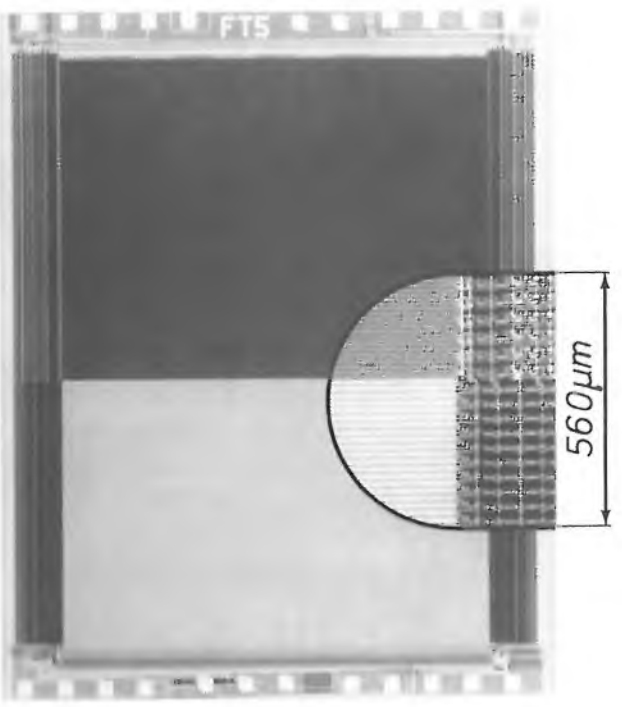

Fig. 8. The accordion imager. The storage section (the light region) is smaller than the image section (the dark region). The storage section is shielded from light by an aluminium layer. The n-channels are vertical, the CCD electrodes horizontal. On the left and right are the shift registers, which generate the voltages on the CCD electrodes. *Insert:* enlarged view of the transition from image section to storage section.

Table I. Allocation of the available chip space to the different sections of the sensor.

Section	Relative area
Image section	35.8%
Storage section	29.3%
CCD output register	2.9%
Digital shift registers	16.8%
Peripheral connections	15.2%

[6] The minimum horizontal dimension follows from the 3.5-μm technology employed. The transfer in the horizontal direction takes place in a three-phase shift register. The length of a cell in this register, which really consists of three shift registers one above the other, is 21 μm. This is why the minimum dimension of an electrode of the shift register, and hence the minimum dimension of a channel, is 7 μm. The pixel matrix must have the standard TV format. This means that the ratio of the horizontal to the vertical dimensions of the image section must be 4:3. Since there are 604 pixels per line and 294 lines, a pixel must have a vertical dimension of 11 μm.

Characteristics of the sensor

To conclude, we shall recapitulate the characteristics of the accordion imager, and compare them with those of its predecessor, the four-phase image sensor. *Table II* gives the main characteristics of both types of sensor.

The area occupied by the accordion imager is only 56% of that of the four-phase device. This makes the accordion imager the smallest solid-state image sensor described in the literature with such a large number of pixels. This reduction of chip area has not entailed any sacrifice of resolution. One of the advantages of the smaller number of electrodes is that it reduces the dissipated power. A lower dissipated power per pixel results in a lower dark current, and therefore better image quality. Dark-current fluctuations, which are local, are one of the main limitations in the use of a solid-state image sensor. These fluctuations can cause bright spots to appear at various points in the picture.

Another advantage is that the electronic control circuits not included on the chip are simpler and more compact. Less polysilicon is required on the chip, and this improves the photosensitivity of the sensor, particularly for blue light. The most important aspect of the accordion imager, however, is that a number of characteristics connected with the chip size and the number of pixels (especially the cost of the chip) are better than for other image sensors, yet it has not been necessary to design a completely new method of production or to develop an entirely new production process.

Table II. Some characteristics of the accordion imager compared with those of the four-phase sensor.

	Four-phase sensor	Accordion imager
Type [1]	frame transfer	frame transfer
Chip area ($y \times x$)	$9.41 \times 7.01 = 66$ mm^2	$7.01 \times 5.45 = 38.2$ mm^2
Number of pixels ($y \times x$)	588×604	588×604
Pixel dimensions ($y \times x$)	15.6×10 µm^2	11×7 µm^2
Read-out rate	11.5 MHz	11.5 MHz
Layout rules	3.5 µm	3.5 µm
Number of electrodes per pixel	4	2

Summary. Solid-state image sensors are silicon chips in which a charge distribution is generated by incident light. The use of such devices in video cameras for the consumer market will depend greatly on the price of the sensor. As with all chips, this is closely dependent on the chip area. With a new read-out mechanism, in which the charge distribution is stretched out and squeezed shut like an accordion, it is possible to build an image sensor with two electrodes instead of the usual four for each line of the frame. The new sensor can be produced with the same technology as used for the four-phase sensor. The electronic control circuits can be fabricated on the chip with the sensor in a single process.

Philips Technical Review 50 years ago

DEMONSTRATION MODEL ILLUSTRATING SUPERHETERODYNE RECEPTION

MARCH 1936

At the World Exhibition held in Brussels last year, a demonstration model was exhibited which illustrated in the most elementary manner the method of operation of modern radio receivers. It is of course generally known that in radio transmission a carrier wave of high frequency is employed and the much lower audio-frequencies are transmitted as a modulation of the amplitude of this carrier wave. The function of the rectifying stage in the receiver is to separate these low audio-frequencies from the high frequency of the carrier wave. Perhaps less well known is the sequence of operations which actually take place in a superheterodyne receiver in which an "oscillator", a "converter valve" and an "intermediate frequency" are used. The main object of the demonstration model described in the present article is therefore to illustrate the principles underlying superheterodyne reception.

The Superheterodyne Principle

In superheterodyne receivers, not only is the incoming high-frequency carrier wave appropriately dealt with, but provision is also made for the simultaneous generation of an additional oscillation by means of an oscillator.

To generate the auxiliary oscillation and to modulate it on the incoming oscillation a special converter valve, the octode, is used in Philips superheterodyne receivers. This valve may be regarded as a triode and a pentode, connected in series, in which the triode serves for the generation of the auxiliary oscillation, while the pentode further handles the alternating current generated in the triode.

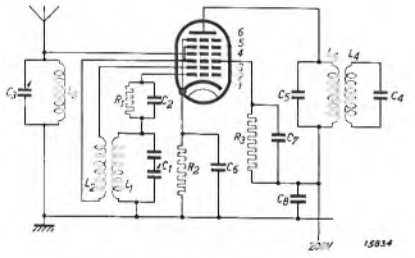

Fig. 1. Circuit diagram of the octode. The circuit L_3C_1 is tuned to the auxiliary oscillation, L_2C_2 to the incoming signals, L_3C_3 and L_4C_4 to the intermediate frequency.
1 = Control grid 2 = Auxiliary anode
3 = Screen-grid 4 = Control grid
5 = Screen-grid 6 = Intercepter grid

Mechanical representation

Electrical oscillations are usually represented diagrammatically by means of a sinusoidal or similar type of wavy line. It appeared therefore that these oscillations, which are usually drawn with chalk on a blackboard, could be usefully reproduced mechanically for general exhibition by means of a sand figure on a slowly-moving belt. This would enable a practical demonstration of the principles of reception and the properties and uses of the carrier wave. In the demonstration model which was evolved for this purpose, the utilisation of the actual carrier wave is also demonstrated by means of a number of cathode ray tubes, which produce a visible trace of the electrical oscillations on their fluorescent screens.

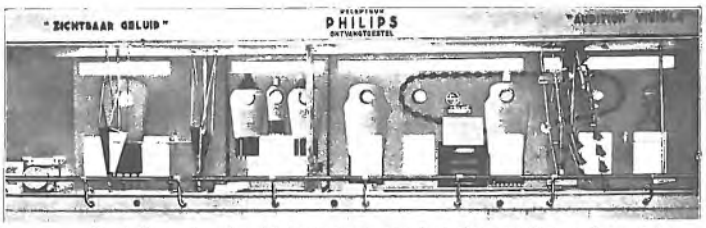

Fig. 2. Front view of model demonstrating superheterodyne reception, as shown at the Brussels 1935 World Exhibition.

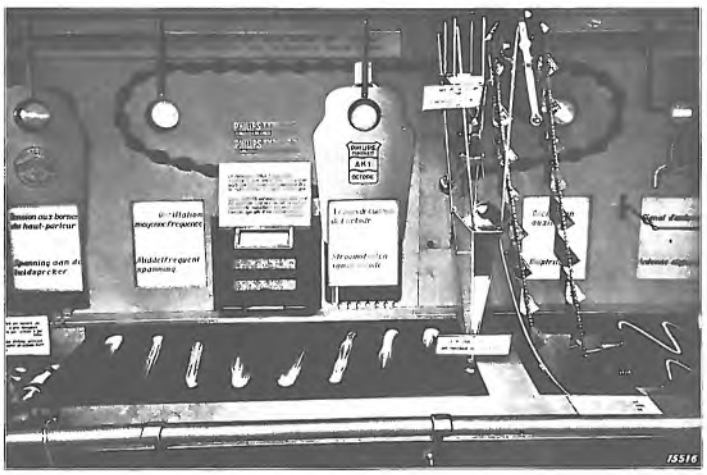

Fig. 3. Sand figures demonstrating the anode current of the octode.

In *fig. 2* the apparatus is shown which was exhibited on the Philips stand at Brussels. The graphing of the various oscillations occurring in radio receivers in the form of sand figures is performed on a moving belt which moves in a horizontal direction from right to left. The belt is only just visible in this picture, but is more clearly shown in *fig. 3*. The feed tubes for the sand and the pendulums fitted with funnels which swing to and fro from back to front and thus produce the sand figures, can be picked out in fig. 2.

PRACTICAL APPLICATIONS OF X-RAYS FOR THE EXAMINATION OF MATERIALS

By W. G. BURGERS.

Differentiation between Natural and Cultured Pearls

A natural pearl is built up of concentric layers of calcium carbonate (mother-of-pearl) which have been deposited by the oyster round any available nucleus (e.g. a grain of sand). Each layer consists of crystallites with a sixfold symmetry, the axis of each crystallite being perpendicular to the layer. This structure is shown schematically in *fig. 2a*.

A "cultured" (or Japanese) pearl is obtained by inserting in the oyster a bead of mother-of-pearl cut from an oyster shell. This shell is built up of plane layers of mother-of-pearl with the sixfold axis of symmetry of the individual crystallites again arranged perpendicular to the layer. The nucleus of a cultured pearl therefore has a structure as shown schematically by the horizontally shaded section in *fig. 2b*. Round this "nucleus" the oyster deposits several thin concentric layers so that in external appearance the finished cultured pearl cannot be distinguished from a natural pearl.

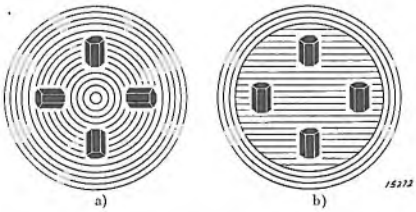

a) b)

Fig. 2. Diagrammatic representation of the structure of a natural and a cultured pearl.
a) The natural pearl is made up of concentric layers of mother-of-pearl (crystallites of calcium carbonate).
b) The cultured pearl consists of a nucleus of plane layers of mother-of-pearl, on the outside of which several thin concentric layers have become secreted.

From the connection between the symmetry of the crystals and the X-ray pattern (which is produced by reflection of the rays at the crystal lattice planes) referred to at the beginning, it follows that the patterns obtained with a natural pearl must always exhibit an arrangement of dots with a sixfold symmetry, which latter cannot be obtained with a cultured pearl. *Figs. 3a and 3b* confirm this conclusion, and show that it is indeed possible to distinguish between natural and cultured pearls by means of X-rays.

a) b)

Fig. 3. a) The diffraction pattern of a natural pearl always exhibits a sixfold symmetry.
b) A cultured pearl gives another type of pattern.

FEBRUARY 1936

PHILAN, a local-area network based on a fibre-optic ring

J. R. Brandsma

Information is one of the main resources of modern life. The availability of up-to-date, reliable and sufficient information at the right place and at the right time is very important for the quality of public, social and economic services. This requires good means of communication, geared to the situation in which they are used. A specific situation is found in factories and offices, where large numbers of people work closely together. Within such a geographically defined area there is a need for the easy exchange of large amounts of information of all kinds and in accordance with an often varying communication pattern. For communications within this business environment ever-increasing use is being made of the 'local-area network' or LAN. At the Philips Research Laboratories Project Centre in Geldrop, near Eindhoven, a novel and versatile concept for a LAN based on a fibre-optic ring has been developed and given shape in the form of a trial system for demonstration purposes. The main aspects of this type of network, which is called PHILAN, are described in the article below.

Introduction

Few people would seriously consider buying a car if the appropriate infrastructure were not available in the form of roads and rules of the road, etc. Without those provisions there would be absolutely no way of making use of the many possibilities offered by that product of modern engineering.

A comparable situation is to be found in the field of information technology. Instead of the car we find one of the many kinds of data-processing equipment, and the infrastructure required consists of a communication network with the appropriate rules or code of practice ('protocols'). In this situation there is of course not much point in storing or rapidly processing large amounts of data at one particular place if it cannot subsequently be sent to the destination with equal rapidity and with a high degree of reliability. In situations where many people have to work closely together or use the same information, as in offices, factories, hospitals and universities, there is a great need for special communication facilities. The requirements these have to meet are the following:

- *Versatility*. Many different kinds of information have to be sent out in parallel (telephone conversations, telex, electronic mail, communication with computers and between computers, monitoring signals such as 'slow-scan TV', radiography, etc., etc.).
- *Universality*. Connections must be as universal as possible, which means to say that at every connection point it must be possible to receive and transmit a wide variety of information (provided the appropriate terminals are present).
- *Flexibility*. Connected terminals must be readily transportable without having to make radical changes such as recabling.
- *Adaptability*. It must be easy to change the kinds of information that can be transmitted and to extend the number of connections.

In the past *ad hoc* solutions to these problems have been sought, and these have tended to result in a rather confused combination of various kinds of communication networks with different types of cables, network structures, wall sockets, etc. The best solution is one that meets all the above requirements with a single communication network, called a 'local-area network (LAN)' [1] or, when special emphasis is placed on the great diversity of the information that can be trans-

Ir J. R. Brandsma is with Philips Research Laboratories, Eindhoven. Until recently the author led the team working on the PHILAN project at the Project Centre in Geldrop, near Eindhoven.

[1] W. A. M. Snijders, Bedrijfscommunicatie en glasvezel, een symbiose, I & I (Inf. & Informatiebeleid), No. 7, 20-30, 1984; D. D. Clark, K. T. Pogran and D. P. Reed, An introduction to local area networks, Proc. IEEE **66**, 1497-1517, 1978.

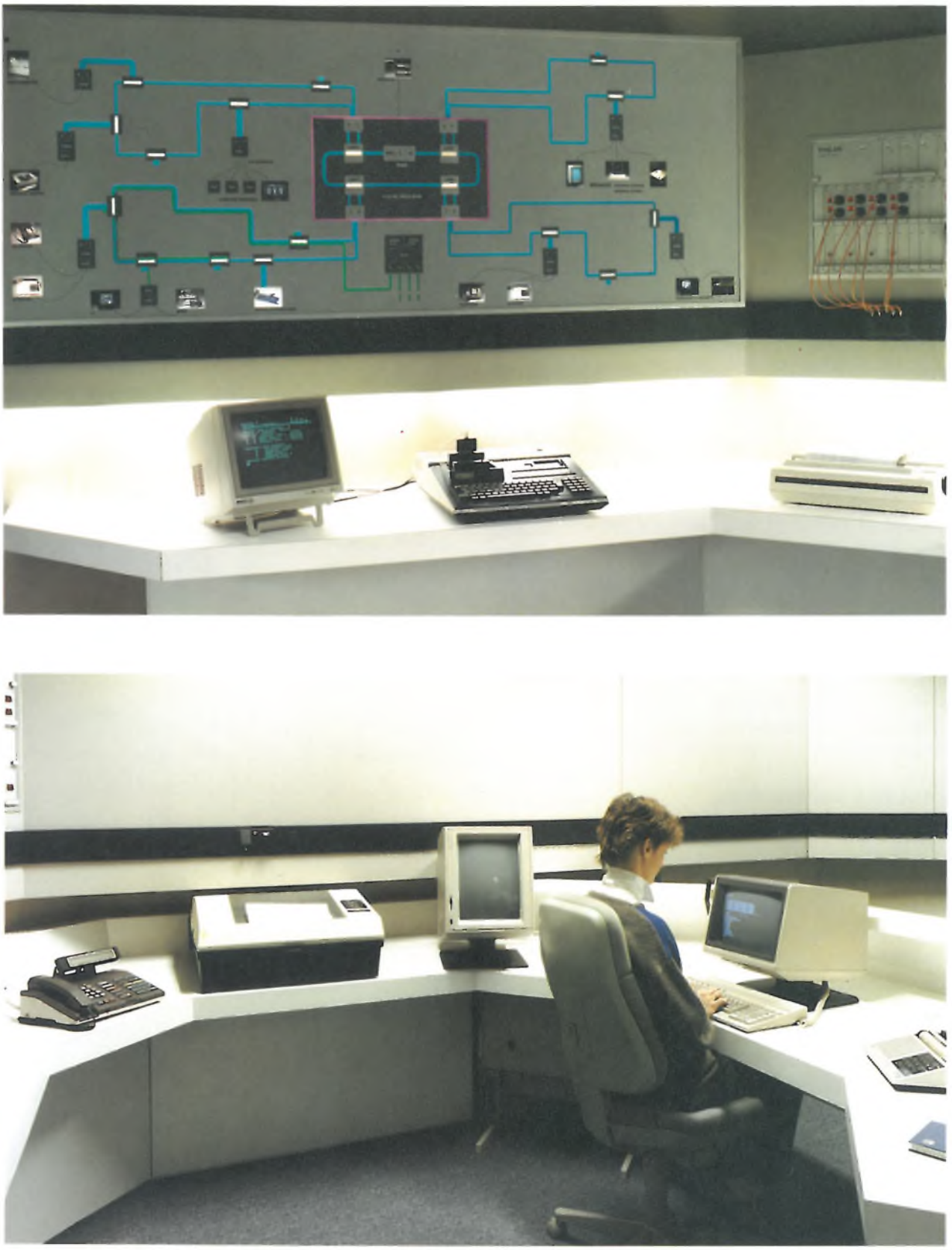

Fig. 1. At the Philips Research Laboratories Project Centre a local-area network based on the PHILAN concept has been built as a trial system for demonstration purposes. The equipment shown in the upper photograph forms the central unit, from which the whole network is controlled. Above it, on a large panel, is a diagram of the complete trial system showing the exact configuration of the network. The lower photograph shows a large number of possible applications of the system. From left to right can be seen an advanced telephone set, a printer, a display screen specially suited to the display of documents, a word processor and an intercom set. The same transmission medium, a single optical fibre, carries the input and output signals of all these devices.

mitted, an 'integrated local-area network (ILAN)'. Owing to the local nature of these LANs, it is not in principle necessary to take account of existing communication networks — usually trunk (long-distance) networks — at the design stage. Designers consequently have a large measure of freedom in the choice of the network structure, the transmission medium and the type of signal.

In this article we shall describe the PHILAN network, a highly sophisticated ILAN network [2], recently developed at Philips, which has been set up as a trial system for demonstration purposes (*fig. 1*). The network has a 'meander-type' ring structure that uses fibre-optic cable. The information (e.g. speech, certain video signals and all kinds of data) is transmitted in digital form at a rate of about 20 Mbit/s, and the error probability is smaller than 10^{-10}.

First of all we shall examine the main considerations that have played a part in the design of PHILAN, such as the various requirements applicable to the transfer of various kinds of information and the possible alternative network structures. We shall then describe the composition ('frame structure') of the digital signals and consider the handling of the traffic between the users of the network in accordance with certain protocols. Finally we shall go somewhat deeper into a number of the building blocks of PHILAN, such as the ring-management system, the ring-access units and a small ingenious optical relay.

Local-area communication

The various kinds of information to be transmitted in a local-area network can be divided into two main groups: continuous information and intermittent information. The first kind is found for example in telephone and video communication and in communication for security and surveillance purposes. The other kind is found in data processing, electronic archiving and in comparable cases of communication between man and machine (computer).

Continuous information requires a connection which is permanently available and whose only side-effect is a small and constant delay. Traditionally this is realized by means of *circuit switching*, in which there is — or at least seems to be — a continuous connection between information source and destination. Intermittent information can best be sent via a data link established by means of *packet switching*, where a channel is occupied only during the transmission of a specific, clearly defined 'packet' of information at a time. Each packet is separately addressed, transmitted and received. Long messages are split into several packets. In a modern local-area network the most efficient operation is achieved by combining both types of information transmission [3].

This can be done for example by first converting all information into digital form, i.e. into bit streams. These separate bit streams can be combined by means of time-division multiplex (TDM) to produce one total bit stream with a much higher bit rate, which can be transmitted via a common transmission medium (e.g. an optical fibre) to which all users are connected. The combined bit stream thus represents a considerable number of communication processes that are taking place simultaneously; the circuit-switched links each have a piece of the combined bit stream that recurs at strictly periodic intervals (e.g. a string of 8 successive bits 8000 times a second) and the packet-switched traffic receives parts of the remaining bit positions as required. We shall return to this point later.

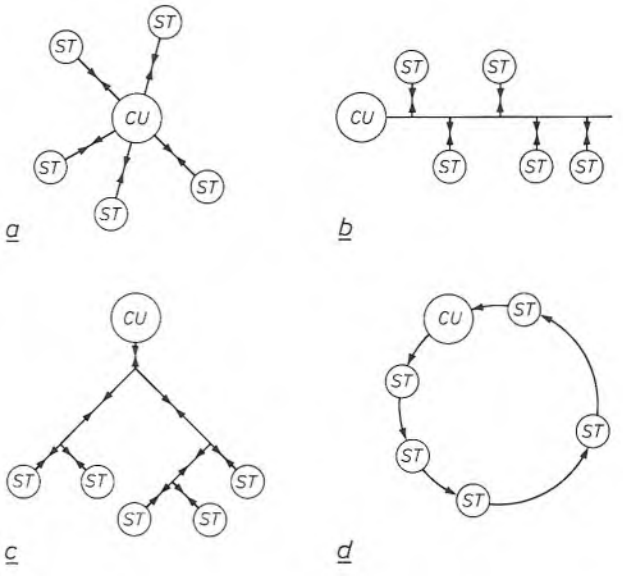

Fig. 2. Four elementary network structures. *a*) Star. *b*) Bus. *c*) Tree. *d*) Ring. *CU* central unit. *ST* station.

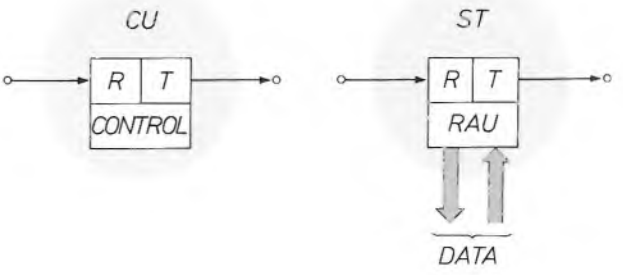

Fig. 3. Basic block diagrams of the central unit *CU* and a station *ST* of a network with ring structure. In both diagrams the receiver unit *R* and the transmitter unit *T* are shown. In *CU* a number of monitoring and management operations are carried out in the part marked *CONTROL*. The station contains a ring-access unit *RAU*, which handles the exchange of data between the ring and the outside world.

An important external characteristic of any communication network is the structure or topology of the network [4][5]. *Fig. 2* shows four basic structures: star, bus, tree and ring. In principle a distinction can always be made between the central unit, which controls the operation of the system, the satellite stations, which function as data source or destination (data sink), and the actual transmission paths.

Every network structure has its own way of handling traffic between stations, and in every structure the role of the central unit is different. In fact with a bus structure it is common practice to decentralize the control in such a way that no separate central unit is needed. Both with the star structure and the tree structure all the data goes from the source via the central unit to the sink. In the ring structure the data circulates from station to station. If a station does not itself have any information to transmit, the incoming information is passed on to the next station. When all stations do that, the result is the formation — via the central unit — of a 'circulating memory', whose capacity depends on the total delay that occurs in the stations and the transmission paths and, of course, on the bit rate.

Another important external characteristic of a communication network is the transmission medium employed. For a LAN three kinds of media enter into consideration: twisted-wire pairs, coaxial cable and fibre-optic cable. Twisted pairs are cheap and easy to install. Coaxial cable has a higher transmission capacity and is popular because of the large number of other existing applications (such as cable TV); this accounts for the large variety of accessories available. Fibre-optic cable offers the largest transmission capacity, little signal attenuation and the unique features of complete electrical insulation and insensitivity to electromagnetic interference.

In the rest of this article we shall mainly be concerned with the ring structure, in which the signals in digital form (briefly: data) are transmitted by means of time-division multiplex. *Fig. 3* shows basic block diagrams of the central unit and a station in such a ring. Both comprise a receiver and a transmitter. The minimum operation that takes place is the unaltered retransmission of the received data. The station also possesses, however, a 'ring-access unit' (RAU), with which data can be read from the ring or written to it. The central unit controls and monitors the operation of the ring; it determines the bit rate and, among its other functions, plays a part in the allocation of transmission capacity to the stations.

From the foregoing it may be deduced that the ring structure has two potential disadvantages. In the first place a ring structure is relatively vulnerable because one defective station or one broken cable can put the whole ring out of action. In the second place the repeated reception and retransmission of data in the form of a bit stream gives rise to a gradually increasing inaccuracy in the bit positions ('jitter'), which may ultimately result in transmission errors. Timely steps therefore have to be taken in the central unit to restore the original accurate time division. This limits the maximum number of stations that can be included in the ring. Both disadvantages can be overcome by segmentation of the ring. This can been done in PHILAN and has resulted in a modified ring structure which we shall refer to as a meander ring.

Table I. List of abbreviations used for component parts of PHILAN.

	Meaning
CRAU	RAU for Circuit-switched traffic
CU	Central Unit
EBS	Electronic Bypass Switch
LN	Local Nucleus
MG	Meander Gate
PRAU	RAU for Packet-switched traffic
RAU	Ring Access Unit
R/T	Receiver/Transmitter
ST	STation
US	USer
WR	Wall Receptacle
WS	Wall Socket

PHILAN

The network structure chosen for the PHILAN system corresponds essentially to a ring, but parts of the ring ('meanders') can be cut off whenever necessary. This is done in a special unit that we call a meander gate or MG. (A list of abbreviations frequently used in this article will be found in *Table I.*) Each meander

[2] J. R. Brandsma, PHILAN: a fiber-optic ring for integrated traffic, Proc. GLOBECOM '85, New Orleans, LA, 1985, pp. 468-471;
J. L. W. Kessels, PHILAN: a LAN providing a reliable message service for real-time applications, Proc. INRIA Conference 'Advanced seminar on real-time local area networks', Bandol, France, 1986;
J. R. Brandsma, A. M. L. Bruekers and J. L. W. Kessels, Method and system of transmitting digital information in a transmission ring, U.S. Patent No. 4 553 234 (12th November 1985).

[3] The term 'integrated local-area network' (ILAN) mentioned earlier is used for communication networks in which this combination is found.

[4] C. D. Tsao, A local area network architecture overview, IEEE Commun. Mag. **22**, No. 8, 7-11, 1984.

[5] D. Hutchison, J. A. Mariani and W. D. Shepherd (eds), Local area networks: an advanced course (Proceedings, Glasgow 1983), Lect. Notes Comput. Sci., Vol. 184, Springer, Berlin 1985.

contains a limited number of stations which are interconnected in accordance with the usual ring structure (*fig. 4*). The transmission medium used in the meanders is fibre-optic cable. The central unit and the meander gates together with the links between them form the local nucleus of PHILAN. This is concentrated at one location and, because of the short distances *inside* the local nucleus, the links used are purely electrical connections.

In each meander gate an interference-free clock signal from the central unit is used to form the signal to be sent to the next meander gate. In this way any jitter that may have arisen in a meander is eliminated, so that in theory an unlimited number of meanders can be connected in cascade.

A more detailed block diagram of a meander is given in *fig. 5*, corresponding to the part *A-A'* in fig. 4. The total digital signal that appears at a given moment in the PHILAN system arrives (in electrical form) at the input of the meander gate. During normal operation an optical equivalent of this signal is formed in the transmitter, which sends it on to the meander. Each possible position in the meander where a station may have to be connected is provided with an optical connector box, called a 'wall receptacle'. If no station is connected, each wall receptacle forms an optical through-connection. If a station is included in the ring, it is connected in the usual way by a special optical plug (see fig. 3). Situated at the end of the meander is the optical receiver of the meander gate. Here the optical signal from the meander is converted into an electrical signal and processed for transmission to the next meander gate.

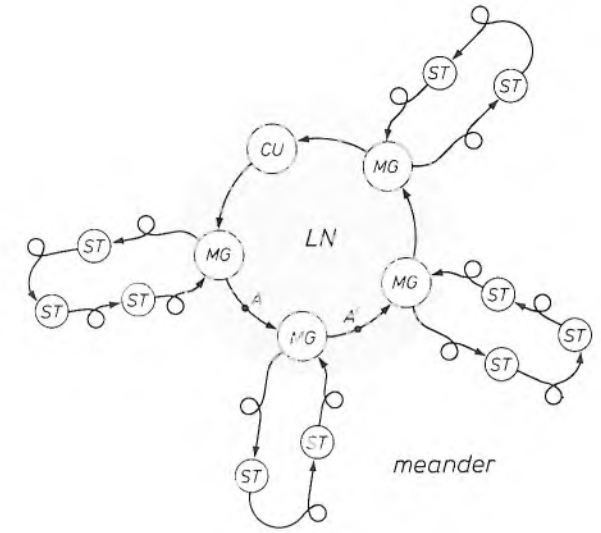

Fig. 4. The meander ring structure of PHILAN. In addition to the central unit *CU* and the stations *ST* found in every ring structure, the PHILAN ring contains a number of meander gates *MG*. These divide the ring into sections, called meanders, each containing a number of stations. The *CU*, the *MG*s and the links between them form the local nucleus *LN* (grey). The transmission medium used in the meanders is fibre-optic cable (indicated by the symbol ——○——); electrical connections are used in the local nucleus.

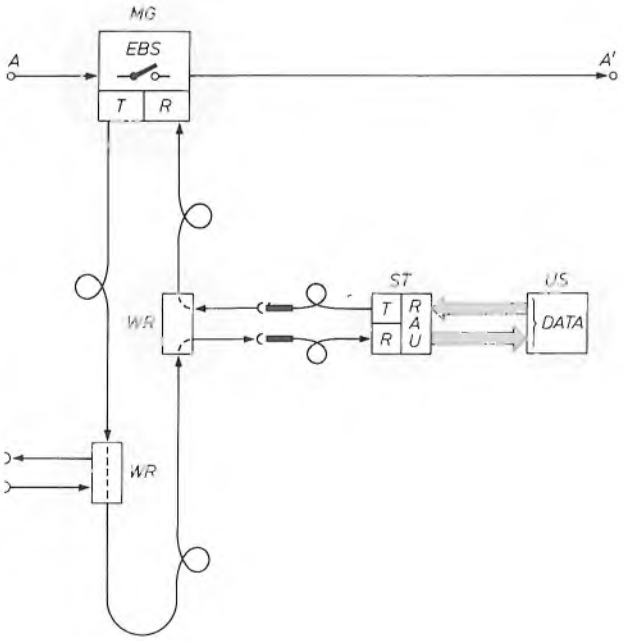

Fig. 5. Basic diagram of a PHILAN meander. The meander gate *MG* forms the link between the actual meander and the rest of the network. This link is established via the optical transmitter *T* and the optical receiver *R*. In addition, *MG* contains an electronic bypass switch *EBS*, which can 'cut off' the meander. At a number of fixed positions along the fibre-optic cable of the meander are wall receptacles *WR*. A user *US* can be connected to a *WR* via a station *ST* and a plug. If there is no plug, *WR* forms an (optical) through-connection. *ST* contains the same optical receiver/transmitter combination *R/T* as *MG*. *US* is coupled to the ring-access unit *RAU* of *ST* via an electrical connection.

Meander length

The total length a meander can have depends on the number of wall receptacles it contains. Upon passing each wall receptacle to which an *active* station is connected the circulating digital PHILAN signal is regenerated (refreshed) before being sent on; any signal attenuation that may have occurred earlier is thus eliminated. A less favourable situation is found in each wall receptacle to which *no active* station is connected. The signal then passes straight through the wall receptacle, involving a nominal attenuation of 1.3 dB. The worst situation occurs when all stations are passive except for one of the two that lie closest to the meander gate. The total attenuation occurring in the meander is then at a maximum. At a given maximum attenuation there is a direct relation between the maximum meander length and the number of wall receptacles in the meander. This relation is shown in *fig. 6* for a total 'power budget' of 32 dB, of which more than 22 dB is available for losses in wall receptacles and fibre-optic cable, given an attenuation of 5 dB/km in the optical fibre. With the very common number of 10 wall receptacles, the maximum meander length is about 2 km.

If for one reason or another a meander is not functioning properly, the electronic bypass switch (*EBS*,

see fig. 5) is closed in the meander gate, thereby cutting out that meander. The rest of the PHILAN system is therefore not affected by the malfunctioning of this meander. This is not the only protective provision made; in each wall receptacle the station connected can be optically bypassed by means of a relay, in the same way as when there is no plug in the socket. This safeguard comes into operation automatically if it is found, for example, that the transmitting unit of a station is not sending out any optical signals. Yet another safety feature is the possibility of making a direct electrical through-connection in a station — between the output of the receiver and the input of the transmitter. This is a feature that plays a particularly important part in the localization of errors ('error diagnosis').

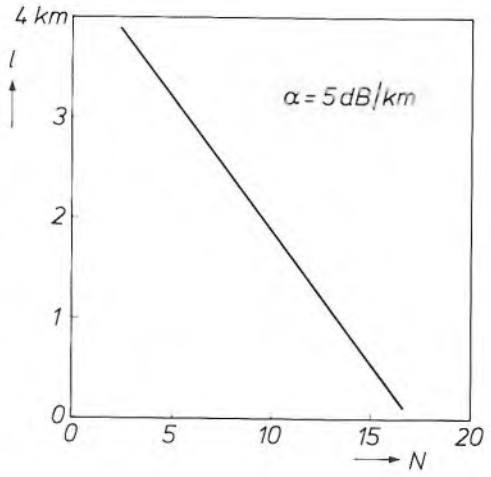

Fig. 6. For each connection point some attenuation of the signal circulating in the ring must be taken into account. In PHILAN the number of connection points N per meander and the maximum meander length l are related by the straight line shown (for a fibre-optic cable with an attenuation of 5 dB/km and a maximum permissible total attenuation in wall receptacles and glass fibre of just over 22 dB).

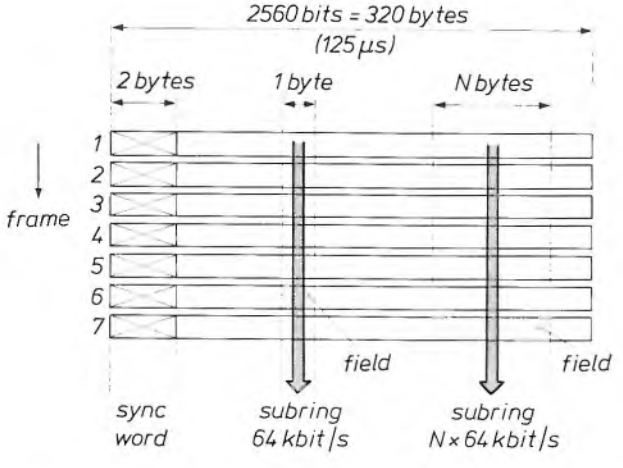

Fig. 7. Frame structure of the digital signal used in the PHILAN ring. Every 2560 successive bits form one frame consisting of 320 bytes of 8 bits. The first two bytes form an unchanging synchronization word, called the 'preamble'. By joining together the bits of one particular byte from each frame a transmission channel ('subring') is formed with a capacity of 64 kbit/s. By taking N bytes together a subring of $N\times64$ kbit/s is obtained. The share of each subring in a particular frame is called a 'field'.

During the design of PHILAN, reliability was a paramount consideration. The aim throughout was to provide *safe communication services*, not only as regards network structure and hardware but also as regards the signals and the protocols used. By this we mean that after a certain time interval the user must have an assurance that his message has arrived correctly at the right destination, without him having to do anything else to verify this. Before looking at this more closely we shall first examine the signal structure used in PHILAN.

The signal structure: frames and subrings

Signal transfer in PHILAN takes place in the form of a continuous series of bits passing through all connected stations in succession at a rate of 20.48 Mbit/s. Each group of 2560 successive bits is identically organized and is called a 'frame'. A frame corresponds to 125 μs. Measures are taken in the central unit to ensure that the signal delay corresponding to one complete circuit or *lap* around the ring is always equal to an integral number of frames. The frames therefore continue to appear at each point in the ring at a fixed rate.

The first 16 bits of a frame always form a special and unchanging synchronization word, called the 'preamble', so that all parts of the PHILAN system remain in synchronism with each other and 'know' exactly when a new frame starts. The remaining bits of the frame belong together in groups of 8 bits ('bytes'). The grouping of the bits of a particular byte from all successive frames results in a transmission channel ('subring') with a capacity of $8/(125\times10^{-6}) = 64$ kbit/s. Similarly a combination of N bytes produces a subring of $N\times64$ kbit/s (*fig. 7*). The bits in one particular frame that belong to the same subring form a 'field'; the size of a field may vary from 1 to 64 bytes (i.e. from 8 to 512 bits).

Between the preamble and the fields that form the subrings there are a further 6 bytes in each frame that have a special function. These are used for intercommunication between the units of the local nucleus (*CU* and *MG*s) or between the units of a particular meander (*MG* and *ST*s). Details will not be given in this article.

Communication within PHILAN takes place by the bits of a particular subring being written by the transmitter of one station and read out by the receiver of another station. Writing and read-out can also take

place in a station simultaneously, in which case it is referred to as a 'swap' [6]. The bits coming from the ring and those destined for the ring are stored in the stations in buffers, which form a kind of separation between the fast (20 Mbit/s) transmission on the ring and the preceding or subsequent processing. Processing rate and transmission rate are thus made independent of each other. One advantage of this is that no processing operations need to be carried out at transmission rate.

All communication takes place through the mechanism of the subrings: this includes both the actual data transfer in packet-switched or circuit-switched traffic and all incidental messages concerning matters such as origin and destination (data source and data sink) and related to the operation of the whole network. Three distinct types may be distinguished: traffic subrings, memory subrings and insertion subrings. Each subring is completely independent; what happens on one particular subring has no influence whatever on the others.

Traffic subrings

As the name suggests, these are the subrings in which the actual traffic in PHILAN takes place, and they account for about 90% of the total ring capacity.

In circuit-switched traffic a subring with the required capacity of $N\times64$ kbit/s is made available for the whole duration of a 'conversation', which in principle may be unlimited. Even in two-way ('full-duplex') traffic between two stations only one subring is required if both stations use the swap operation.

In packet-switched traffic a subring is made available for the transfer of one packet (a maximum of 8 kbytes). This subring covers a field of 1, 4, 16 or 64 bytes per frame; on this basis there are four categories of traffic subrings with a capacity of 64, 256, 1024 and 4096 kbit/s respectively. Owing to the limited dimensions of the fields, a packet will in general be distributed over more than one frame. Messages that are longer than the longest possible packet are in turn divided into a number of packets.

Traffic subrings will generally be referred to here from now on as 'channels'.

Memory subrings

Memory subrings function as a 'circulating memory' for various system data that may be of interest to all connected stations. They are used for example to allocate a channel to a particular station for a particular time for the transmission of a data packet. This takes place in principle in the following way. In each frame the channel controller (a part of the central unit) places the number of a free channel — if there is one — in a field of the memory subring. By means of a swap, each connected station may substitute a zero for this number and thus 'seize' the channel concerned. The channel controller also continuously performs the swap operation on the memory subring and finds out, by receiving the number zero, when the channel is occupied. When a channel becomes free, this is communicated to the channel controller by returning the appropriate number in a similar way via the memory subring.

The channel controller monitors the free channels continuously. Each of the four categories of channels for packet-switched traffic has its own memory subring. Depending on the actual volume of messages the channel controller may transfer channels from one category to another by combination or splitting. The channel controller also ensures that no channel numbers can become permanently lost or are duplicated in circulation as a consequence of transmission errors.

Insertion subrings

In each frame two times 8 bytes are reserved for forming two 'insertion subrings'. They each therefore have a transmission capacity of 512 kbit/s and are used in packet-switched traffic for exchanging information ('protocol messages') between the various connected stations. One insertion subring is used for sending protocol messages that connect a transmitter and a receiver for the duration of the complete message ('call messages'). The other insertion subring is used for exchanging protocol messages during actual packet-switched traffic between partners that have already been connected. These messages prevent packets from being lost through overflow of storage

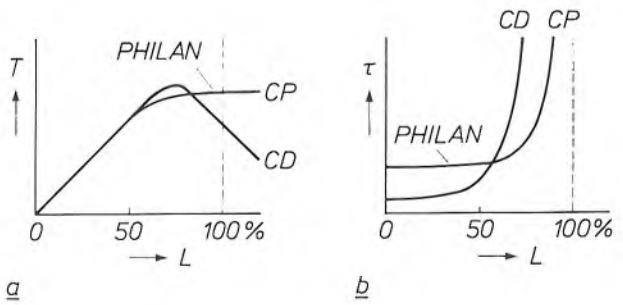

Fig. 8. Comparison of the network stability for packet-switched traffic in two types of LAN. The first type of network, of which PHILAN is an example, offers the special feature of collision prevention (*CP*) between the transmitted packets. In the other type of network mutual interference is permitted and subsequently restored ('collision detection' or *CD*). *a*) With increasing traffic load L, the effective throughput T in PHILAN increases monotonically to the maximum value; in the other system, T becomes smaller at large values of L. *b*) The price to be paid for this benefit is a somewhat longer average delay τ for the packets in the PHILAN network when the traffic load L is small. At high values of L, PHILAN again has the advantage. (If L is 100% or higher, the mean delay in both systems is infinitely large.)

buffers in the receiver (flow control) or as a consequence of transmission errors (error control).

The name of this type of subring derives from the manner in which it is used: each station can insert a protocol message of 8 bytes into a field in this subring by means of a swap operation. The present contents of the field are read into a receiving buffer and replaced by new contents. The present contents may however represent a valid message for a subsequent station on the ring and should not therefore be destroyed. In the next frame it is consequently reinserted (again via the swap operation). In this way each protocol message goes through the whole PHILAN system until it finally comes back like a kind of echo at the station which originally sent it out. This station then finally removes the message from the ring.

The total time that elapses before an echo arrives depends on the number of stations in which swapping has been carried out, but the maximum delay is known beforehand. The correct reception of an echo at the place of origin means that the protocol message in question has passed correctly through all operating stations. If, on the other hand, no correct echo is received within the maximum delay, the same protocol message is sent once again. This procedure forms the basis on which the correct transmission of information can be guaranteed in the PHILAN system ('safe-message service').

One of the main advantages of the signal structure and associated protocols adopted for PHILAN is network stability: an increasing volume of traffic does *not* — as in some other networks — lead to a lower effective transmission capacity, caused by the fact that an ever-decreasing proportion of the packets are transmitted correctly at the first attempt (*fig. 8*). In addition, special measures have been taken to ensure that PHILAN functions fairly, i.e. without any discrimination against transmitters or receivers in the allocation of transmission capacity.

An illustrative example

The function of the various subrings may be illustrated by the example given in *fig. 9*. This shows two users *US-A* and *US-B*, between which a packet-switched connection has to be built up via the stations *ST-A*, *ST-B* and the rest of the PHILAN system. *US-A* and *US-B* are connected by means of a standardized link known as a 'VMEbus'[7] with *ST-A* and *ST-B* respectively. These stations have a ring-access unit specially designed for packet-switched traffic and are therefore designated *PRAU*. Let us assume that *US-A* is the initiator of the connection and that *US-B* is not engaged; this means that *PRAU-B* constantly monitors the first insertion subring, which is used for sending call messages.

When *US-A* wants a connection, he sends a request for it, including the address of *US-B*, over the VMEbus to *PRAU-A*. The latter places a call for *US-B* on the first insertion subring by means of the swap operation. This call also contains the address of *US-A*. In response, *PRAU-B* performs two actions. He places a call for *US-A* on the same insertion subring to indicate that he is ready to receive information, and he informs *US-B* that a message is about to be received. When the call for *US-A* by *PRAU-A* has been received, *US-A* is requested, via the VMEbus, to fill the packet buffer of *ST-A* with a packet. *US-A* does this and at the same time indicates how large the packet is and also whether it is the last packet of this message.

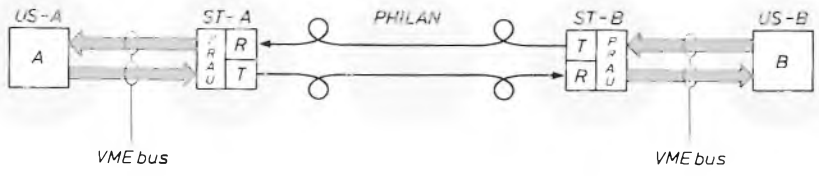

Fig. 9. Simplified representation of a packet-switched link between users *US-A* and *US-B*. Between each user and the corresponding station *ST* electrical signals are exchanged via a standardized connection, called a VMEbus. The stations are connected by fibre-optic cables with the rest of the PHILAN system (not further specified here). *PRAU* ring access unit for packet-switched traffic. *R* optical receiver. *T* optical transmitter.

PRAU-A then occupies a free traffic subring (channel) by means of a swap on the memory subring in the category with the capacity selected by *PRAU-A*. Next, *PRAU-A* sends a start message to *PRAU-B* via the second insertion subring and at the same time gives information about the channel used, the size of the packet and whether it is the last packet or not. *PRAU-B* then switches to reception on the relevant channel, waits for the arrival of the packet and writes it into his packet buffer. *PRAU-B* then places the number of the used channel into the memory subring by means of a swap operation to indicate that the channel is free again. In addition an

[6] *Read-out* alone does not affect the signal circulating on the ring; this only happens when new information is *written to* certain bit positions (possibly as part of a swap operation).

[7] A number of manufacturers in the computer field (in particular Motorola, Mostek and Signetics/Philips) have defined a collective standard for communication links in applications of 8-bit, 16-bit and 32-bit microprocessors. It is called the 'VMEbus', but is now also referred to as the 'IEC 821 bus' or the 'IEEE P1014'. The abbreviation VME stands for 'Versa Module Europe', but the full name has now no more than historical interest. An organization called VITA (VMEbus International Trade Association) has been set up to disseminate information on the VMEbus. It has its own journal, 'VMEbus Systems', published by Intratech Communications, St Clair Shores, Michigan 48081, U.S.A.

error-detection procedure is carried out to check whether the packet has been correctly received and, if this is so, the packet is made available to *US-B* via the VMEbus. Finally, confirmation of this and a request for the next packet are sent by *PRAU-B* to *PRAU-A* via the second insertion subring. *PRAU-A* then requests *US-A* for the next packet, again occupies a free channel, and so on.

If *PRAU-B* discovers that a particular packet has not been correctly received, he immediately sends a message back to *PRAU-A* via the second insertion subring with a request for the relevant packet to be retransmitted. This is done as soon as a free channel has been found. This entire procedure is repeated for as long as is necessary for all packets of a particular message to be sent correctly from *US-A* to *US-B*. The connection between *US-A* and *US-B* is cancelled as soon as *PRAU-A* has received confirmation that *PRAU-B* has received the last packet of the message correctly.

The actual procedure differs in one particular respect from what has been suggested so far: each *PRAU* does not have only one packet buffer; it has two — equivalent — packet buffers of 64 kbits each. While *US-A* fills one packet buffer of *PRAU-A*, the contents of the other packet buffer of *PRAU-A* are sent to one of the packet buffers of *PRAU-B*, and at the same time the other packet buffer of *PRAU-B* is emptied by *US-B*. If the transmission procedure takes place at the maximum rate, packets of the same message are handled simultaneously at three places in the PHILAN system: on the actual ring and on the two VMEbuses of *A* and *B*. In this way messages of any given length can be transmitted from *A* to *B* at a maximum rate of about 4 Mbit/s.

The component units of PHILAN

The stations

As we have seen (fig. 5), a station can be divided into a receiver/transmitter combination *R/T* and a ring-access unit *RAU*. The two main tasks of *R/T* are to perform the opto-electrical and the electro-optical conversions of the digital signals circulating in the PHILAN ring. A more detailed block diagram of *R/T* is given in *fig. 10*. Whereas the electrical signals between *R/T* and *RAU* take the form of a simple bit stream (with no encoding), an elementary form of encoding (biphase coding [8]) has been adopted, for various technical reasons connected with transmission [9], for the digital signals to be transmitted by optical fibre (*fig. 11*). The transmitter has therefore been provided with an encoder and the receiver with a special receive filter, a clock-recovery circuit and a decoder.

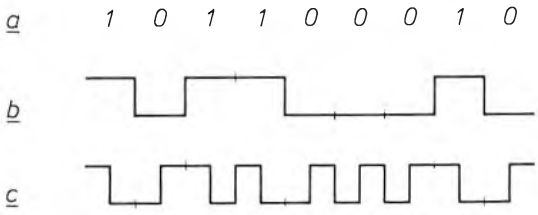

Fig. 11. *a*) Arbitrary bit stream consisting of ones and zeros. *b*) Corresponding 'uncoded' binary signal; a '1' is represented by a high level and an '0' by a low level. *c*) The same bit stream after biphase encoding. A '1' is now represented by a sequence of a high level and a low level, an '0' by the reverse. This encoding gives a transmission signal with a better frequency spectrum, and the required clock signal is easier to recover at the receiver end.

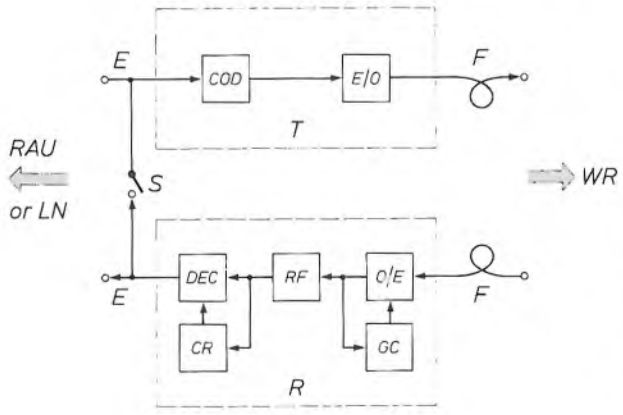

Fig. 10. Optical receiver/transmitter combination *R/T* used in each station (and also in each meander gate) of the PHILAN system. *E* electrical connection. *F* fibre-optic cable. *COD* biphase encoder. *E/O* electro-optical converter. *O/E* opto-electrical converter for the signal coming from the fibre-optic cable. *GC* gain control for the electrical signal. *RF* receive filter. *DEC* biphase decoder. *CR* clock recovery. *S* electrical bypass switch. *WR* wall receptacle. *RAU* ring-access unit. *LN* local nucleus.

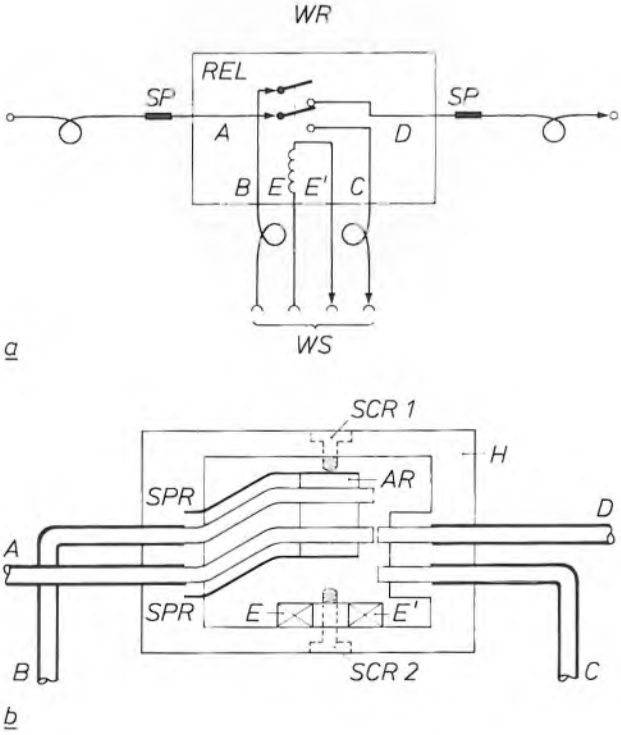

Fig. 12. *a*) Basic diagram of the wall receptacle *WR*. Two optical splices *SP* are used to include *WR* permanently in the meander ring. A station *ST* can be connected by means of a wall socket *WS*, which contains two optical contacts and two electrical contacts. The heart of *WR* is a relay *REL* which controls two optical switch contacts. *b*) Cross-section through the relay *REL*. *A*, *B*, *C*, *D* optical fibres. *SPR* leaf springs. *E*, *E'* connections for the relay coil. *SCR1*, *SCR2* set screws. *AR* armature. *H* housing [11].

There are two versions of the ring-access unit, each built around a standard microprocessor (type '68000'): a CRAU for circuit-switched traffic and a PRAU for packet-switched traffic. At the user end a CRAU has a connection (in both directions) of 2.048 Mbit/s. This gives the user access to 32 channels on the PHILAN ring, each with a capacity of 64 kbit/s, or to one or more combinations of a number of these channels.

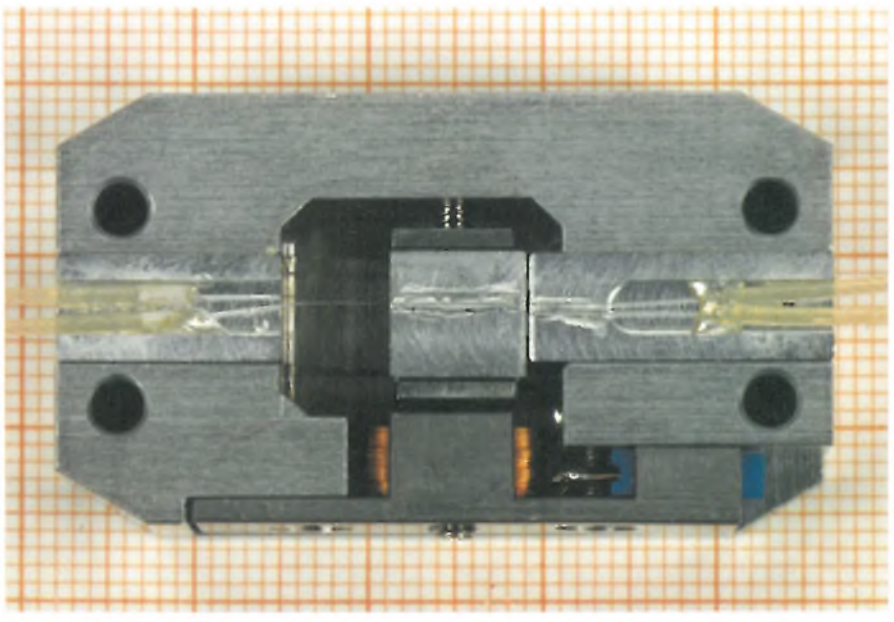

Fig. 13. Photograph of the interior of the relay *REL* in fig. 12. The optical fibres are bonded by adhesive into V-grooves, which are made in a single operation in both the housing and the armature during manufacture. This means that there is no need for extremely tight tolerances. Set-screws on either side determine the two extreme positions of the armature. The two leaf springs that attach the armature to the housing are hardly visible in this photograph.

Signalling information between a user and a CRAU is exchanged via a VMEbus [7].

The VMEbus is also used with the PRAU for exchanging the actual packets and the related messages between user and station. As already mentioned, packets can be sent over the PHILAN ring at different rates, from 64 to 4096 kbit/s. The maximum packet length is always 64 kbits (8 kbytes); longer messages have to be sent in more than one packet. Each PRAU possesses hardware for error detection after the reception of each packet. This is done by means of the Cyclic Redundancy Code (CRC) [10].

The wall receptacles

In PHILAN the optical wall receptacles occupy a place of their own. Their first task is to make it possible to modify the number of PHILAN connections in a simple and reliable way. In addition they must be capable of forming an optical 'bypass' and, in spite of the critical mechanical requirements found here, they must be an economic proposition. The answer to this problem has been found in the use of a specially developed optical relay capable of switching fibre-optic cables. The basic diagram of the wall receptacle is shown in *fig. 12a*, a cross-section of the relay used in it is given in fig. 12*b*, and a photograph of the relay is shown in *fig. 13*. When the coil of the relay is not energized (e.g. when there is no plug in the socket) the relay forms an optical through-connection; otherwise the optical signals go via the connected plug (*fig. 14*). The nominal attenuation in the relay is only 0.7 dB.

The meander gates

The three main functions of the meander gates were touched upon earlier in this article (see fig. 5):

• Using the same type of receiver/transmitter combination R/T found in each station, an opto-electrical connection and an electro-optical connection are

[8] See for example p. 348 in the special issue: F. W. de Vrijer, Modulation, Philips Tech. Rev. **36**, 305-362, 1976;
see also: P. J. van Gerwen and W. A. M. Snijders, Communication system for bi-phase transmission of data and having sinusoidal low-pass frequency response, U.S. Patent No. 4 573 169 (25th February 1986).

[9] Such as measures to deal with the large spread (by a factor of 1000) in the strength of the received optical signal, to facilitate clock generation in the receiver and to optimize the signal-to-noise ratio after reception.

[10] See p. 129 in: A. S. Tanenbaum, Computer networks, Prentice-Hall, Englewood Cliffs, NJ, 1981.

[11] W. A. M. Snijders and J. P. Klomp, Optical switch, European patent application No. 0181657-A1 (21st May 1986).

established between the local nucleus and the individual meanders.

- In appropriate cases the *EBS* switch can be used to 'cut off' a particular meander.
- Any jitter produced in the meander is eliminated.

In addition the synchronization pattern (preamble) at the beginning of each frame is regenerated.

To enable the electronic bypass *EBS* to be switched on and off without interfering with the rest of the PHILAN system (e.g. with the synchronization), the signal delay between input and output of the meander gate must be the same before and after switching. Special measures are taken to ensure that this delay always amounts to 256 bits.

In addition, when *EBS* comes into operation, the meander gate has to take a number of extra measures to guarantee the 'safe-message service' of PHILAN. This service is based on operation with echoes (page 17) and in certain circumstances these echoes can give rise to erroneous conclusions, since a correct echo will *not* have passed through an operational station in any cut-off meander.

Finally, each meander gate also monitors the synchronization of all the stations in the corresponding meander and takes special measures to restore the synchronization if this is lost.

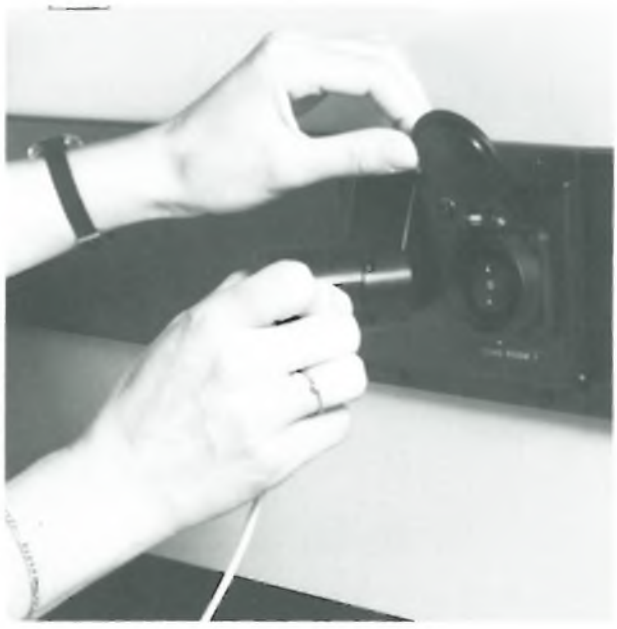

Fig. 14. Wall socket and plug for the PHILAN meander ring. This provides a reliable and easily detachable double optical and double electrical connection (see fig. 12*a*) [12].

The central unit

The central unit *CU* of PHILAN (fig. 3) functions as a 'ring management system'. In its simplest version it contains a monitor and two channel controllers for circuit-switched and packet-switched traffic, respectively (*fig. 15*).

The main tasks of the monitor are the generation and monitoring of the correct frame structure of the PHILAN signal, and to make up the delay experienced by the signal in one lap of the meander ring to an integral number of frame periods.

The channel controllers are responsible for recording free channels and making them available as required.

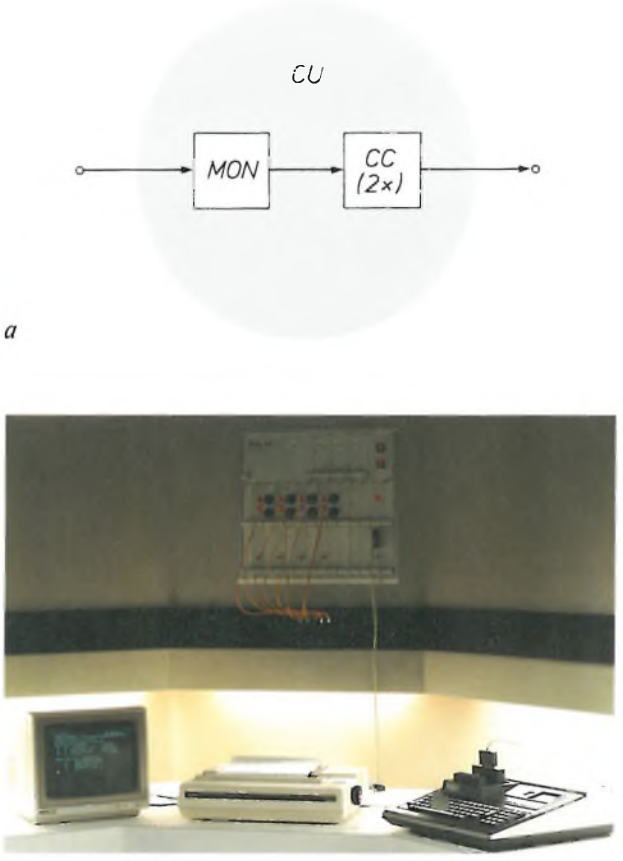

a

b

Fig. 15. *a*) In its simplest form the central unit *CU* in PHILAN consists of a monitor *MON*, which monitors the signal structure, and two channel controllers *CC*. If required, other equipment can be added for error diagnosis, management and direct control by an operator. *b*) Photograph of the extended central unit used in the demonstration system at the Project Centre. The specific PHILAN circuits are contained in a wall rack (top centre). Below it can be seen, from left to right, a display screen, a printer and a P2000 computer, with a keyboard and a cassette deck. These are used as the input and output peripherals for the operator. (See also fig. 1.)

[12] J. W. Faber and J. P. Klomp, Optical connector device, European patent application No. 0189609-A1 (6th August 1986).

Possible extensions

So far we have confined the description of PHILAN to the basic configuration; there are, however, a number of important extensions that can be made. Two of these will be mentioned briefly to conclude this article. In the first place it is possible in principle to connect the central units of several PHILAN systems with each other so as to form larger transmission networks. In the second place, specially developed hardware can be added to the central unit, the meander gates and the stations to increase the diagnostic and control capabilities of the system, enabling the system to make regular fully automatic checks on the functioning of all meander gates and stations. One such check is the measurement of the optical transmitting power of each station. All information about the state of the network is recorded in the central unit and can be displayed on a screen or communicated to an operator by means of alarm signals. Conversely, the operator using the keyboard can give instructions to the central unit to carry out specific tasks.

By making the appropriate additions to the PHILAN basic configuration the optimum local-area network can thus be created for practically any situation.

Summary. PHILAN is an integrated local-area network in which digital information is transmitted at a bit rate of about 20 Mbit/s in time-divison multiplex. The system has a ring network structure, with sections called meanders that can be cut off in the event of local malfunctioning. The transmission medium used in the meanders is fibre-optic cable. Both circuit-switched and packet-switched traffic can be handled simultaneously in the PHILAN system. For packet-switched traffic the use of specific protocols gives practically 100% reliability ('safe-message service'). Connections to the meanders are made via wall receptacles, in which a double optical plug connection is established. Each wall receptacle contains a specially developed relay for electromechanical switching of two fibre-optic cables. In addition to a relatively simple basic configuration, there are more elaborate versions of the PHILAN system with sophisticated provisions for error diagnosis and control. At the Philips Research Laboratories Project Centre a PHILAN trial system has been built for demonstration purposes.

Investigation of a new type of rechargeable battery, the nickel-hydride cell

J. J. G. Willems

The author describes the research work on a new type of rechargeable battery, which has resulted in a hermetically sealed nickel-hydride cell. The new cell has stable electrode material and an effective control of the hydrogen and oxygen flow in the system. These features have enabled a first experimental version to operate well for more than a thousand cycles of high-rate charge and discharge.

Brief historical background

The first galvanic cell — or more accurately 'battery' of galvanic cells — was Alessandro Volta's pile (the 'voltaic pile') of 1800, which consisted of a stack of sheets of zinc and silver (or copper), separated from each other by pieces of cardboard soaked in a saline solution (*fig. 1*) [1]. As became clear much later, the electrical energy from each individual cell is due to the oxidation of the zinc to form zinc ions, with the release of electrons:

$$Zn \rightarrow Zn^{2+} + 2e^-, \qquad (1)$$

and to the reduction of water to gaseous H_2, with the uptake of electrons:

$$2H_2O + 2e^- \rightarrow H_2 + 2OH^-. \qquad (2)$$

Why these particular materials fulfil these functions can be explained by their relative position in the electrochemical series of the elements (*fig. 2*). This thermodynamically determined position in the series is not the only significant factor, however: it is also necessary to take the kinetics of the process into account.

The silver (or copper) is not used up in the voltaic cell, but acts as a catalyst in the reduction of the water; its only other function is that of a conductor of current (*fig. 3*). Zinc is still used as the material for negative electrodes, for example in dry batteries, because of its negative electrode potential, but the use of water (zero electrode potential in fig. 2) as the oxidizer at the positive electrode has remained confined to this first galvanic cell: the electromotive force (e.m.f.) available from this element is only 0.5 V.

In 1836 John Daniell developed a galvanic cell in which copper ions from a copper-sulphate solution are reduced at a positive copper electrode to metallic copper for the required electron transfer:

$$Cu^{2+} + 2e^- \rightarrow Cu. \qquad (3)$$

The negative electrode consisted of a rod of amalgamated zinc, which was immersed in dilute sulphuric acid. The amalgamation prevents an excessive side

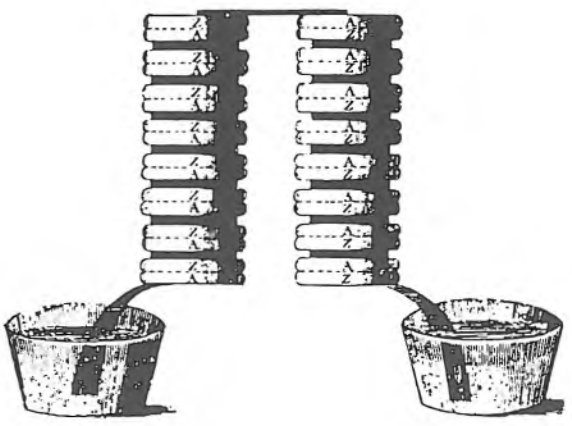

Fig. 1. The voltaic pile, as illustrated in the first publication (in Phil. Trans. R. Soc. 90, 403, 1800) [1]. *A* stands for silver (argent) and *Z* for zinc.

Dr Ir J. J. G. Willems, now with the Lighting Division, Philips NPB, was formerly with Philips Research Laboratories, Eindhoven.

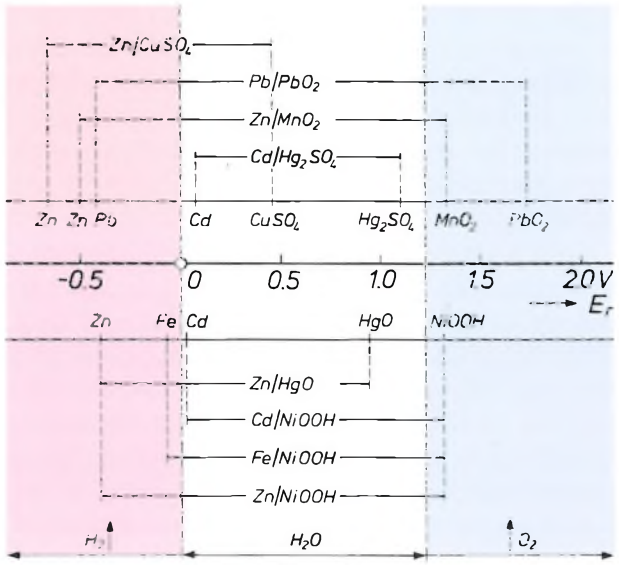

Fig. 2. The electrode potential E_r of some of the more familiar electrode materials (combined with an electrolyte), determined with respect to the potential of a reversible hydrogen electrode in the same electrolyte. Oxidation potential increases from left to right (from non-noble to noble in the electrochemical series of the elements). If the electrode potential is lower than 0 V (the electrode potential of the voltaic couple water/hydrogen), the electrode material tends to reduce H_2O to H_2 (the red region); if the electrode potential is higher than +1.23 V (the electrode potential of the couple water/oxygen), the material then tends to oxidize H_2O to O_2 (the blue region). Only in the Weston cell (Cd/Hg_2SO_4) do both electrode couples show no tendency to decompose water. The electrode potentials of materials used in combination with an acid or neutral electrolyte are shown above the horizontal axis; the potential values of materials used in an alkaline medium are shown below the horizontal axis.

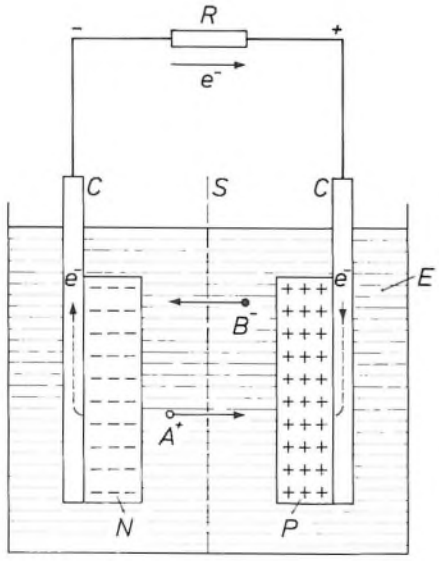

Fig. 3. Diagram of a current-producing galvanic cell. *P* active positive electrode material. *N* active negative electrode material. *e* electrons. *E* electrolyte. A^+ positive ions. B^- negative ions. *C* current collectors. *S* separator. *R* external load.

reaction between the zinc and the sulphuric acid. Even with the cell not working, hydrogen would otherwise have been liberated and the zinc would have been used up. (This process is equally detrimental to the operation of the voltaic pile.) To prevent copper ions from being deposited on the zinc — this happens because of their position in the electrochemical series — the two electrodes are contained in separate compartments, each with its own electrolyte. A porous diaphragm, originally of cow's gullet, permitted the necessary transfer of ions between the electrodes.

The first rechargeable battery, Gaston Planté's lead-acid cell, dates from 1860. It consisted of two interwound lead sheets separated by flannel strips and immersed in sulphuric acid. The electrodes were formed by repeated charging from primary cells. (Current generators like the dynamo had already been invented, but they were not yet widely used.)

The development of dry cells also dates from the same period, about 1865. In the dry cell the oxidizing substance is a solid (a metal oxide) and the electrolyte is effectively 'immobilized', so that the battery can be made 'leakproof'. Georges Leclanché used a mixture of manganese dioxide and carbon for the positive electrode, and a carbon rod inserted into the mixture was the current conductor. The electrolyte consisted originally of a saturated solution of ammonium chloride; in a later development this was thickened (immobilized) by means of starch or lime, or both. Amalgamated zinc, which was then coming into use for the manufacture of batteries, again served for the negative electrode. Today, more than a century later, the Leclanché cell is still the most widely used dry battery.

Apart from their use as a current source, batteries were soon required to meet the need for a constant-voltage reference source. These 'standard cells' operate in phase equilibrium; when they are being used it is only the position of the equilibrium that changes, though only very slightly. The nature of the substances reacting in the cell does not change. In the Weston cell (1892) the positive mercury/mercurous-sulphate electrode and the negative cadmium amalgam/cadmium-sulphate electrode are immersed in a saturated solution of crystals of these salts. The e.m.f.

[1] Further historical data will be found in:
G. W. Vinal, Primary batteries, Wiley, New York 1950, see especially the first chapter, pp. 1-24;
G. W. Heise and N. C. Cahoon, The primary battery, Vol. 1, Wiley, New York 1971, first chapter, pp. 1-58;
S. U. Falk and A. J. Salkind, Alkaline storage batteries, Wiley, New York 1969, first chapter, pp. 1-41.
For the general principles of the battery discussed here, see for example:
V. S. Bagotskii and A. M. Skundin, Chemical power sources, Academic Press, New York 1980;
J. O'M. Bockriss *et al.* (eds), Comprehensive treatise of electrochemistry, Vol. 3, Plenum, New York 1981.

of the Weston cell is 1.01463 V at 25 °C and its variation with temperature is only -4.05×10^{-5} V/°C.

A major objective in the development of batteries was, and still is, to make the most efficient use of the relatively expensive electrode materials, and this is most easily done with rechargeable batteries. To start with such batteries will be required to have no spontaneous side-reactions that give an unproductive loss of active material, in other words minimum 'self-discharge'. This requirement led to the development of alkaline accumulators at about the turn of the century. These included the nickel-cadmium cell and the nickel-iron cell (Junger and Edison). Alkaline reagents are in general less reactive with metals and metal oxides than acids.

It is difficult to avoid such non-productive side reactions completely, since most electrode materials are not thermodynamically stable in combination with aqueous electrolytes and are thus always inclined to react with water with the formation of hydrogen or oxygen, depending on the value of the electrode potential. As can be seen in fig. 2, it is only for the pair of electrodes in the Weston cell that the position of the electrode potentials is such that no spontaneous decomposition of water can take place. A possible way around this difficulty would be to use non-aqueous electrolytes, but the usual practice has been to manage with electrodes that, although not thermodynamically stable, are sufficiently stable kinetically. In other words, the electrode materials are chosen or treated in such a way (for example by amalgamation) that their rate of reaction with the electrolyte is very slow.

The extent to which unwanted amounts of hydrogen or oxygen are nevertheless produced then often depends on the state of charge of the battery and on the charging rate. This is because the battery can only be fully charged if the charging voltage is *greater* than the cell e.m.f., which implies moving further into the unstable region (fig. 2). The charging voltage will have to be higher the faster the battery is to be charged. Overcharging the battery, which is usually unavoidable because it is impossible to know exactly when the battery is fully charged, also causes the formation of hydrogen and oxygen. The same applies to over*dis*charge, which may be the consequence of differences in capacity between the series-connected cells of a battery. Here a cell that has discharged first can be forced by adjacent cells to discharge itself still further, a process inevitably accompanied by the formation of hydrogen and oxygen.

This problem of unwanted gas generation becomes particularly serious when it is intended to produce a completely sealed rechargeable battery, one that can be used in all positions and without requiring maintenance, preferably for many years. The dry battery may be seen as an early answer to this problem, without however achieving the goal of rechargeability. Moreover, as pre-war users will have found to their displeasure, the 'leakproof' dry battery was by no means the same thing as the hermetically sealed battery now in view.

Good results in this respect have now been achieved with nickel-cadmium cells. Since 1950 these cells have been provided with an excess of cadmium hydroxide, $Cd(OH)_2$, at both electrodes (*fig. 4*). In overcharging and overdischarging the current tries to find a path, oxidizing or reducing materials with the appropriate characteristics, and this can give a high gas pressure in a sealed cell. The excess of $Cd(OH)_2$ 'channels' any such unwanted current so that it causes no damage, or very little.

If on overcharging the nickel electrode starts to form oxygen, the cadmium electrode will still not be

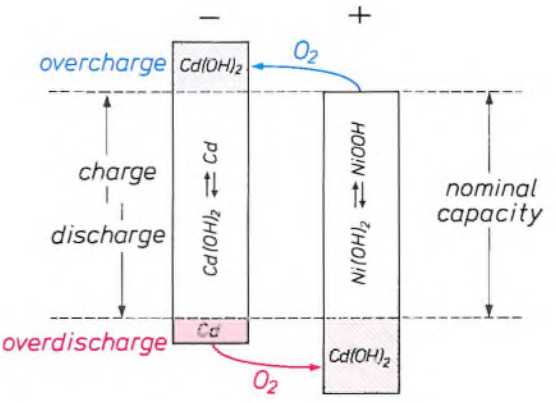

Fig. 4. Diagram illustrating the protection from overcharging and overdischarging in a sealed cadmium battery, introduced in about 1950. Adding $Cd(OH)_2$ to both electrodes introduces an oxygen cycle during both overcharging (blue region) and overdischarging (red region). The added $Cd(OH)_2$ is indicated by hatching. An excess of cadmium (red) is also added at the cadmium electrode; this is explained on p. 32.

fully charged because of the excess of $Cd(OH)_2$. It will therefore not generate hydrogen (fig. 2) and continue to convert $Cd(OH)_2$ into metallic Cd. This conversion, however, is now no longer used for the process of energy storage but for reducing the oxygen formed at the nickel electrode and retaining it as $Cd(OH)_2$. So from that stage onwards there is no change in the state of charge of the two electrodes (since the nickel electrode was already fully charged).

In over*dis*charging the electrodes change roles as compared with the roles they took in overcharging. Because of the addition of $Cd(OH)_2$ to the nickel elec-

trode, this electrode in the empty state will take on the potential of the cadmium electrode, and so will again be able to counteract the evolution of hydrogen. The oxygen produced at the empty cadmium electrode in overdischarging is reduced in a similar reaction cycle at the nickel electrode. It could be said that there was a deliberately engineered 'chemical bypass', which channels both forms of an unwanted passage of current via an oxygen cycle.

As mentioned, because of the position of its electrode potential, the excess of $Cd(OH)_2$ is in principle capable of *preventing the evolution of hydrogen gas* (both upon overcharging at the cadmium electrode and overdischarging at the nickel electrode). This is therefore important because the evolution of hydrogen is a much greater problem than that of oxygen, since hydrogen gas once formed is *not* converted at the nickel electrode owing to kinetic impediments, and consequently a channelling comparable with the oxygen cycle is not possible.

Even though $Cd(OH)_2$ can be introduced into the battery as explained, the evolution of hydrogen can never be completely eliminated. Some hydrogen may form because of the ageing of $Cd(OH)_2$, particularly during charging at high currents and on overdischarging. Hermetically sealed NiCd cells are therefore always provided with a safety valve that opens if too much hydrogen gas accumulates.

For some time now a similar expedient has been used in the lead-acid accumulator so that it can also be produced as a hermetically sealed battery. The greater reactivity of the acid electrolyte makes it even more difficult in this case to prevent the accumulation of gas, which requires at the very least a specially adapted cell construction, at the expense of durability.

The investigations at Philips Research Laboratories that will now be described should be viewed against this background of efforts to achieve a hermetically sealed rechargeable battery that can be used in all positions, has a very long service life, can be charged and discharged at a very high rate and can withstand considerable overcharging and overdischarging.

Initial study of $LaNi_5$ and $LaNi_4Cu$ as electrode material

In this section we shall be considering the use of hydrogen as 'fuel' for a rechargeable battery, and not as the product of an unwanted side reaction, as it so often was in the previous section. This implies that it must be possible to oxidize hydrogen at the surface of an electrode while the battery is being discharged, and that hydrogen can be stored in this electrode while the battery is being charged. Our investigations at Philips Research Laboratories of materials for such an electrode were mainly made with $LaNi_5$ and related compounds. Water from an aqueous electrolyte can be reduced electrochemically at these materials, the hydrogen evolved can be stored as a hydride and the stored hydrogen can then be reoxidized to form water:

$$LaNi_5 + 6H_2O + 6e^- \underset{\text{discharge}}{\overset{\text{charge}}{\rightleftarrows}} LaNi_5H_6 + 6OH^-. \quad (4)$$

The formation of hydrogen in this case is therefore, once again, not an unwanted side reaction but part of the chemical system responsible for the storage of energy. $LaNi_5H_6$ can be used here as the active material of the *negative* electrode, which is converted into $LaNi_5$ during the discharge; the $LaNi_5H_6$ is then reformed by the charging. The metal hydride may be compared in this respect with the cadmium at the negative pole of the NiCd cell:

$$Cd(OH)_2 + 2e^- \underset{\text{discharge}}{\overset{\text{charge}}{\rightleftarrows}} Cd + 2OH^-. \quad (5)$$

If we compare the electrode reactions of $LaNi_5$ with those in Volta's cell — since water is converted in both — we see, however, that the reactions in the voltaic pile have exactly the opposite function. In the voltaic pile water is converted into hydrogen, and electrons are taken up, during discharge at the positive pole, whereas with $LaNi_5$ this occurs during charging at the negative pole (and then the conversion in the opposite direction on discharge results in the production of electrons).

Reactions of this kind are also used with the familiar reversible hydrogen electrode, with platinum as the electrode material. The difference compared with $LaNi_5$ in this case is that the hydrogen gas has to be supplied, since hydrogen is not absorbed by platinum. An electrode of this type cannot therefore be used for the storage of electrical energy.

About fifteen years ago it was discovered that intermetallic compounds such as $LaNi_5$ and TiFe are capable of absorbing large amounts of hydrogen gas and of desorbing it at pressures of the order of 1 atmosphere and at room temperature [2]. *Fig. 5* shows the absorption and desorption isotherms of the $LaNi_5$-H_2

[2] Publications on hydrogen-absorbing compounds discovered in the past 15 years include:
H. Zijlstra and F. F. Westendorp, Solid State Commun. **7**, 857-859, 1969;
J. H. N. van Vucht, F. A. Kuijpers and H. C. A. M. Bruning, Philips Res. Rep. **25**, 133-140, 1970;
J. J. Reilly and R. H. Wiswall Jr., Inorg. Chem. **13**, 218-222, 1974;
F. A. Kuijpers, Philips Res. Rep. Suppl. 1973, No. 2;
H. H. van Mal, Philips Res. Rep. Suppl. 1976, No. 1;
K. H. J. Buschow, P. C. P. Bouten and A. R. Miedema, Rep. Prog. Phys. **45**, 937-1039, 1982.

system at a number of temperatures [3]. As the figure illustrates, in a temperature range up to about 80 °C the system has a phase transition between a hydrogen-poor phase and a hydrogen-rich phase at a constant equilibrium pressure, called the plateau pressure. At room temperature $LaNi_5$ absorbs six hydrogen atoms at a plateau pressure of 2 atmospheres, and at a pressure of 1.6 atm the hydride formed is converted back to $LaNi_5$, accompanied by the desorption of hydrogen gas. The amount of hydrogen that can be absorbed and desorbed in this way per unit volume is enormous: 40% greater than the hydrogen density in liquid hydrogen at 20 K. Even at a temperature of 80 °C large amounts of hydrogen gas can still be reversibly stored in $LaNi_5$ at a pressure of less than 20 atmospheres. The resultant absorption-desorption hysteresis, which is greater at higher plateau pressures and gives an energy loss, is of course an unwanted effect. Compared with TiFe, $LaNi_5$ has lower plateau pressures at the same temperatures and a much lower absorption-desorption hysteresis.

On repeated absorption and desorption of hydrogen gas, $LaNi_5$ disintegrates into small fragments (*fig. 6*), forming a fine powder with a specific surface area of 0.25 m^2/g. The powder has a high catalytic activity, which, combined with the high diffusion coefficient for H atoms in the metal lattice, results in high sorption rates. At 20 °C complete hydrogen desorption takes no more than a few minutes. In addition, $LaNi_5$ and $LaNi_5H_6$ are both good electrical conductors. All in all, $LaNi_5$ therefore seems to be a promising electrode material for a rechargeable battery.

How does $LaNi_5$ behave in the presence of the electrolyte, however? To find this out we carried out a number of experiments with this material and related compounds in a 'half-cell' arrangement. The materials, which are very hard and brittle, were pulverized by repeated hydrogen gas absorption/desorption cycles, and then mixed with powdered copper. This mixture was cold-pressed to form a porous pellet, which was found to satisfy all electrode requirements [3]. The electrolyte used in the cell was a 6 M KOH solution, a platinum plate was used as the counter-electrode and an Hg/HgO/6 M KOH electrode was used as the reference electrode (*fig. 7*) [3]. *Fig. 8* shows a charge and discharge curve for an $LaNi_5$ electrode as measured in this cell. As can be seen, there is close correspondence with the absorption and desorption curves in fig. 5. Starting from the fact that the absorption of one hydrogen atom is associated with the transfer of one electron (eq. 4), it can be shown that the theoretical charge-storage capacity for the composition $LaNi_5H_6$ is 372 mAh/g, which is slightly more than the theoretical storage capacity for a cadmium electrode (366 mAh/g). This is important because our aim was to be able to use the $LaNi_5$ elec-

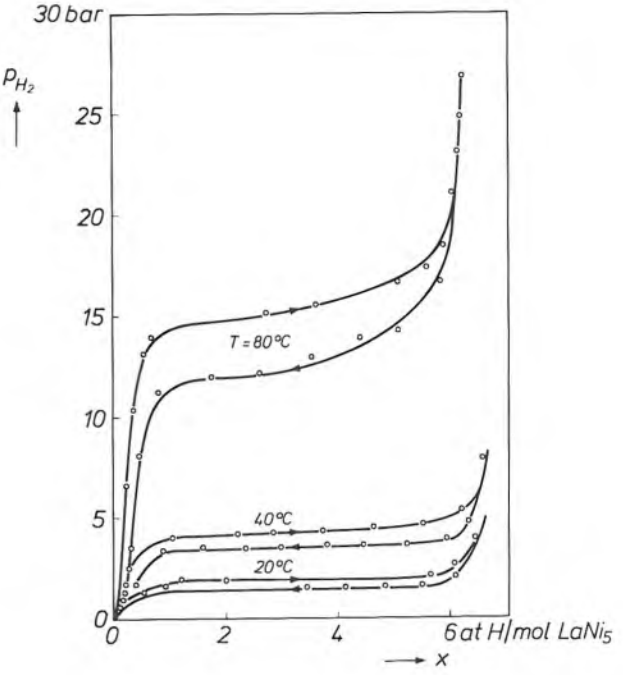

Fig. 5. Absorption and desorption isotherms (hydrogen pressure p_{H_2} as function of the concentration of hydrogen atoms x) of the $LaNi_5$-H_2 system at 20, 40 and 80 °C.

Fig. 6. If $LaNi_5$ is made to absorb and desorb hydrogen repeatedly, it gradually disintegrates into small fragments, seen here in a small heap under the piece of metal gauze acting as a sieve. (This is the effect of a single absorption of hydrogen by an $LaNi_5$ casting.)

trode as an alternative to the cadmium electrode in a nickel-cadmium battery, for reasons that will appear shortly.

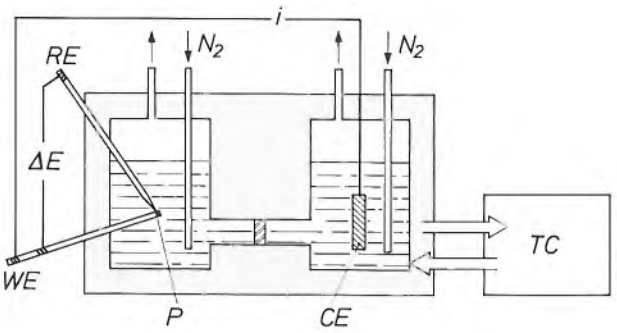

Fig. 7. Diagram of the experimental arrangement used for many of the 'half-cell' electrochemical measurements. *WE* working electrode; a porous pellet *P* of the active material being investigated, e.g. $LaNi_5$, is attached to its tip. *RE* reference electrode, usually an Hg/HgO/6 M KOH electrode. *CE* platinum counter-electrode. The electrolyte is kept free from oxygen by purging with nitrogen. The half-cells have a water-jacket and are kept at a temperature of 25 °C by a thermostat *TC*.

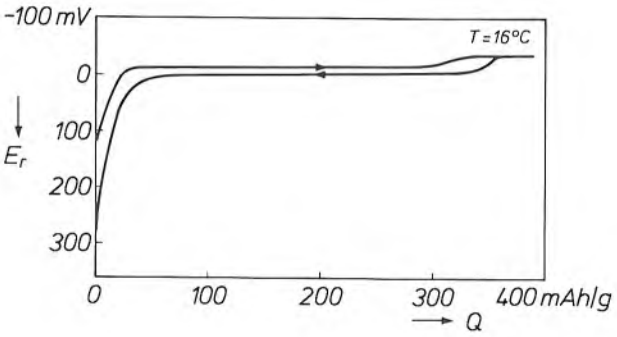

Fig. 8. Charge and discharge curve for an $LaNi_5$ electrode, with respect to the reversible hydrogen electrode, as a function of the charge *Q*, measured in 6 M KOH at 16 °C.

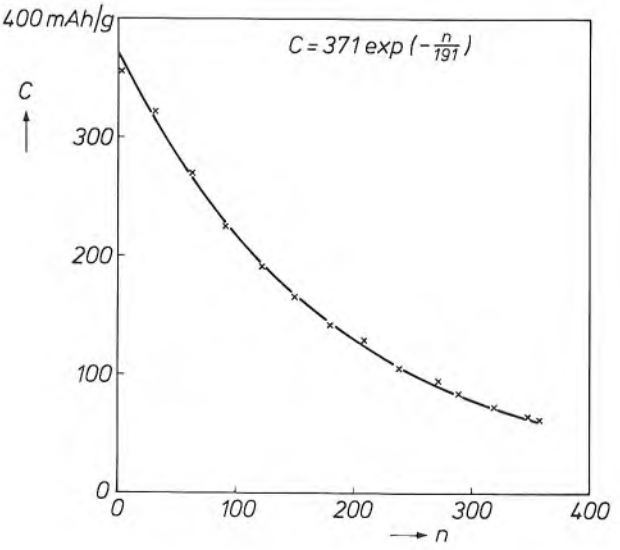

Fig. 9. Storage capacity *C* of an $LaNi_5$ electrode as a function of the number of charge/discharge cycles (*n*).

Although $LaNi_5$ has these desirable properties, it has one major disadvantage. The electrochemical experiments discussed soon revealed that the storage capacity of $LaNi_5$ electrodes decreases drastically after repeated charging and discharging. As can be seen in *fig. 9*, the storage capacity then decreases exponentially — by as much as 40% after only 100 cycles. This rules out $LaNi_5$ as an electrode material for rechargeable batteries — at least if it is to meet the strict requirements formulated in the previous section.

In our investigation we therefore set ourselves the primary goal of establishing the cause of this drastic decrease in storage capacity. We included in our investigations the compound $LaNi_4Cu$, which had been investigated previously at our Laboratories. This material also absorbs large amounts of hydrogen, but it does so at a lower plateau pressure more suitable for practical purposes, and gives the same exponential decrease in storage capacity on repeated charging and discharging.

This experimental investigation relied mainly on X-ray diffraction analyses and electron microscopy [3], in addition to the electrochemical methods described. *Fig. 10* shows X-ray diffraction diagrams of powdered specimens of $LaNi_5$, $LaNi_4Cu$ and their hydrides, obtained after exposing the specimens to hydrogen gas at 150 atm for 24 hours. Diagrams *a* and *d* give the pattern of a phase consisting of hexagonal crystals (space group P6/mmm). Diagrams *c* and *e* show the same pattern as *a* and *d*, with the difference that all peaks have clearly been shifted to smaller diffraction angles, indicating the same hexagonal structure but with larger lattice spacings, resulting in a volume increase of 20% or more, due to the absorption of hydrogen.

We studied the effect of the periodic absorption and desorption of hydrogen by repeatedly charging and discharging electrodes of $LaNi_5$ and LaNi4 Cu in a solution of 6 M KOH, and then making diffraction diagrams of powders of the electrode material thus treated (*fig. 11*). After a number of charge/discharge cycles a number of small peaks and 'shoulders' start to appear in the diagrams — in addition to the diffraction pattern of the original material and large peaks at 21.7° and 25.3°, which are attributable to the copper powder. The small peaks are due to $La(OH)_3$ and the

[3] A more extensive and detailed description of these investigations will be found in the thesis by J. J. G. Willems, Metal hydride electrodes; stability of $LaNi_5$-related compounds, Philips J. Res. **39**, Suppl. No. 1, 1984.
Major contributions to this research were made by J. R. van Beek and H. C. Donkersloot; see for example:
J. R. van Beek, H. C. Donkersloot and J. J. G. Willems, in B. W. Baxter (ed.), Power Sources, Vol. 10 (Proc. 14th Int. Power Sources Symp., Brighton 1984), Academic Press, London 1985, pp. 317-338.

'shoulders' to free Ni (or to $Ni_{0.8}Cu_{0.2}$). These diffraction peaks become distinctly larger as the number of cycles increases.

The conclusion is that the periodic charging and discharging of the electrode in 6 M KOH assists the conversion of $LaNi_5$ (or $LaNi_4Cu$) in the presence of water into $La(OH)_3$ and Ni (or $Ni_{0.8}Cu_{0.2}$):

$$LaNi_5 + 3\,H_2O \rightarrow La(OH)_3 + 5\,Ni + \tfrac{3}{2}\,H_2, \quad (6)$$

or

$$LaNi_4Cu + 3\,H_2O \rightarrow La(OH)_3 + 5\,Ni_{0.8}Cu_{0.2} + \tfrac{3}{2}\,H_2. \quad (7)$$

Scanning electron microscopy (SEM) gave the following supplementary picture of the degradation process in $LaNi_5$ on periodic electrochemical charging and discharging.

Fig. 12a shows the state of the material in an unused electrode. The cracks that can be seen were produced when the electrode was made, during the pulverization in an H_2 atmosphere (fig. 6). After 12 charge/discharge cycles (fig. 12*b*) the first needles of $La(OH)_3$ appear at the surface, and the number of cracks and tears has been increased. In fig. 12*c*, after 25 cycles, the number of needles is considerably larger, and the grain size has fallen on average by a factor of three. In fig. 12*e* the specimen is completely overgrown with $La(OH)_3$, and in fig. 12*f* (after 359 cycles) the conversion of $LaNi_5$ into $La(OH)_3$ is practically complete.

The 'driving force' for the decomposition of $LaNi_5$ in 6 M KOH is the strong affinity of $LaNi_5$ for water. The gain in Gibbs free energy for this oxidation reaction is 472 kJ/mol of $LaNi_5$ — nearly *four times* the heat of formation of $LaNi_5$.

The actual oxidation reaction will occur at the interface between the metal and the electrolyte. As we have

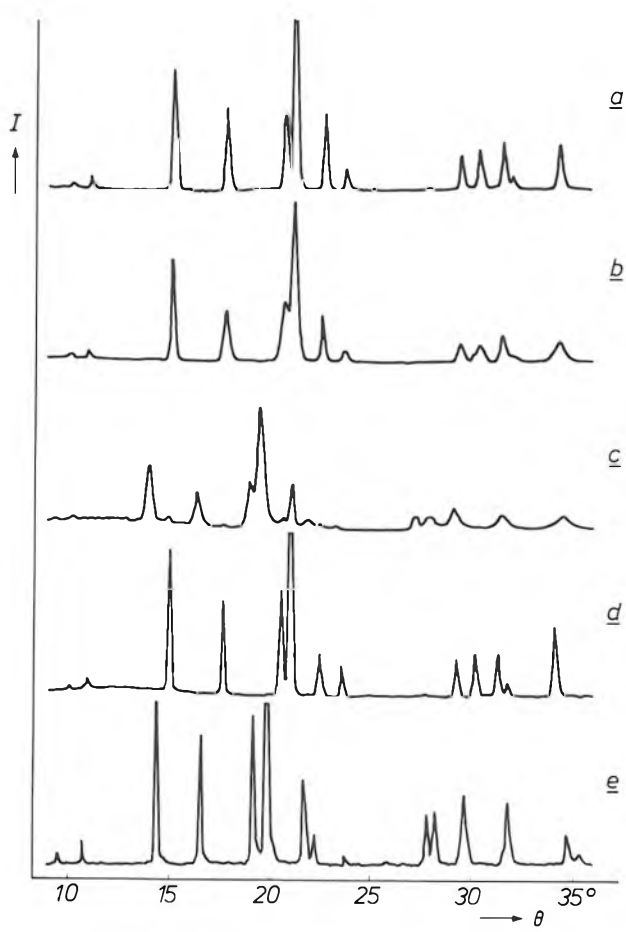

Fig. 10. X-ray diffraction diagrams of powdered specimens of $LaNi_5$ and $LaNi_4Cu$ before and after hydrogen absorption (exposure to hydrogen gas at 150 atm for 24 hours). *a*) Ground $LaNi_5$. *b*) $LaNi_5$ pulverized by 100 cycles of absorption and desorption of hydrogen. *c*) $LaNi_5H_6$, formed by causing the material of (*a*) to take up hydrogen. *d*) Ground $LaNi_4Cu$. *e*) The same material as (*d*) after absorption of hydrogen.

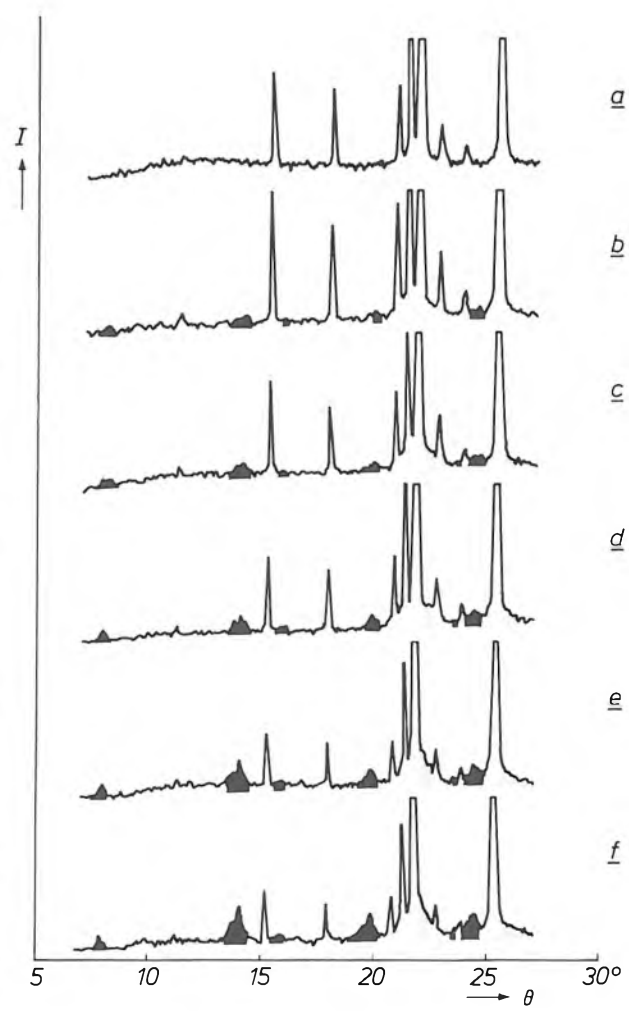

Fig. 11. X-ray diffraction diagrams of dismantled $LaNi_4Cu$ electrodes that have been charged and discharged a number of times in 6 M KOH. The photographs show the effect of zero (*a*), 23 (*b*), 65 (*c*), 87 (*d*), 148 (*e*) and 188 (*f*) charge/discharge cycles. The positions of the reflection peaks due to $La(OH)_3$ are shown in black, and those due to $Ni_{0.8}Cu_{0.2}$ are shown in grey. The large peaks at 21.7 and 25.3° can be attributed to the copper powder added to the electrode material. The other peaks are due to $LaNi_4Cu$.

seen, however, the conversion is not limited to the surface, but is virtually complete. This is remarkable, since the mobility of lanthanum at room temperature in the $LaNi_5$ lattice is virtually zero. Nor is the rate at which this lanthanum is converted into $La(OH)_3$ proportional, as might be expected, to the area of the active *surface*, but rather to the *amount of active material remaining*, i.e. to the amount of stored hydrogen, as is evident from the exponential decay of the storage capacity. This suggests that the decomposition of $LaNi_5$ is connected with the absorption and desorption process.

This led us to the view that the 'respiration' of the lattice might produce a kind of peristaltic movement, which would drive the lanthanum present inside the lattice up to the surface.

The search for a more stable electrode material

From the work of H. H. van Mal, K. H. J. Buschow and F. A. Kuijpers [2] at our Laboratories it was already known that the partial substitution of Co for Ni in $LaNi_5$ had the effect of considerably reducing the increase of volume on hydriding. Altogether we made some twenty intermetallic AB_5 compounds in which La and Ni were partially replaced by other metals. As can be seen in *fig. 13*, the substitution of Co for 3.3 Ni atoms has the strongest effect in the desired direction. The substitution of 1 or 2 atoms has much less effect, and the substitution of 4 or 5 atoms gives rise to widely deviating effects, which are not yet properly understood [3]. Apart from a diminished decrease of capacity on repeated charging and discharging, we see that in all cases the initial capacity is also reduced.

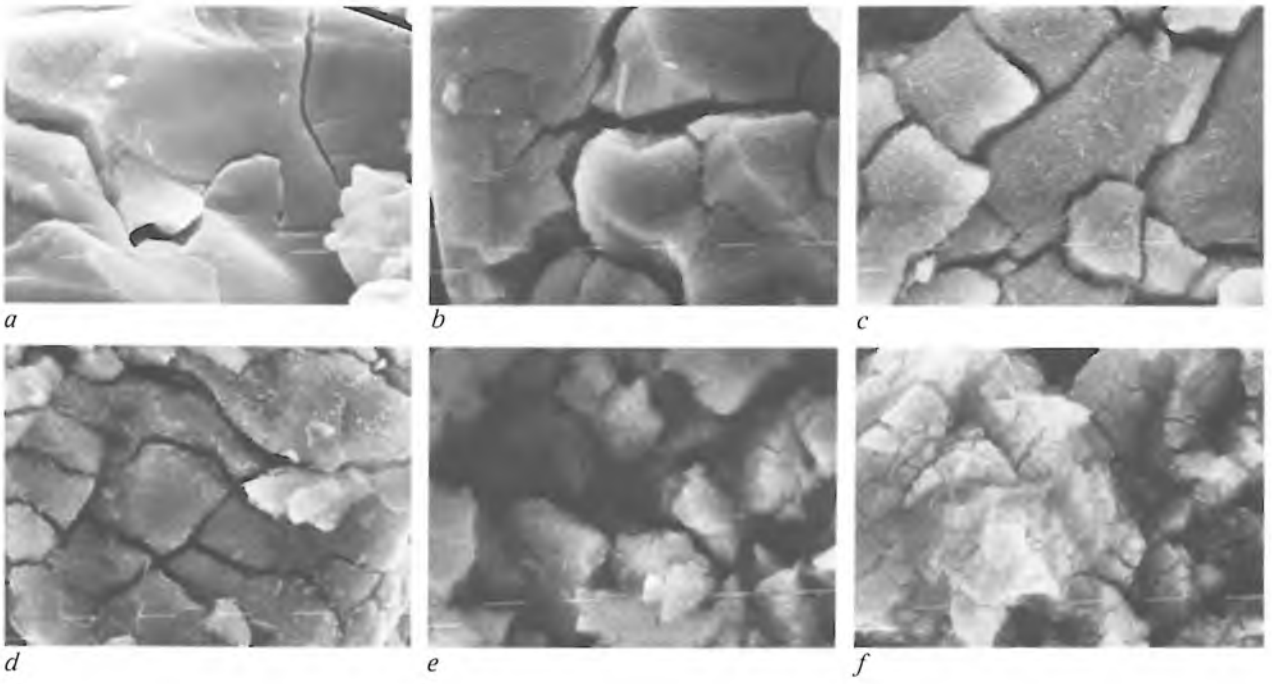

Fig. 12. SEM micrographs of $LaNi_5$ electrodes after repeated charging and discharging. The results are shown after zero (*a*), 12 (*b*), 25 (*c*), 63 (*d*), 176 (*e*) and 359 (*f*) charge/discharge cycles. One 'dash' represents 1 μm. $La(OH)_3$ needles, which are visible from (*b*) onwards, have completely overgrown the original material in (*f*).

The mechanical stresses associated with the 'respiration' of the lattice will of course increase with the changes in volume that take place on the absorption and desorption of hydrogen. In the case of $LaNi_5$ the increase of volume due to the absorption of hydrogen may be as much as 24% of the initial volume.

We therefore looked for related hydrogen-absorbing intermetallic compounds that expand less during this absorption than $LaNi_5$, and thus give less diffusion and oxidation of lanthanum.

The stability of some compounds, particularly those with 2 or 3 atoms of Co (*fig. 14*), can be significantly improved by adding a small amount of aluminium to the constituent components in the preparation of the compounds. The stability of $LaNi_5$ itself is not affected by this small addition. A similar improvement in stability is also obtained by adding small amounts of silicon. Both additives would be expected to impede the diffusion of lanthanum in the metal lattice or cause a protective skin to form on the surface.

No comparisons will be given of all the substitutions that we investigated or their effects. We found that the compound $La_{0.8}Nd_{0.2}Ni_{2.5}Co_{2.4}Si_{0.1}$ answered our purpose extremely well. This electrode material has an initial capacity of 290 mAh/g and the capacity remaining after a thousand charge/discharge cycles is still 70% (*fig. 15*). The excellent properties of this compound are also illustrated by the SEM micrographs in *fig. 16*. These show that after 666 cycles there are only relatively few $La(OH)_3$ needles present and that the fragments formed still have the jagged character of uncorroded crystals (see fig. 12).

The question remained as to whether the stability improvement achieved really was connected with a diminished expansion in volume on hydriding. To start with, we established that the decrease in the capacity of the electrodes only occurs during repeated charging and discharging and is not the consequence of mere contact with 6 M KOH over a long period. We also measured the volume increment ΔV due to H_2 absorption by X-ray diffraction methods and plotted the results against the fraction S_{400} of the capacity remaining after 400 cycles (*fig. 17*). The measured points are grouped along two straight lines in the figure, showing that a decreasing volume increment does in fact result in improved stability, and that this is most pronounced in compounds that contain small amounts of Al or Si.

We thus arrived at the following picture for explaining the corrosion of $LaNi_5$-type compounds. The rate-determining step in the corrosion process is the transport of lanthanum to the interface between the electrode and the electrolyte. Under normal conditions the mobility of lanthanum in the metallic AB_5 lattice is virtually zero at room temperature. This is not the case at the phase boundary. As indicated in *fig. 18*, a phase boundary is always present during charging and discharging in the grains of the intermetallic compound. During charging and discharging continuous 'recrystallization' takes place from a hydrogen-poor phase to a hydrogen-rich phase, and vice versa. Since the hydrogen-rich phase has a larger unit cell (figs 10 and 17) than the hydrogen-poor phase, the lattice at the phase boundary is deformed, so that the mobility of the lanthanum in this zone can assume high values. During charging and discharging this phase boundary, and hence the zone of enhanced mobility, migrates through the grains, and therefore the lanthanum can be transported from the bulk of the grains towards the surface, even at room temperature. The lowest mobility is found when the volume expansion due to hydriding is smallest, of course.

Small amounts of aluminium or silicon lead to the formation of a closed skin at the surface of the grains,

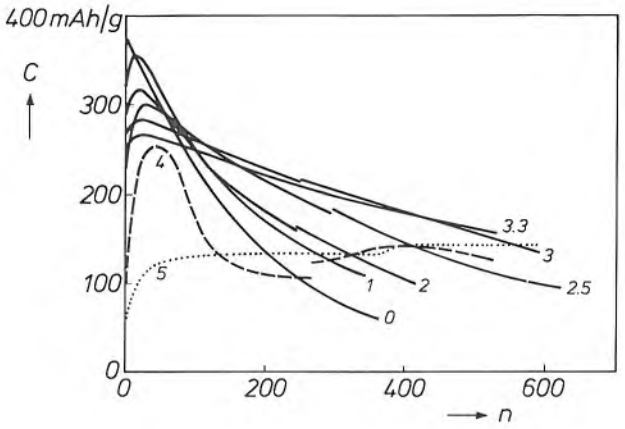

Fig. 13. The effect of substituting cobalt for nickel in $LaNi_5$ on the curve for the storage capacity C as a function of the number of charge/discharge cycles (n). The number of nickel atoms replaced by cobalt atoms is shown beside each curve. The optimum effect is found when 3.3 nickel atoms are replaced by cobalt.

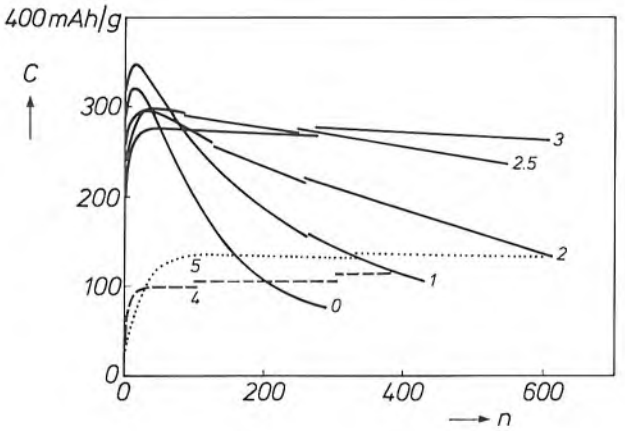

Fig. 14. As in fig. 13, but after the addition of 0.1 atomic fraction of Al. The addition of small amounts of Si has the same effect.

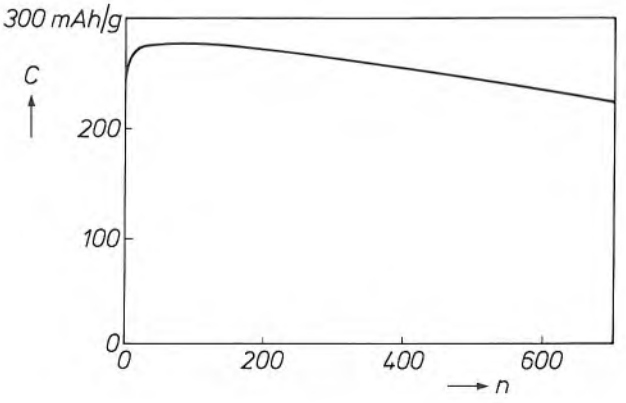

Fig. 15. The storage capacity C of an electrode of $La_{0.8}Nd_{0.2}Ni_{2.5}Co_{2.4}Si_{0.1}$ as a function of the number of charge/discharge cycles n. The improvement in stability with respect to $LaNi_5$ is clear from a comparison with fig. 9.

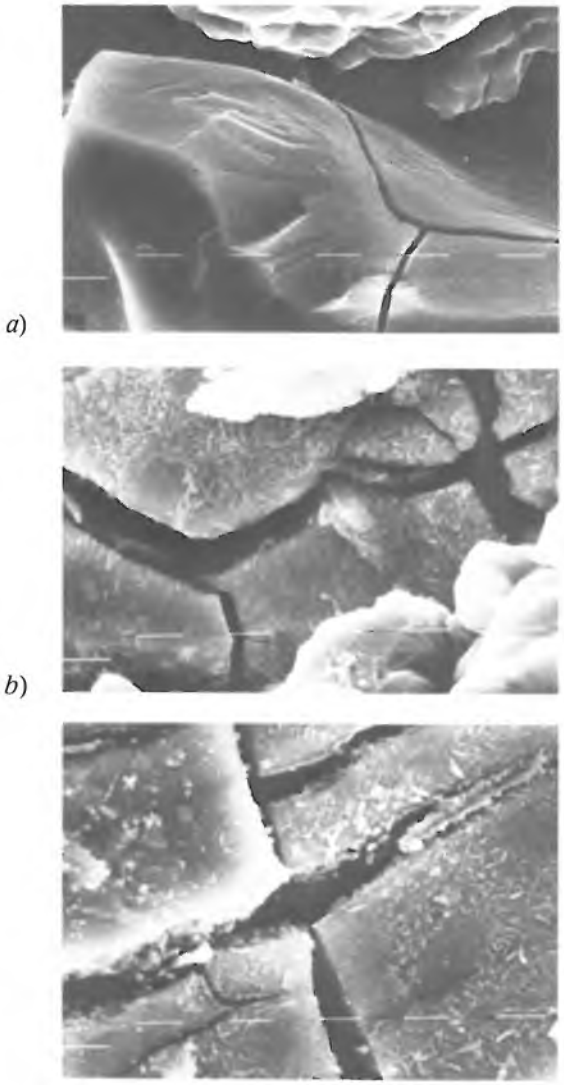

Fig. 16. SEM micrograph of $La_{0.8}Nd_{0.2}Ni_{2.5}Co_{2.4}Si_{0.1}$ electrodes after zero (*a*), 41 (*b*) and 666 (*c*) charge/discharge cycles. One 'dash' represents 1 μm.

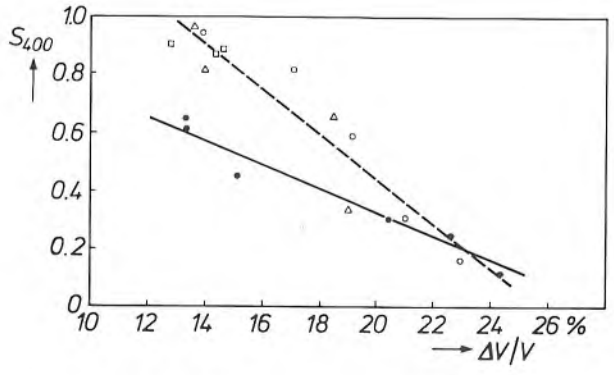

Fig. 17. Effect of the relative volume expansion $\Delta V/V$ on the stability of an electrode made from $LaNi_5$ and related compounds. The stability is expressed as the fraction S_{400} of the storage capacity remaining after 400 charge/discharge cycles. The filled circles relate to materials of the type $LaNi_{5-x}Co_x$, the open symbols to materials of the same type with small amounts of aluminium or silicon added. For small volume changes the materials with added aluminium or silicon are clearly the most stable.

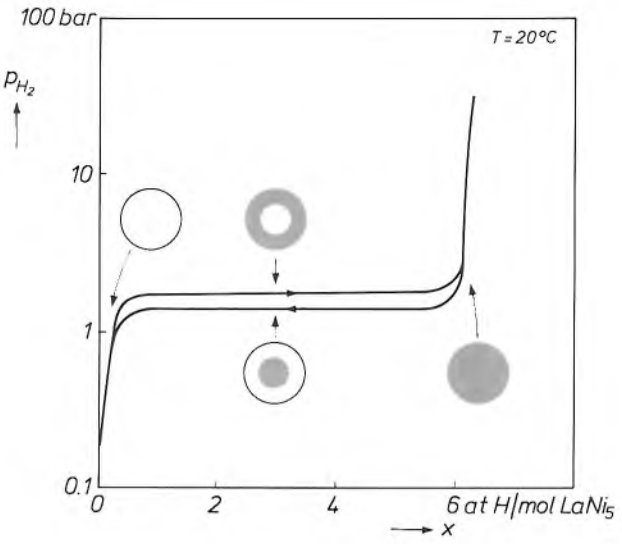

Fig. 18. Schematic representation of the phase boundary shift between the hydrogen-poor and hydrogen-rich phases in $LaNi_5$ grains on charging and discharging. The hydrogen-poor phase is white, the hydrogen-rich phase is shown grey.

which acts as an additional restriction of the exposure of lanthanum to the electrolyte. This skin is thought to be composed of islands of cobalt and nickel with an aluminium- or silicon-containing oxide between them. Its inhibiting effect can only be maintained if the volume changes are not too great, if not the enclosing skin disintegrates; this explains why it is not found in $LaNi_5$ itself (fig. 14).

Is the hydride electrode a suitable alternative to the cadmium electrode of the NiCd cell?

Most electrodes of rechargeable batteries with an aqueous electrolyte are charged and discharged in a dissolution-precipitation mechanism. The discharge of the positive electrode in the lead-acid battery, for example, proceeds as follows:

dissolution:

$$PbO_2 + 4H^+ + 2e^- \rightarrow Pb^{2+} + 2H_2O, \quad (8)$$

followed by precipitation:

$$Pb^{2+} + HSO_4^- \rightarrow PbSO_4\downarrow + H^+, \quad (9)$$

and charging of the negative electrode of the NiCd cell:

dissolution:

$$Cd(OH)_2 + 2OH^- \rightarrow [Cd(OH)_4]^{2-}, \quad (10)$$

followed by precipitation:

$$[Cd(OH)_4]^{2-} + 2e^- \rightarrow Cd\downarrow + 4\,OH^-. \quad (11)$$

In the first case the soluble intermediate product is an ion, Pb^{2+}, and in the second case an ion complex, $[Cd(OH)_4]^{2-}$. In view of the relatively low concentra-

tions of these ionic intermediates, large surface areas and short diffusion paths are required to obtain acceptable rates of charge and discharge. This makes it necessary to use electrodes with an appropriate porous structure. An undesirable feature of this charging and discharging mechanism is therefore that changes in shape occur during charging and discharging because of the redistribution of the active material within the porous electrode. The main processes are:

- nucleation and growth of the new solid phase at the surface of the active material still present;
- passivation, which consists of shielding the active material by a thin layer of non-active material formed around it, e.g. the sulphation of both electrodes of the lead-acid cell;
- recrystallization, leading to the formation of larger grains or more stable modifications, as found for instance during the ageing of the cadmium electrode in the NiCd battery, and finally
- dendrite formation, which may cause failure by internal short-circuiting.

The worst effects of these processes are that they diminish the size of the active area and reduce its accessibility. These effects increase strongly with the rates of charge and discharge and with the 'depth of discharge'. Consequently, during average charge and discharge periods of 5 to 20 hours the percentage of optimally used active material is only between 25 and 45%. (This is why, for example, the capacity of the cadmium electrode in the nickel-cadmium cell has to be much larger than the nominal capacity of the nickel electrode.) On repeated discharging in less than an hour, which may be required in some applications, the percentage of active material optimally utilized is much lower than the stated percentage of 25%.

Electrodes without soluble intermediates, such as the nickel electrode, do not suffer from such limitations. Here charge and discharge take place via a solid-state transition, which may be written as:

$$Ni(OH)_2 + OH^- \underset{\text{discharge}}{\overset{\text{charge}}{\rightleftarrows}} NiOOH + H_2O + e^-. \quad (12)$$

Owing to the absence of the degradation effects described, which are connected with the dissolution-precipitation mechanism, the nickel electrode has developed into one of the most valued products of present-day battery technology — it can be charged and discharged thousands of times at high current without noticeable deterioration.

As we have seen above, the hydride electrode is charged and discharged via a solid-state transition:

$$M + xH_2O + xe^- \underset{\text{discharge}}{\overset{\text{charge}}{\rightleftarrows}} MH_x + xOH^- \quad (13)$$

(where M could for example represent the compound $La_{0.8}Nd_{0.2}Ni_{2.5}Co_{2.4}Si_{0.1}$).

When both types of electrode are combined as the positive and negative poles of a rechargeable nickel-hydride battery, the overall cell reaction for charging and discharging is:

$$M + xNi(OH)_2 \underset{\text{discharge}}{\overset{\text{charge}}{\rightleftarrows}} MH_x + xNiOOH, \quad (14)$$

so that during operation of the cell there is no net consumption of electrolyte. This permits a simple and compact construction with little electrolyte [3].

The resultant new type of rechargeable battery should have the following four desirable features:

- No cadmium or other toxic heavy metals.
- A high energy density, especially when used at high discharge rates. Both the NiCd cell and the nickel-hydride cell have a theoretical energy density of about 200 Wh/kg, but at the discharge rates in common use the actual energy density of the NiCd cell will not be more than 40 to 50 Wh/kg, partly because of the low degree of utilization of active material. In view of this considerable reduction in the theoretical energy density, the nickel-hydride cell, which has no dissolution-precipitation mechanism and consumes no electrolyte, seems to offer much better prospects.
- A high power density. Equation (14) shows that charging and discharging a nickel-hydride battery is rather like pumping hydrogen atoms, or protons, from one electrode to the other. Owing to the high mobility of the hydrogen atom and of the proton, the system should be capable of handling high current densities with low internal resistance, so that this electrode combination should result in a battery that can be charged and discharged at high rates.
- The possibility of effective protection from overcharging and overdischarging. In overcharging, the chemical bypass mechanism operates in the same way as in the NiCd cell, via an oxygen cycle. In overdischarging, however, the situation is different from that in a nickel-cadmium cell: the hydrogen gas evolved in the nickel-hydride cell is turned to good use, since it introduces a chemical bypass in the form of a hydrogen cycle:

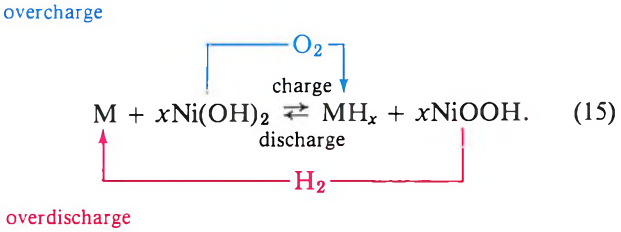

(15)

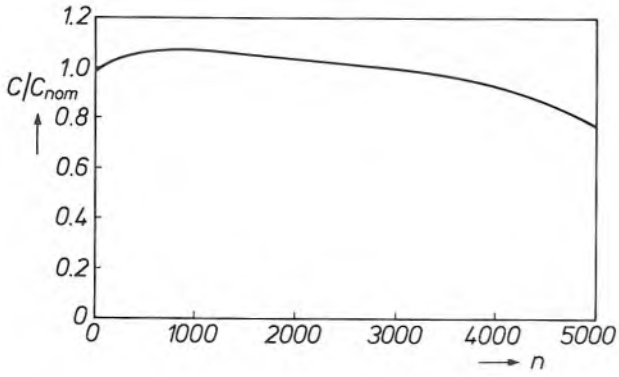

Fig. 19. The relative storage capacity C/C_{nom} of an experimental nickel-hydride cell as a function of the number of charge/discharge cycles n. The hydride electrode is overdimensioned by a factor of 1.85 with respect to the nickel electrode. C_{nom} is 300 mAh.

Experimental nickel-hydride cell

In provisionally completing this experimental investigation, in which only half-cells have as yet been tested, we made a number of experimental nickel-hydride cells. At this point we were not trying to establish whether such a battery had all the good features that seemed likely in the previous section. This would have required the construction of an optimum battery that could provide the predicted high energy density and power density. Our aim was simply to show that predictions based on half-cell measurements were reasonably valid for the complete battery.

We were particularly interested in the validity of the following two hypotheses, which found support in the

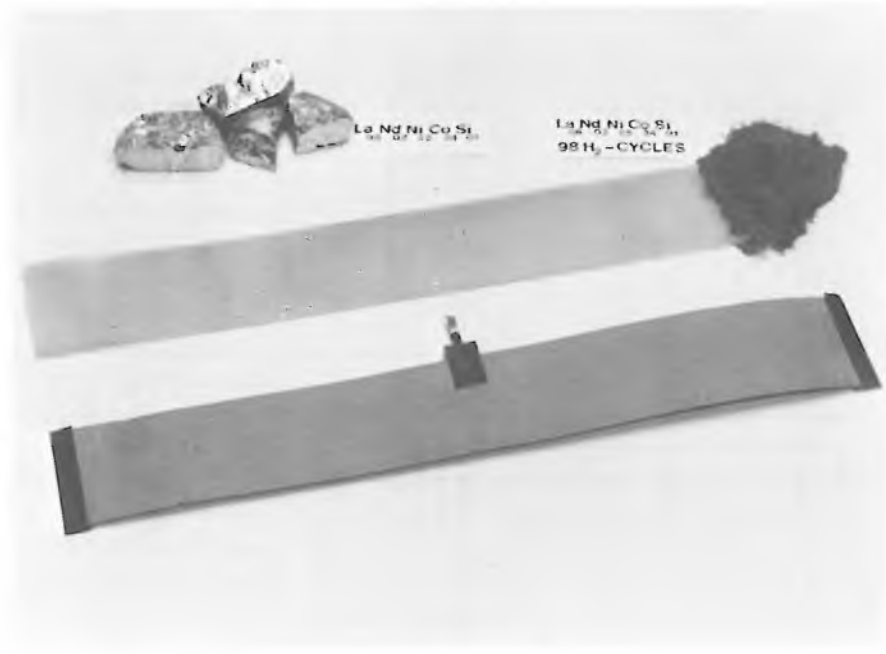

Fig. 20. One of our methods of manufacturing the hydride electrode. Metal castings of composition $La_{0.8}Nd_{0.2}Ni_{2.5}Co_{2.4}Si_{0.1}$ (top left) are pulverized by repeated absorption and desorption of hydrogen gas (top right) and the resultant powder is applied as a paste to a strip of expanded nickel.

Fig. 21. Illustrating the second manufacturing step. A hydride electrode (grey; see the lower strip in fig. 20) is rolled up with a sintered nickel electrode (black) and a separator (white) to form a cylindrical battery. After addition of electrolyte the battery is hermetically sealed.

Fig. 22. A complete experimental nickel-hydride cell and pressure vessel.

investigation described here: firstly, that electrodes made from $La_{0.8}Nd_{0.2}Ni_{2.5}Co_{2.4}Si_{0.1}$ would only give a 30% decay in storage capacity after 1000 charge/discharge cycles (fig. 15) and secondly, that no such decay of storage capacity would occur if the active material did not take part in the expansion and contraction process of hydrogen absorption and desorption.

To test these two hypotheses we made the hydride electrode, which we combined with a nickel electrode (overdimensioned by a factor of 1.85), so that we had active material that would expand and contract and material that would not do so.

Overdimensioning is also necessary in a practical battery (although usually by a much smaller factor), as part of the approach for protecting the cells of a hermetically sealed battery from overcharging and overdischarging. As soon as the overdimensioning ceases to exist because of the decay of storage capacity, a steep rise in gas accumulation will soon put an end to the life of the battery. (Battery life is defined here as the time for which the battery will operate before the gas pressure in the sealed unit rises above a specified value, e.g. 20 bars.)

From the measured decrease in the storage capacity of active material that participates 100% in hydrogen absorption and desorption (fig. 15) we can calculate the cell life for an overdimensioning of 1.85 times. For our experimental battery we calculated a life of 4000 charge/discharge cycles.

Fig. 19 shows the capacity decay of this battery as a function of the number of charge/discharge cycles. After 4000 cycles the storage capacity was still 92% of the nominal value, and even after 5000 cycles, that is to say after 60 weeks of continuous high-rate charging and discharging, the storage capacity was still better than 78% of the nominal value. After these 5000 cycles the pressure in the cell was about 10 bars.

The conclusion from these results is that the capacity decay of the new electrode material in a complete cell is at all events not greater than that found from the measurements on the half-cell.

Figs 20 and *21* illustrate one of the ways in which we made such experimental nickel-hydride cells. The intermetallic compound $La_{0.8}Nd_{0.2}Ni_{2.5}Co_{2.4}Si_{0.1}$ was pulverized by repeated hydrogen-gas absorption/desorption cycles, and the powder was then mixed with fine nickel powder and applied as a paste to a strip of expanded nickel. The positive electrode was made by impregnating a porous sintered-nickel plate with $Ni(OH)_2$. The electrolyte was a solution of 5 M KOH and 1 M LiOH. The two electrodes, separated by a polyamide strip, were rolled up to form a cylindrical package and placed in a nickel-plated steel can. After addition of the electrolyte the battery can be hermetically sealed or (as in our experiments) placed in a pressure vessel fitted with a pressure gauge (*fig. 22*).

Summary. $LaNi_5$ and related compounds have been investigated for their usefulness as electrode material in hydrogen-based rechargeable batteries. Although $LaNi_5$ and $LaNi_4Cu$ give the required rapid absorption and desorption of large amounts of hydrogen, they are not suitable electrode materials because of the very large decay in their storage capacity with repeated charging and discharging. It was found that this capacity loss is due to the conversion of the active material into $La(OH)_3$, which proceeds more rapidly as the volume changes in the active material caused by repeated charging and discharging become larger. Partial substitution of Co for Ni gives smaller volume changes and hence a more stable electrode material. The stability is further improved by adding small quantities of aluminium or silicon. The capacity of electrodes made from the newly developed $La_{0.8}Nd_{0.2}Ni_{2.5}Co_{2.4}Si_{0.1}$ was found to have decayed by only 30% after 1000 charge and discharge cycles. The experimental — hermetically sealed — nickel-hydride battery made with this material combines a long life with high energy density and power density, and effective protection from overcharging and overdischarging. It also contains no toxic heavy metals such as cadmium.

Dielectric resonators for microwave integrated oscillators

G. Lütteke and D. Hennings

Microwave oscillators used in radar and telecommunications must operate at constant frequency and generate little noise. Until recently this meant that oscillator circuits had to include a cavity resonator that functioned as a selective filter. The dimensions of the cavity resonator, however, were not compatible with the miniaturization of microwave integrated circuits in which waveguides and coaxial lines have been replaced by microstrip. Dielectric resonators are much more suitable for microwave integrated circuits, because they are small. Careful consideration must be given to the choice of the ceramic material for these resonators, to ensure high frequency stability and good noise characteristics.

Introduction

Now that direct television broadcasts via geostationary satellites have become a reality, there is a need for inexpensive circuits for microwave reception. Microwave integrated circuits (MICs) combine small dimensions and low weight with low cost. Modern MIC technology uses bipolar transistors and field-effect transistors with ever higher cut-off frequencies, and special active devices for the microwave region such as Gunn diodes and IMPATT diodes (IMPATT stands for 'IMPact Avalanche and Transit Time'). In MIC technology these components are interconnected by microstrip lines, which consist of a thin metal conductor (the strip) separated from a metal ground layer by a dielectric [1].

For telecommunication microwave links and for satellite television the frequency of the microwave carrier is required to be highly constant. A high signal-to-noise ratio is also essential. These requirements can only be met by the use of frequency-stabilizing selective band filters in the oscillator circuits. Until recently this meant using relatively large cavity resonators, which had to be made of Invar to ensure low temperature sensitivity. With these resonators a relative frequency stability of 10^{-6} °C^{-1} and Q-factors (quality factors) of more than 10 000 have been achieved.

Because of their size, cavity resonators are not very compatible with the structure of microwave integrated circuits. Efforts have therefore long been made to replace these resonators by ceramic types, which can be smaller because the permittivity of ceramic is higher than that of air. Many attempts to produce such resonators foundered because no ceramic materials could be found that combined a high permittivity and Q-factor with a low temperature dependence. It was not until the seventies that it was discovered that barium nonatitanate ($Ba_2Ti_9O_{20}$) was a suitable material for microwave dielectric resonators. This material was also found to be suitable for selective filters consisting of a number of coupled dielectric resonators. The dimensions of these filters can be kept within reasonable limits even at the lower frequencies. Its high permittivity also makes the material an excellent substrate material for microwave integrated circuits operated at relatively low frequencies. In addition, with specific microstrip dimensions low characteristic impedances can be achieved. (The characteristic impedance of a microstrip line is approximately inversely proportional to the square root of the permittivity of the dielectric.)

The temperature dependence of the frequency f_R, of electromagnetic standing waves in a dielectric reso-

Dr G. Lütteke is with Philips GmbH Apparatefabrik Krefeld, and was formerly with Philips GmbH Forschungslaboratorium Aachen (PFA), Aachen, West Germany. Dr D. Hennings is with PFA.

[1] J. H. C. van Heuven and A. G. van Nie, Microwave integrated circuits, Philips Tech. Rev. 32, 292-304, 1971.

nator is expressed by the temperature coefficient τ_{f_R}, which is defined as:

$$\tau_{f_R} = \frac{1}{f_R} \frac{df_R}{dt}, \quad (1)$$

where t is the temperature. This temperature coefficient is a function of the thermal expansion coefficient and of a similarly defined temperature coefficient for the permittivity. In oscillator circuits it is not desirable to make τ_{f_R} for the resonator exactly zero. This is because the overall temperature coefficient for the resonant frequency of the complete oscillator includes a small negative contribution from the other components in the circuit, and this has to be compensated by a positive contribution from the resonator.

To keep the dimensions of the resonator within reasonable limits the relative permittivity ε_r of the material must be high. (If we compare the dimensions of a cavity resonator and a dielectric resonator, we see that the cavity resonator at the same frequency and height/diameter ratio is about $\sqrt{\varepsilon_r}$ times as large as the dielectric resonator [2].) In addition it must be possible to control the temperature coefficient of the resonant frequency in a small range by varying the composition of the material. The region of miscibility ratios of the two compounds $BaTi_4O_9$ and $Ba_2Ti_9O_{20}$ in the phase diagram of the BaO-TiO_2 system is particularly suitable for controlling the temperature coefficient. With resonators of $Ba_2Ti_9O_{20}$ containing about 30% of $BaTi_4O_9$, oscillator circuits for 10 GHz have been made whose frequency stability is comparable with that of oscillators that have Invar cavity resonators. The dimensions of the dielectric resonators are very much smaller, however.

In this article we shall first look at the theoretical background of dielectric resonators in connection with measurements of material properties. We shall then deal with the composition of the ceramic materials for these resonators. After discussing various kinds of oscillator circuits, we shall conclude with a number of applications of stable oscillator circuits for microwave frequencies.

The dielectric resonator and the measurement of material properties

A dielectric resonator is usually a cylindrical body made of a material that has a high permittivity. Electromagnetic standing waves are set up in the resonator, and their wavelength is determined by the dimensions and the permittivity. Part of the high-frequency electromagnetic field extends beyond the resonator. This stray field can be used for coupling the resonator to the microwave circuit.

Ceramic materials with a high permittivity have been known for a long time. Barium titanate ($BaTiO_3$) can have ε_r-values as high as 10 000. Most ceramic materials, however, are unsuitable for use in resonators because their dielectric losses are excessively high at microwave frequencies. In ferroelectric materials like barium titanate these losses are due to the dielectric relaxation of the domain walls. The magnitude of the dielectric losses is determined by the loss factor $\tan\delta_m$, where δ_m is the loss angle of the material. The magnitude of the loss factor follows from the equation giving the complex permittivity ε:

$$\varepsilon = \varepsilon_r \varepsilon_0 (1 - j \tan\delta_m), \quad (2)$$

where ε_0 is the permittivity of free space. In resonators the dielectric losses must be kept as small as possible. This is expressed in the Q-factor Q_m, which is defined as the reciprocal of the loss factor.

It is also important that the relative permittivity should not vary much as a function of temperature and that the thermal expansion coefficient of the material should be small. This can be seen from the expression for the temperature coefficient τ_{f_R} for the resonant frequency of dielectric resonators [3]:

$$\tau_{f_R} = -\tfrac{1}{2}(\tau_{\varepsilon_r} + 2\tau_\alpha), \quad (3)$$

where τ_{ε_r} is the temperature coefficient of the permittivity and τ_α is the thermal expansion coefficient. A low value of τ_{f_R} can thus be obtained by using a material in which the quantities τ_{ε_r} and τ_α largely compensate one another. A problem is that for some materials there are no published values for these quantities, so that they have to be measured.

For these measurements we used the arrangement shown schematically in *fig. 1a* [4]. In a cylindrical sample microwave resonances are generated whose geometry is comparable with the geometry of resonances in a dielectric resonator. The sample is mounted between two metal plates. A variable-frequency signal from a network analyser is applied to the sample via a coaxial line and excites a field in it. The signal is returned to the analyser by a second coaxial line. The metal plates act as a waveguide operating below its cut-off frequency. This means that the high-frequency field emerging from the sample decreases rapidly with increasing radial distance. To reduce the effects of eddy-current losses in the metal plates, the sample is given a high length/diameter ratio.

The resonant modes in a cylindrical dielectric resonator are related to the modes in a cavity resonator. In a *cavity resonator* only transverse modes, designated TE_{mnp} and TM_{mnp}, can occur. The subscripts m, n and p are integers relating to the number of periods of the electric or magnetic field in the circum-

ferential, radial and axial directions respectively. Either the electric field (the TE_{mnp} mode, the subscripts relating to the magnetic field) or the magnetic field (the TM_{mnp} mode, the subscripts relating to the electric field) is a purely transverse field, that is to say with no axial component. The non-transverse magnetic or electric field associated with a transverse electric or magnetic field does therefore have an axial component. In a cylindrical, non-metallized *dielectric resonator* only transverse modes with rotational symmetry ($m = 0$) can be excited. In dielectric resonators, however, there may also be non-transverse modes, which do not have rotational symmetry. In these modes, called HE_{mnp} or 'hybrid' modes, both the magnetic and electric fields have an axial component.

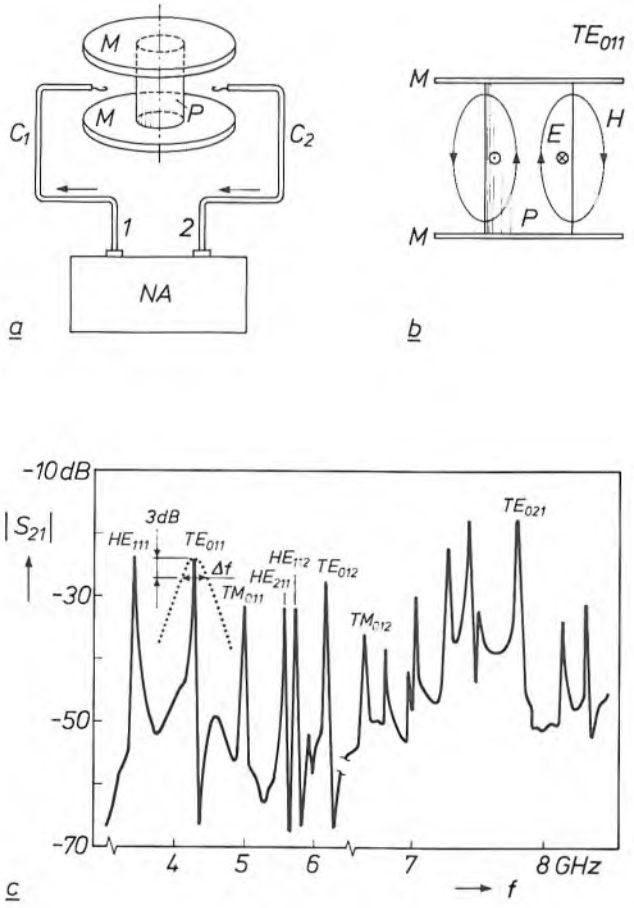

Fig. 1. Measurement of materials for dielectric resonators. *a*) Experimental arrangement. A cylindrical ceramic sample *P* is placed between two metal plates *M*. Microwave resonances are excited in the sample by a signal from a network analyser *NA* (Hewlett Packard 8410). The signal is supplied to the sample from port *1* of the analyser via a coaxial cable C_1, and is returned via a second cable C_2 to port *2* of the analyser. Both coaxial cables are terminated in a loop in a plane perpendicular to the axis of the resonator. *b*) Diagram illustrating the TE_{011} mode in the sample. *E* electric line of force. *H* magnetic line of force. *c*) Example of a frequency spectrum measured with the network analyser. The modulus of the ratio S_{21} of the voltages at terminals *2* and *1* is plotted in dB as a function of frequency *f*. The spectrum is a combination of two measurements with different linear frequency scales. The modes corresponding to some of the peaks are indicated. The peak for the TE_{011} mode has been magnified in the horizontal direction: the dotted line. The Q-factor of the material can be determined from the width Δf of the peak at 3 dB below the peak.

Of the many modes that can occur in a cylindrical resonator, only the transverse mode TE_{011} is of practical significance. In fig. 1*b* the electric and magnetic lines of force of the TE_{011} mode in the sample under test are shown schematically. The (transverse) electric lines of force are circles whose centres lie on the axis of the sample. The magnetic lines of force are approximately in the axial direction in the material and are rather like those of a magnetic dipole. Since each magnetic line of force lies in a plane through the axis and also extends beyond the material, the TE_{011} mode can easily be coupled to the network analyser by coaxial cables.

Fig. 1*c* shows a frequency spectrum measured with the arrangement of fig. 1*a*. Such a spectrum will only contain peaks due to the transverse modes TE_{0np} and TM_{0np} and the hybrid modes HE_{mnp}. It can be seen that the mode with the lowest frequency is the HE_{111} mode. Around the peak due to the TE_{011} mode in the figure an indication is given of how the Q of the material Q_m can be determined from the shape of the peak. Q_m is approximately equal to the ratio of the resonant frequency to the width Δf of the resonance peak, measured 3 dB below the peak. (A value of 3 dB corresponds to a power ratio of 0.5.) The permittivity can be calculated from the resonant frequency and the dimensions of the sample.

A dielectric resonator used in oscillator circuits has the shape of a flat cylinder. It is not clamped between metal plates, but is mounted with some axial and radial play in a metal case. The magnetic field can therefore extend outside the resonator in the axial direction; see *fig. 2a*. The mode indicated here is therefore called the $TE_{01\delta}$ mode. The coupling to the rest of the circuit is made with a microstrip line; see fig. 2*b*. To limit the losses in the ground plane of the microwave circuit the resonator is mounted at the bottom of the housing on a quartz-glass ring; see fig. 2*c*. The resonator has a height/diameter ratio of about 0.4, so that the differences in frequency between the $TE_{01\delta}$ mode and the neighbouring modes are relatively large. The side walls of the case are far enough away from the resonator to

[2] M. W. Pospieszalski, On the theory and application of the dielectric post resonator, IEEE Trans. **MTT-25**, 228-231, 1977.

[3] D. Hennings and P. Schnabel, Dielectric characterization of $Ba_2Ti_9O_{20}$ type ceramics at microwave frequencies, Philips J. Res. **38**, 295-311, 1983.

[4] B. W. Hakki and P. D. Coleman, A dielectric resonator method of measuring inductive capacities in the millimeter range, IRE Trans. **MTT-8**, 402-410, 1960;
W. E. Courtney, Analysis and evaluation of a method of measuring the complex permittivity and permeability of microwave insulators, IEEE Trans. **MTT-18**, 476-485, 1970.

minimize the excitation of eddy currents in them by the r.f. field. The case is nevertheless small, because the field decreases rapidly in the radial direction, since the upper and the lower plate also function here as a radial waveguide operating below its cut-off frequency.

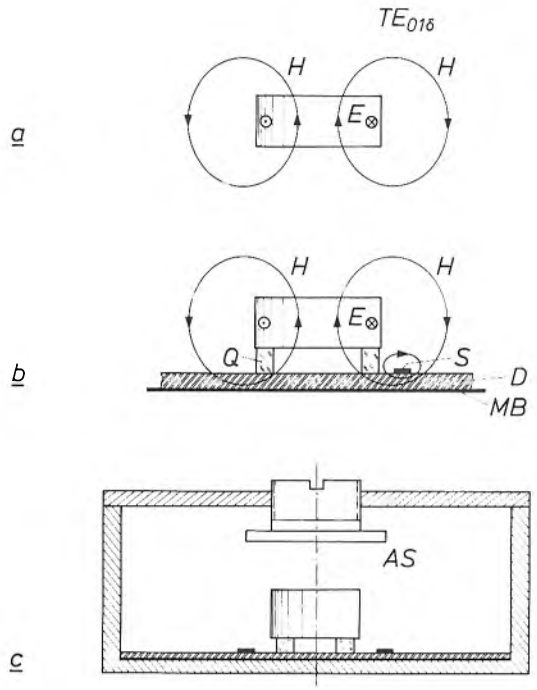

Fig. 2. *a*) Diagram of the $TE_{01\delta}$ mode in a dielectric resonator for oscillator circuits. (This mode should strictly be classified as $TE_{0\gamma\delta}$, since the magnetic field also extends from the resonator in the radial direction.) *b*) Coupling the resonator to a microstrip line in a microwave integrated circuit. *Q* quartz-glass ring. *S* strip of the microstrip line. *D* dielectric substrate. *MB* metal base. *c*) The dielectric resonator in its metal case, which contains the rest of the oscillator circuit (not shown). *AS* adjusting screw for fine tuning of the resonant frequency.

The resonant frequency is difficult to predict exactly from the dimensions of the resonator and the case. The frequency setting is therefore made with a tuning screw, which varies the distance over which the magnetic field of the $TE_{01\delta}$ mode extends in the axial direction. The resonant frequency can be set very accurately in this way.

Choice of material

It was discovered in the fifties that barium nonatitanate ($Ba_2Ti_9O_{20}$), because of its relatively high permittivity ε_r and very small temperature coefficient τ_{ε_r}, was a suitable material for stable ceramic capacitors [5]. Much later it turned out that the properties of this material also make it suitable for use in dielectric resonators for frequencies up to 10 GHz [6].

In the phase diagram of the quasi-binary system $BaO\text{-}TiO_2$, see *fig. 3a*, lines for the compound $BaTi_4O_9$ (80 mol.% TiO_2) and for pure TiO_2 lie on opposite sides of the line for the compound $Ba_2Ti_9O_{20}$ (81.818 mol.% TiO_2). These three materials all have a high permittivity (that of TiO_2 is very high) and a low loss factor; see *Table I*. The temperature coefficient τ_{f_R} of resonators made with TiO_2 and $BaTi_4O_9$ is relatively large, whereas it is almost zero for $Ba_2Ti_9O_{20}$. The compounds $BaTi_4O_9$, $Ba_2Ti_9O_{20}$ and TiO_2 are not miscible with one another, but they can be combined by sintering to form a dense type of ceramic with a porosity of less than 0.5%. It therefore seems sensible to obtain the small — but not zero — temperature coefficient required by making the two-phase ceramics $BaTi_4O_9\text{-}Ba_2Ti_9O_{20}$ or $Ba_2Ti_9O_{20}\text{-}TiO_2$.

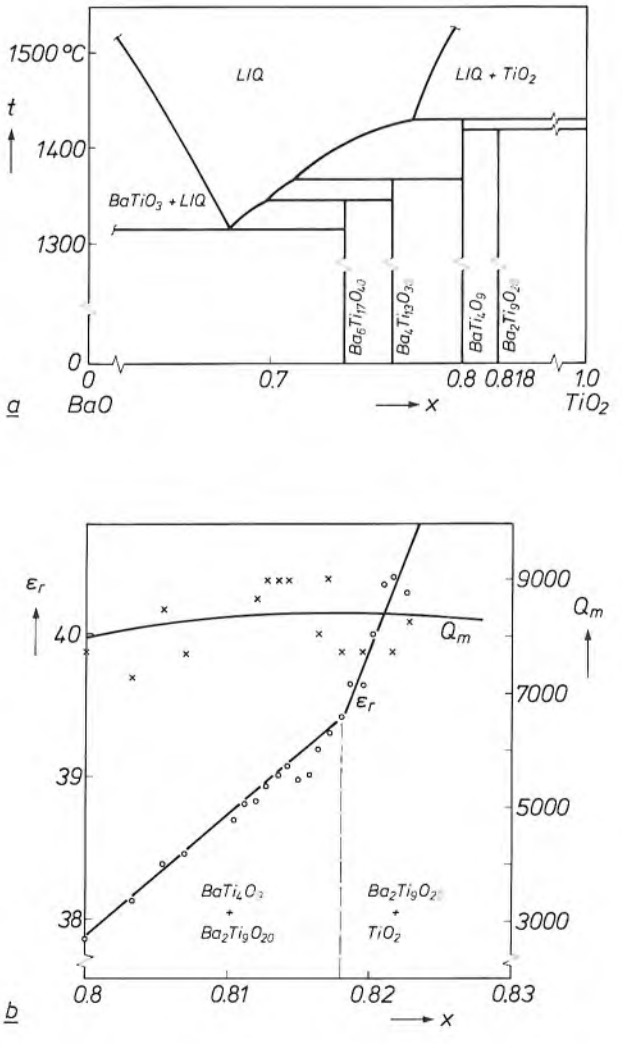

Fig. 3. Part of the phase diagram of the quasi-binary system $BaO\text{-}TiO_2$ [6]. *t* temperature. *x* molar quantity of TiO_2. *b*) Relative permittivity ε_r and Q-factor Q_m as a function of *x*, as the result of a number of measurements with the arrangement of fig. 1*a*. The regions for the two-phase ceramics $BaTi_4O_9\text{-}Ba_2Ti_9O_{20}$ and $Ba_2Ti_9O_{20}\text{-}TiO_2$ are separated by a dashed line.

Table I. Permittivity ε_r, temperature coefficient τ_{f_R} and loss factor $\tan\delta_m$, measured at 4 GHz for $BaTi_4O_9$, $Ba_2Ti_9O_{20}$ and TiO_2 samples.

	ε_r	τ_{f_R} [°C^{-1}]	$\tan\delta_m$
$BaTi_4O_9$	37.5	20×10^{-6}	1.6×10^{-4}
$Ba_2Ti_9O_{20}$	39.3	≈ 0	1.1×10^{-4}
TiO_2	100	1550×10^{-6}	2×10^{-4}

Fig. 3*b* shows that samples made from such two-phase ceramics have a permittivity that is a monotonically increasing function of the molecular content x of TiO_2. The Q-factor $Q_m = 1/\tan\delta_m$ is seen to be high and to change relatively little as a function of x. *Fig. 4* shows the temperature coefficient τ_{f_R} as a function of temperature for samples of the two-phase ceramic $(Ba_2Ti_9O_{20})_{1-y}$-$(BaTi_4O_9)_y$ with differing mixture ratios y. For pure $Ba_2Ti_9O_{20}$ the value of τ_{f_R} at 0 °C happens to be exactly equal to zero. This material might therefore be used for making resonators that have a broad minimum at 0 °C in the curve for the resonant frequency as a function of temperature, which approximates to a parabola. However, we want

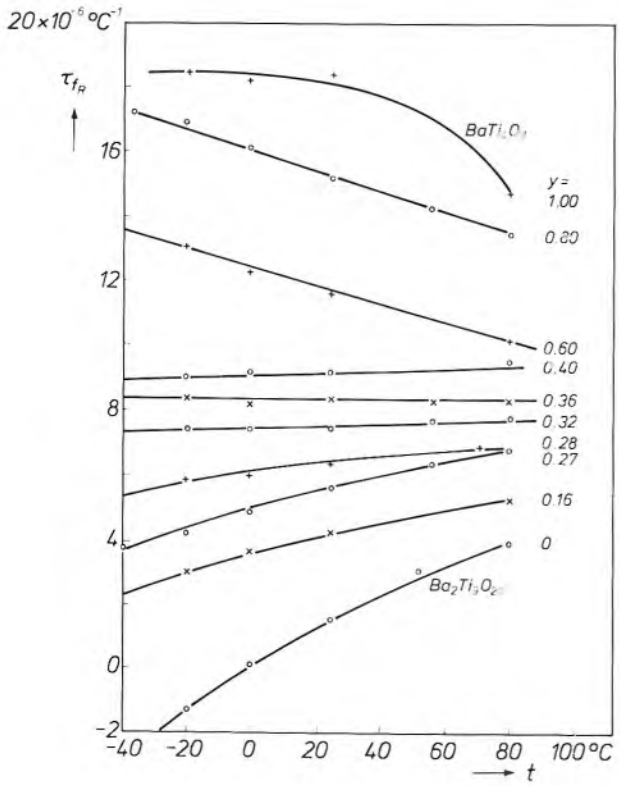

Fig. 4. Temperature coefficient τ_{f_R} for the resonant frequency f_R of ceramic samples as a function of temperature t. Each curve corresponds to a different value of the molar content y of $BaTi_4O_9$ in the two-phase ceramic $(Ba_2Ti_9O_{20})_{1-y}$-$(BaTi_4O_9)_y$.

the temperature coefficient of the resonant frequency to be independent of temperature and to have a small positive value. In this way we can compensate for negative temperature coefficients of other elements in the oscillator circuit.

Fig. 4 shows that this condition is satisfied by ceramic samples of $Ba_2Ti_9O_{20}$ containing about 30% of $BaTi_4O_9$. Resonators made of this material have been used in oscillator circuits that gave a frequency drift of only 150 kHz at 10 GHz in a temperature range from −20 to 100 °C [7]. The product of Q_m and the resonant frequency f_R (in GHz) of ceramic resonator materials is generally found to be practically constant in the range from 2 to 15 GHz, and is therefore used as a figure of merit. With the new materials described here we have reached values of about 45 000 for this product.

The oscillator circuit

Coupling to the resonator

There are various types of microwave oscillator circuit. If a dielectric resonator is used to stabilize the resonant frequency, it is always connected to the active element in the circuit by a microstrip line, the 'coupling line'. The coupling line is terminated by a load impedance, usually a matched load — a resistance equal to the characteristic impedance Z_0 of the line, so that there is no reflection at the termination. The terminating impedance is connected between the strip of the coupling line and the ground plane of the microwave integrated circuit; see *fig. 5a*.

The resonator may be regarded as a tuned circuit consisting of a resistance, an inductance and a capacitance connected in parallel, as in fig. 5*b*. Unloaded, the circuit has a Q-factor Q_R and an angular resonant frequency ω_R, and is considered to be coupled to the rest of the circuit by an ideal transformer with a turns ratio of n. If the tuned circuit plus transformer is replaced by another equivalent tuned circuit connected directly into the circuit, the values R, L and C change to R_1, L_1 and C_1 (see fig. 5*c*), and we can write:

$$R_1 = n^2 R.$$

The coupling factor β is defined as the ratio of this

[5] G. H. Jonker and W. Kwestroo, The ternary systems BaO-TiO_2-SnO_2 and BaO-TiO_2-ZrO_2, J. Am. Ceram. Soc. **41**, 390-394, 1958.

[6] H. M. O'Bryan, J. Thomson and J. K. Plourde, A new BaO-TiO_2 compound with temperature-stable high permittivity and low microwave loss, J. Am. Ceram. Soc. **57**, 450-453, 1974.

[7] C. Tsironis and D. Hennings, Highly stable FET DROs using new linear dielectric resonator material, Electron. Lett. **19**, 741-743, 1983.

resistance to the characteristic impedance of the coupling line:

$$\beta = \frac{R_1}{Z_0} = \frac{n^2 R}{R_0}, \qquad (4)$$

where R_0 is the load impedance. The magnitude of the coupling factor is largely determined by the distance between resonator and strip.

The impedance Z_1 is defined as the impedance between the strip and the ground plane at the position of the resonator and looking towards the load. This impedance is a function of the angular frequency ω of the microwave signals and can be expressed in terms of the quantities defined above:

$$Z_1(\omega) = Z_0 \left\{ 1 + \frac{\beta}{1 + jQ_R(\omega/\omega_R - \omega_R/\omega)} \right\}. \qquad (5)$$

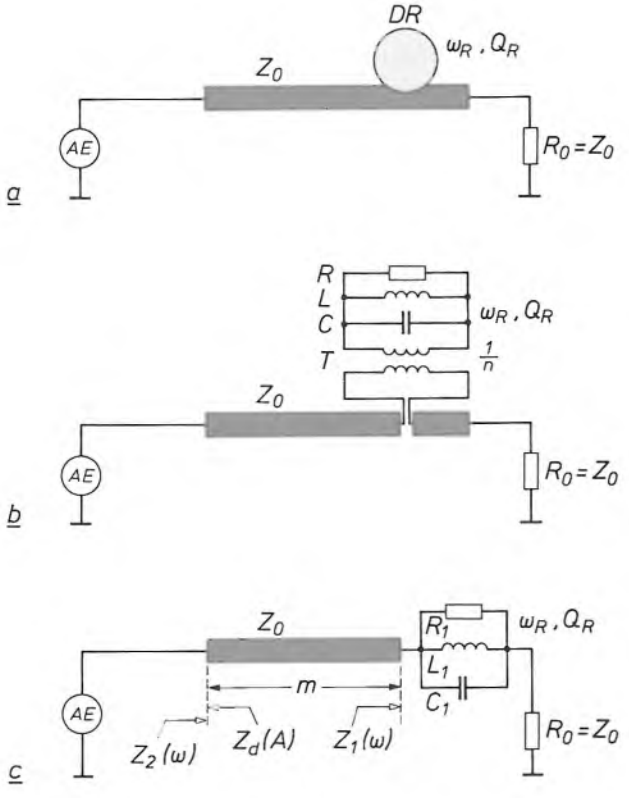

Fig. 5. Coupling of the dielectric resonator *DR* to the active element *AE*. *a)* Diagram showing the coupling line, a microstrip line of characteristic impedance Z_0. The coupling line is terminated by a resistance R_0, equal to Z_0. ω_R, Q_R angular resonant frequency and Q-factor of the resonator. *b)* Circuit with the resonator replaced by a parallel tuned circuit of R, L and C. The tuned circuit is connected to the coupling line by a transformer T with turns ratio n. *c)* Circuit with the tuned circuit and transformer replaced by a tuned circuit of R_1, L_1 and C_1. m length of the coupling line. $Z_1(\omega)$ the impedance between strip and ground plane near the resonator, looking towards R_0; ω angular frequency. $Z_2(\omega)$ as $Z_1(\omega)$, but at the input to the coupling line. $Z_d(A)$ input impedance of the active element; A amplitude of the oscillation.

Any non-variable impedance can be represented as a point on a Smith chart [8]; $Z_1(\omega)$ represents a circle on the chart (see *fig. 6*).

A Smith chart can be used to represent both the vector reflection coefficient, i.e. the voltage ratio of the incident and reflected microwave signals, and the real and imaginary components of the impedance normalized to the characteristic impedance. The voltage standing-wave ratio or VSWR can be read from these quantities in the diagram. This is the ratio of the voltages at the nodes and antinodes in the standing wave resulting from the incident and reflected signals.

The circle $Z_1(\omega)$ goes through M, the centre of the Smith chart, when $\omega = 0$ and $\omega = \infty$, because Z_1 is equal to the characteristic impedance Z_0 at these values of ω. The point for $\omega = \omega_R$, i.e. for resonance of the tuned circuit in fig. 5*c*, corresponds to the right point of intersection of the circle $Z_1(\omega)$ with the line h in the chart, since then $Z_1 = Z_0 + R_1$, from eq. (5). (Line h corresponds to impedances that are purely resistive.) The diameter of the circle is equal to $R_1 = \beta Z_0$; this diameter therefore increases as the resonator is more closely coupled to the microstrip line.

It is a property of the Smith chart that a point on the chart moves along a circle of centre M when the position where the impedance is being considered moves along a transmission line (in our case the microstrip line). If we want the impedance $Z_2(\omega)$ that the active element 'sees' at the input to the coupling line — the impedance at that point due to the coupling line, resonator and load — we find it by rotating the circle $Z_1(\omega)$ clockwise through an angle θ with respect to M. This angle is given by

$$\theta = \frac{2m}{\lambda} 360°,$$

where m is the length of the coupling line and λ is the wavelength. The locus for the load of the active element corresponds almost exactly to the circle $Z_2(\omega)$ thus obtained.

The oscillation condition for the complete circuit can be expressed as

$$Z_d(A) + Z_2(\omega) = 0, \qquad (6)$$

where the input impedance Z_d of the active element is a function of the amplitude A of the oscillation.

Oscillation can only occur if the complex input impedance of the active element contains a negative real component. (This is the case in Gunn and IMPATT diodes when the supply voltage satisfies certain conditions; in transistors the oscillation condition can only be satisfied by using negative feedback.) Within the limited frequency range determined by the $TE_{01\delta}$

mode of the resonator, only the real component of Z_d changes with varying amplitude; the reactance is virtually constant. On the Smith chart $-Z_d(A)$ therefore corresponds well to a line of constant reactance: an arc of a circle with its centre-point on the line v. The operating point of the circuit is the point of intersection of the lines for $Z_2(\omega)$ and $-Z_d(A)$.

The frequency and amplitude of the oscillation can be adjusted by moving the operating point. The location of the line $-Z_d(A)$ depends on the supply voltage of the active element and — in the case of transistors — on the coupling between the three terminals. The location of the locus $Z_2(\omega)$ depends on the length of the microstrip line between the active element and the resonator. The diameter of $Z_2(\omega)$ is determined by the coupling factor. The resonant frequency ω_R of the actual resonator depends on its dimensions and the setting of the tuning screw. An appropriate choice for the characteristic impedance — which determines the scale of the Smith chart — will ensure that point B, which represents the point $-Z_d(A = 0)$, lies inside the circular locus. It is easy to see that the operating point will then always be in a stable situation.

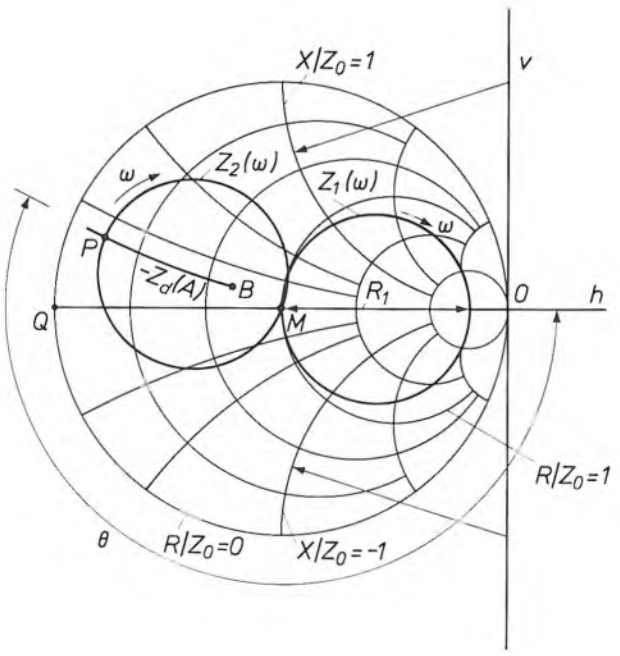

Fig. 6. Smith chart [8] for the coupling of the resonator to the active element. Every point inside the large circle represents an impedance $Z = R + jX$, normalized to the characteristic impedance Z_0. Circles through O with their centres on line v correspond to a constant ratio X/Z_0. X is positive above line h, and negative below it. Circles through O with their centres on line h correspond to a constant ratio R/Z_0. For O: $R = \infty$, $X = \infty$. For M: $R = Z_0$, $X = 0$. For Q: $R = 0$, $X = 0$. The thicker circles represent the impedances $Z_1(\omega)$ and $Z_2(\omega)$; see fig. 5. The circle $Z_1(\omega)$ intersects h at M for $\omega = 0$ and $\omega = \infty$. The second intersection of the circle with h corresponds to $Z_1(\omega_R) = Z_0 + R_1$. θ angle through which the circle for $Z_1(\omega)$ has to be rotated around M to obtain $Z_2(\omega)$; for $\theta = 360°$, m is equal to a half-wavelength. The line $-Z_d(A)$, see also fig. 5, is seen to correspond to a line of constant reactance. The point B corresponds to $-Z_d(A = 0)$ and lies within $Z_2(\omega)$. P, the intersection point of the lines $-Z_d(A)$ and $Z_2(\omega)$, is the operating point, which in this case has a stable position.

Terminating the coupling line with a pure resistance equal to the characteristic impedance of the line has the advantage that components in the signal whose frequency differs from ω_R are attenuated. The resonator is then 'electrically inoperative' for components at such frequencies. It can be shown that terminating the coupling line with a *reactance* does not give one single stable operating point, but three different operating points. However, one of these is in an unstable situation. The other two, although stable, correspond to frequencies that are very close together, so that the ultimate frequency of the oscillation is not predictable. Terminating the microstrip line with a reactance does not therefore produce a circuit of any practical use.

The various types of oscillator circuit

Fig. 7 shows five oscillator circuits, each containing a three-terminal active element [9]. The active element can be a bipolar transistor or a field-effect transistor. The microstrip lines in the various circuits are terminated by their characteristic impedance Z_0. The resistance that acts as a load in the circuits shown should be considered as equivalent to the actual transmitting or receiving circuits. The main difference between the microwave circuits is in the position of the load resistance. All these oscillator circuits were originally used with cavity resonators.

Fig. 7*a* shows the simplest type of oscillator circuit. The terminating resistance of the microstrip line acts not only as a damping resistance (R_D) but also as the load (R_L). The dielectric resonator is used as a 'reaction-type' resonator.

Fig. 7*b* shows a circuit with a 'transmission-type' resonator. The load is connected to the resonator by a second microstrip line. The resonator is not so tightly coupled to this line as to the first line. The signal goes from the active element via the resonator to the load, so that components at frequencies outside the passband of the resonator are strongly attenuated.

In the circuit of fig. 7*c* the damping resistance and the load are connected to different terminals of the transistor. There is a matching network for the load resistance. The resonator is coupled to the microstrip line in such a way that the maximum energy is reflected

[8] P. H. Smith, Transmission line calculator, Electronics 12, No. 1 (January), 29-31, 1939;
L. V. Blake, Transmission lines and waveguides, Wiley, New York 1969.

[9] I. M. Clarke and B. F. van der Heijden, Dielectric resonator oscillators, Proc. Military Microwaves '84, London 1984, pp. 591-595.

at the resonant frequency. A standing wave is then set up in the microstrip line between the active element and the resonator. This circuit is therefore referred to as an oscillator with a 'reflection-type' resonator.

In the circuit of fig. 7*d* two of the terminals of the active element are connected to a microstrip line coupled to the resonator. These lines with the resonator form a feedback path, and the device is therefore referred to as an oscillator with a 'feedback-type' resonator. The load forms part of the impedances Z_{31} or Z_{23}, which are connected to the third terminal of the transistor.

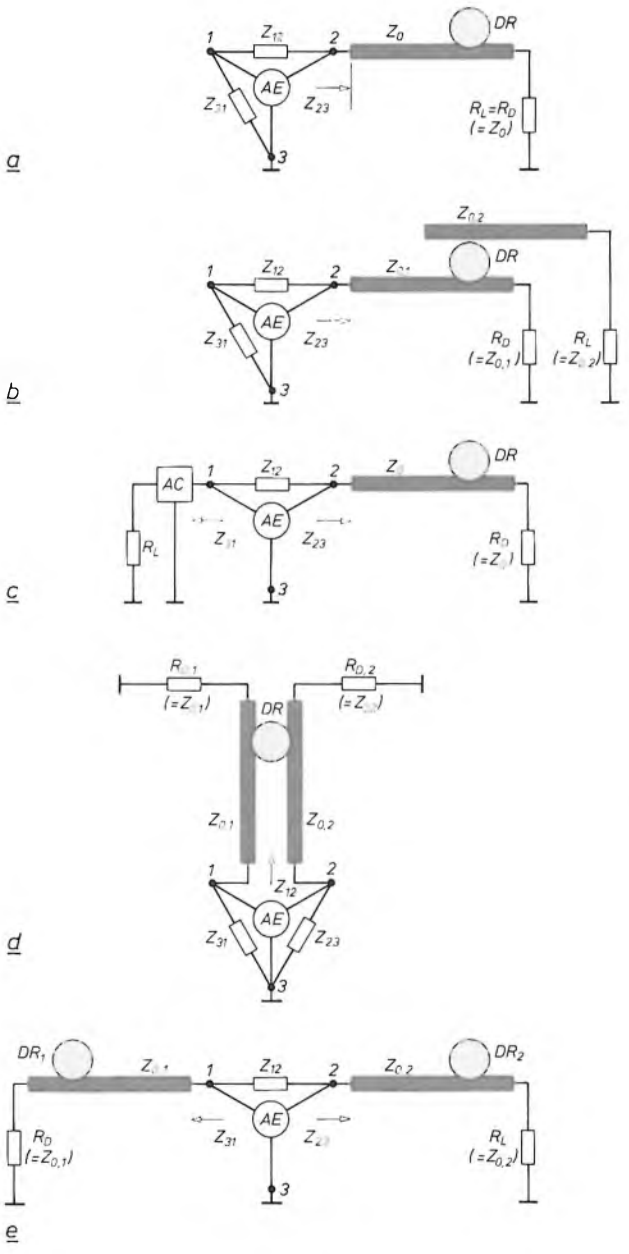

Fig. 7. The different oscillator circuits. *a*) Oscillator with reaction-type resonator. *1*, *2*, *3* terminals of the active element. Z_{12}, Z_{31}, Z_{23} impedances between the terminals. R_L load. R_D damping resistance. R_L and R_D are combined here to form a single resistance equal to the characteristic impedance Z_0 of the coupling line. *b*) Oscillator with transmission-type resonator. $Z_{0,1}$, $Z_{0,2}$ characteristic impedances of the coupling lines. *c*) Oscillator with reflection-type resonator. *AC* matching network for the load. *d*) Oscillator with feedback resonator. $R_{D,1}$, $R_{D,2}$ damping resistors in the coupling lines. *e*) Oscillator with two resonators: DR_1 and DR_2.

All these circuits have one resonator. However, two resonators can be used, which will give even better frequency stability; see fig. 7*e*. This circuit may be regarded as a combination of a reaction-type and a reflection-type resonator. The line with the reaction resonator is terminated by the load, the other by the damping resistance. A problem with this oscillator circuit is the mechanical tuning of the two resonators, since it only oscillates when both resonators are accurately tuned to the same frequency.

For completeness *fig. 8* shows the ways in which the base, collector and emitter of a bipolar transistor, or the source, drain and gate of a field-effect transistor can be connected to terminals *1*, *2* and *3* of the circuits in fig. 7. Fig. 8*a* relates to oscillators with the reaction-type or transmission-type resonator, fig. 8*b* to the oscillator with reflection-type resonator, and fig. 8*c* to the oscillator with feedback-type resonator. The first three circuits in fig. 7 also operate with Gunn or IMPATT diodes. Terminal *1* and the impedances Z_{12} and Z_{31} should then be omitted in fig. 7*a* and *b*. In fig. 7*c* terminal *1* should be omitted and the impedances Z_{12} and Z_{31} combined.

Frequency stability

The resonant frequency of the oscillator circuit varies slightly in practice. The variations may be divided into long-term and short-term variations. The long-term variations are a consequence of temperature fluctuations; their magnitude depends on the temperature coefficient τ_{f_0} for the oscillator resonant frequency f_0 (defined in a similar way to τ_{f_R}, see eq. 1). The short-term variations are random and are referred to as phase noise.

The temperature coefficient τ_{f_0} depends on the thermal behaviour of the active element, the dielectric resonator, the microstrip line and the case in which the microwave circuit is mounted. With a suitable design, the effect of the microstrip line and the case on τ_{f_0} can be made small compared with the effect of other elements. τ_{f_0} then depends almost entirely on the thermal characteristics of the active element and the resonator.

The temperature coefficient of the oscillator circuit can be expressed as [10]:

$$\tau_{f_0} = \frac{F(\beta)}{Q_R} \frac{d\phi_d}{dt} + \tau_{f_R}, \qquad (7)$$

where $F(\beta)$ is a function of the coupling factor and ϕ_d

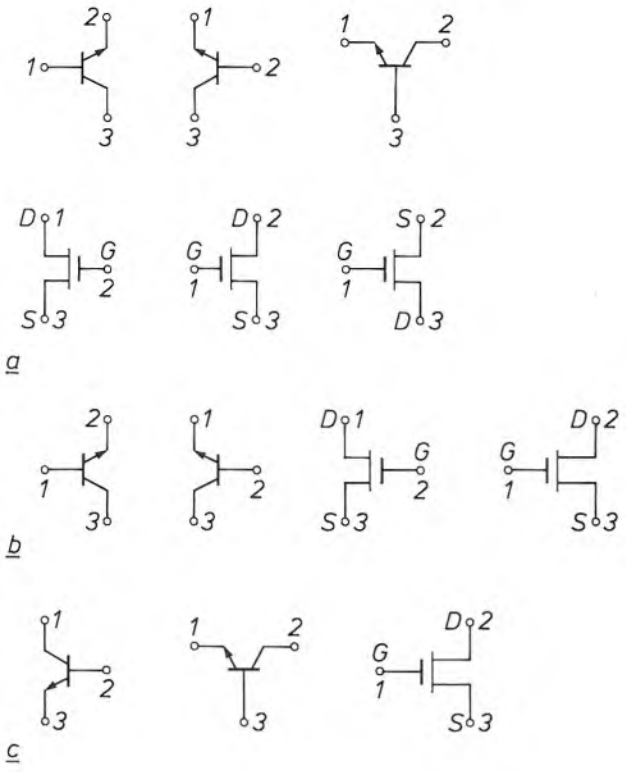

Fig. 8. The various ways in which a bipolar transistor or a field-effect transistor can be incorporated in the circuits of fig. 7. The numbering of the terminals corresponds to that in fig. 7. *a*) The active elements for the oscillators of fig. 7*a* and *b*. *b*) The active elements for the oscillator of fig. 7*c*. *c*) The active elements for the oscillator of fig. 7*d*.

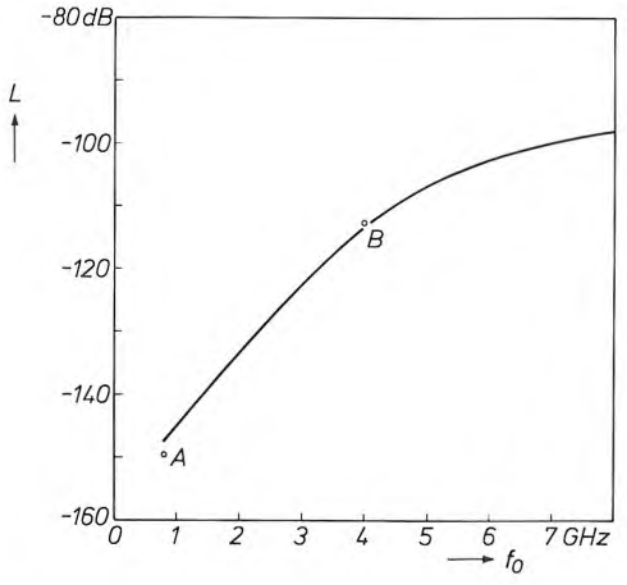

Fig. 9. Power density of the phase noise of microwave oscillators with dielectric resonators as a function of the oscillation frequency f_0. The curve is the result of an extrapolation using eq. (9) and literature data [13] (*A*) together with results of our own measurements (*B*). Plotted along the vertical axis is the ratio L in dB of the power density in W/Hz of the (single-sideband) power density spectrum of the phase noise at a distance of 10 kHz from the resonant frequency, and the output power of the oscillator.

is the argument associated with the input impedance Z_d of the active element (see fig. 5*c*). The first term in (7) is negative for all active (semiconductor) elements and has a value in the range from -2×10^{-6} to -10×10^{-6} °C^{-1}. Since $|\tau_{f_0}|$ should be as small as possible, τ_{f_R} should have a low positive value. The correct value of τ_{f_R} can be achieved, as we have seen, by using a mixed ceramic with a particular ratio of $Ba_2Ti_9O_{20}$ to $BaTi_4O_9$ for the resonator material, or by building a sandwich resonator of two different materials [11].

The (single-sideband) power density of the phase noise (i.e. the noise power per unit bandwidth) is generally related to the output power P_0 of the oscillator. This relative power density $L(f-f_0)$ of the phase noise at a 'distance' $f-f_0$ from the oscillator frequency is proportional to ${f_0}^2$ and the absolute temperature, and inversely proportional to the square of the Q-factor of the oscillator Q_0 [12]. If we compare two spectra of the phase noise at different frequencies f_0 and f_0', different output powers P_0 and P_0' and different Q-factors Q_0 and Q_0' at the same temperature, we obtain the following equation for the ratio of the relative power densities:

$$\frac{L(f-f_0)}{L'(f-f_0)} = \frac{{f_0}^2 {Q_0'}^2 P_0'}{{f_0'}^2 {Q_0}^2 P_0}. \qquad (8)$$

If in addition the coupling factors of the resonators are identical, the Q-factors of the oscillators in eq. (8) can be replaced by those of the resonators. It is also known that the maximum available output power of microwave oscillators is inversely proportional to the square of the oscillator frequency. Equation (8) can therefore be written as:

$$\frac{L(f-f_0)}{L'(f-f_0)} = \frac{{f_0}^4 {Q_R'}^2}{{f_0'}^4 {Q_R}^2}. \qquad (9)$$

This equation gives an idea of the phase noise to be expected at high frequencies. It has been used in *fig. 9* together with data from the literature [13] (point *A*) and data from our own measurements of relative power densities of the phase noise at 4 GHz (point *B*). The Q-factors Q_R are comparable, because resonators of pure $Ba_2Ti_9O_{20}$ were used in both cases. Fig. 9 and

[10] T. Makino and A. Hashima, A highly stabilized MIC Gunn oscillator using a dielectric resonator, IEEE Trans. **MTT-27**, 633-638, 1979;
C. Tsironis and V. Pauker, Temperature stabilization of GaAs MESFET oscillators using dielectric resonators, IEEE Trans. **MTT-31**, 312-314, 1983.

[11] C. Tsironis and P. Lesartre, Temperature stabilization of GaAs FET oscillators using dielectric resonators, Proc. 12th Eur. Microwave Conf., Helsinki 1982, pp. 181-186.

[12] K. Kurokawa, Injection locking of microwave solid-state oscillators, Proc. IEEE **61**, 1386-1410, 1973.

[13] G. D. Alley and H.-C. Wang, An ultra-low noise microwave synthesizer, IEEE Trans. **MTT-27**, 969-974, 1979.

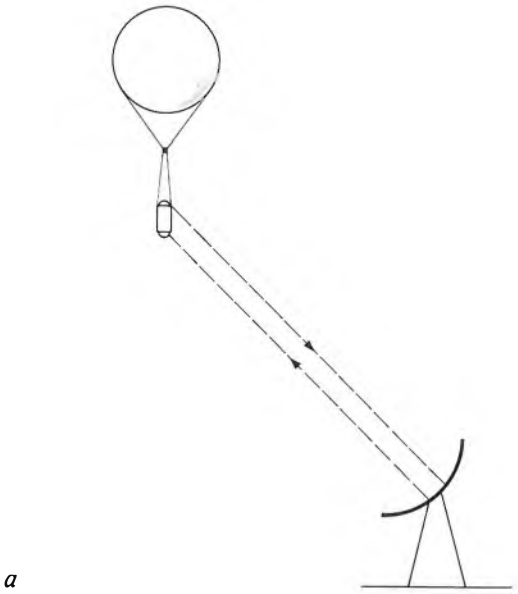

a

b

Fig. 10. *a*) Principle of locating the position of a radiosonde by means of a transponder, a combination of a transmitter and a receiver. The transponder, which is suspended from the balloon of the radiosonde, responds to a signal transmitted by a parabolic antenna on the ground. The position of the radiosonde can be determined from the angles at which the ground station receives a signal from the transponder, and from the time that elapses between the transmission and reception of the signal. *b*) The transponder, complete with antennas, which are located underneath the top and bottom shielding caps. The transmitted power is 200 mW and is sufficient for a range of 50 km. The transponder contains a microwave oscillator with dielectric resonator and is a product of the Philips GmbH supply centre Systeme und Sondertechnik in Bremen.

eq. (9) show that at high frequencies the phase noise increases steeply. It has also been found that bipolar transistors are very suitable for use in oscillator circuits with low phase noise.

Applications

Dielectric resonators will mainly be used to replace the cavity resonators now used for stabilizing microwave oscillators — for example in microwave receivers for satellite television [14]. In addition, various applications have emerged that would be inconceivable without dielectric resonators. Two of them will be described below.

An oscillator for a transponder in a radiosonde

A transponder is a combination of a transmitter and a receiver. Nowadays a radiosonde can carry a microwave transponder for locating its position; see *fig. 10*. The transponder must be small and light, and also inexpensive — since the transponder is not usually recovered after the flight.

The transponder responds to the signal from a transmitter on the ground. If the frequency and an identifying modulation of the signal correspond to preset input data, the transponder replies by sending out a signal at the same frequency with the same modulation. The position of the radiosonde can be determined from the time between the transmission of the search signal and the reception of the reply signal and from the angles from which the reply signal is received.

The signal in the transponder, which has a frequency of 9.2 GHz, is obtained by frequency-doubling and then amplifying the 4.6-GHz output signal of an oscillator. The signal is modulated by switching the oscillator on and off in a fixed pattern. Three different circuits have been developed for the oscillator, with reaction, transmission or reflection-type resonators; see fig. 7*a-c*. The active element of the oscillator circuits is a bipolar transistor, which is connected as shown in the second diagram in fig. 8*a* or *b*. The circuits are designed such that terminals *1* and *2* are not connected ($Z_{12} = \infty$). In the circuits with a reaction-type or transmission-type resonator (fig. 7*a* and *b*) Z_{31} is a purely capacitive feedback impedance. In the circuit with the reflection-type resonator (fig. 7*c*) the matching network AC transforms the load resistance of 50 ohms into a high resistance between collector and emitter. This circuit also has a capacitive feedback impedance between terminals *1* and *3*.

The value of the feedback impedance must be set very accurately, or the oscillator circuit will resonate in the $HE_{11\delta}$ or $TM_{01\delta}$ mode, whose resonances are at

frequencies close to that of the required $TE_{01\delta}$ mode; see fig. 1*c*. It is very difficult to set the frequency exactly, because the input impedance Z_d of the active element changes as a result of transients when the oscillator is switched on and off.

The three different oscillator circuits are illustrated in *fig. 11*. The type of circuit can be recognized from the shape of the lines on the ceramic substrate. The dielectric resonator of pure $Ba_2Ti_9O_{20}$ is mounted directly on the substrate and has a diameter of 14 mm and a height of 5 mm. The height of the aluminium case is therefore no more than 14 mm; the length and width are both 50 mm. The complete oscillator weighs as little as 80 g. The oscillation frequency can be tuned through a band of ± 30 MHz by means of a screw in the cap.

The transistors used in the circuits are leadless chips designed for microwave frequencies. At a supply voltage of 9 V and an input current of 32 mA, the output power of the oscillators is 30 mW. *Fig. 12a* gives a plot of frequency as a function of temperature for the transmission-type resonator. The curve corresponds to a temperature coefficient of -5.1×10^{-6} °C^{-1}. If the resonators had been made of $Ba_2Ti_9O_{20}$ with about 30% of $BaTi_4O_9$, the absolute value of the tem-

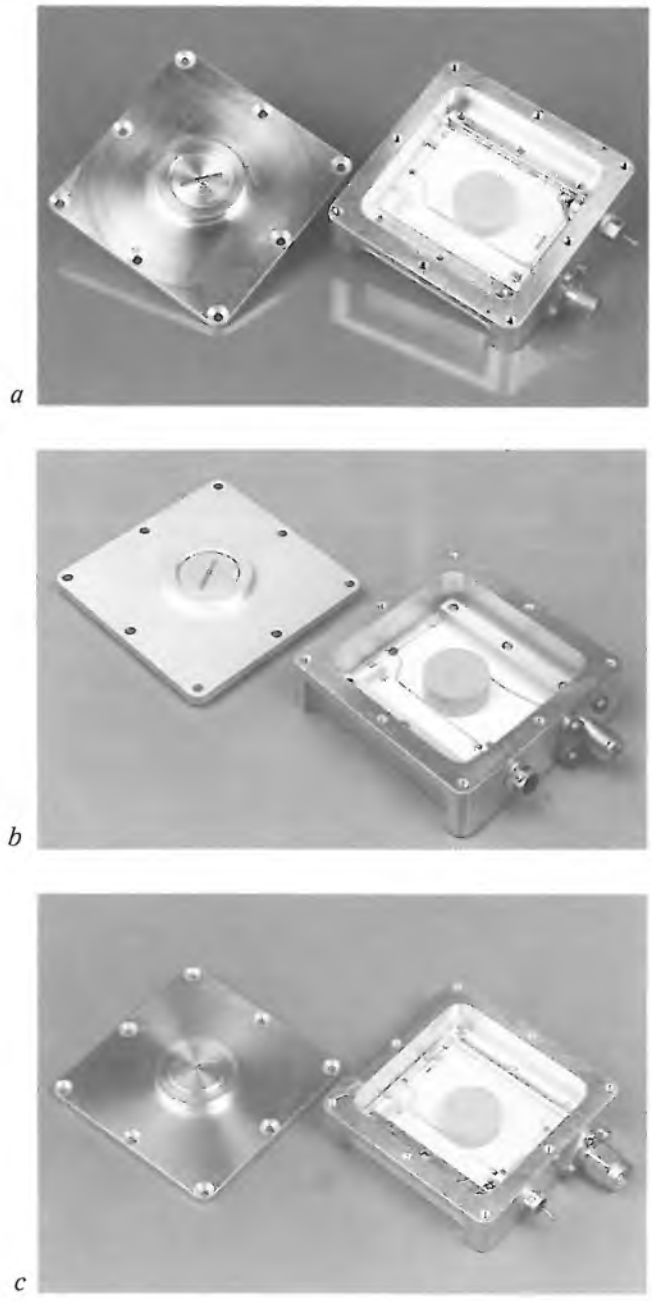

Fig. 11. The various oscillators for the transponder in fig. 10 that have been built and tested. *a*) Oscillator with reaction-type resonator. *b*) Oscillator with transmission-type resonator. *c*) Oscillator with reflection-type resonator. The tuning screw for fine tuning of the oscillator frequency is clearly visible in the cap of the housing of all three oscillators; see fig. 2*c*.

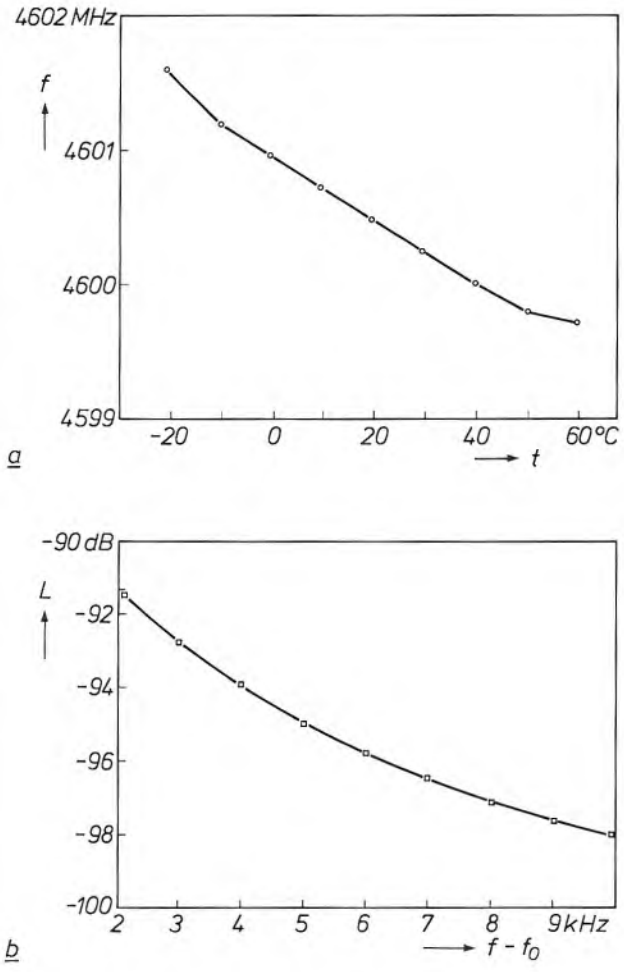

Fig. 12. *a*) Plot of the frequency f as a function of temperature t for the oscillator with transmission-type resonator in fig. 11*b*. (The corresponding temperature coefficient of -5.1×10^{-6} °C^{-1} can be improved by using a somewhat different composition for the resonator material.) *b*) The (single-sideband) power density spectrum of the phase noise of the oscillator with reaction-type resonator in fig. 11*a*. See also the caption to fig. 9.

[14] P. Harrop, P. Lesartre and T. H. A. M. Vlek, Low-noise 12 GHz front-end designs for direct satellite television reception, Philips Tech. Rev. **39**, 257-268, 1980.

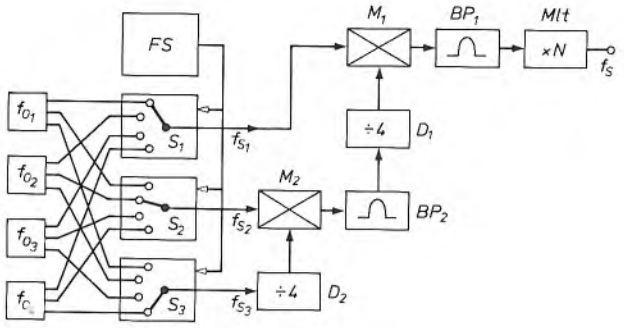

Fig. 13. Block diagram of the circuit of a direct microwave synthesizer. f_{O_1} to f_{O_4} microwave oscillators with different frequencies and stabilized by dielectric resonators. *FS* frequency selector. S_1 to S_3 four-position switches. f_{S_1} to f_{S_3} signals that can optionally have the frequency of one of the oscillators f_{O_1} to f_{O_4}. M_1, M_2 mixers. D_1, D_2 frequency dividers, for making the signal frequency four times smaller. BP_1, BP_2 bandpass filters. *Mlt* multiplier that multiplies the frequency of the signal by N. f_S output signal.

perature coefficient would have been even smaller and less than 10^{-6} °C^{-1}. Fig. 12*b* shows the result of noise-spectrum measurements on the circuit with the reaction-type resonator. The spectrum contains some amplitude noise as well as phase noise. The noise from the oscillator is so low that the result of the measurement almost corresponds to the noise spectrum of the highly sensitive spectrum analyser (Hewlett-Packard 8566 A).

The complete transponder, shown in fig. 10*b*, contains in addition to the oscillator circuit a number of batteries and the transmitting and receiving circuit with the accompanying antennas. The antennas are located underneath the protective caps at top and bottom. The transmission power is 200 mW, sufficient for a range of 50 km. The transponder is manufactured by the Philips GmbH supply centre Systeme und Sondertechnik, in Bremen.

Oscillators for direct frequency synthesis

Microwave synthesizers — circuits for synthesizing signals at microwave frequencies — are usually *indirect* synthesizers. This means that the frequency of the output signal is stabilized by a phase-locked loop (PLL) in the circuit. The operation of *direct* microwave synthesizers is based on the direct mixing of highly stable reference signals. Circuits in which the reference signals are generated by oscillators stabilized by cavity resonators tend to be rather large. Compact circuits that give a stable output signal can be built using oscillators with dielectric resonators [15].

Fig. 13 shows a possible block diagram for such a circuit. There are four oscillators, and the output signal can have 64 different frequencies. The oscillators are connected to the output by switches, mixers, bandpass filters, dividers and a multiplier. The frequency f_S of the output signal is given by

$$f_S = N\left(f_{S_1} + \frac{f_{S_2} + f_{S_3}/4}{4}\right),$$

where f_{S_1}, f_{S_2} and f_{S_3} are each set equal to one of the frequencies f_{O_1}, f_{O_2}, f_{O_3} or f_{O_4} of the oscillators. The multiplication factor N of the multiplier can be small when dielectric resonators are used. Large values of N are necessary when crystal-stabilized oscillators are used, since these oscillators operate at a frequency of about 100 MHz. A high value of N increases the noise component in the output signal. Circuits using microwave oscillators stabilized by dielectric resonators can therefore deliver an output signal that combines high stability with very low noise.

[15] G. Lütteke, Dielectric resonator stabilised reference oscillators, IEE Colloq. on Microwave programmable sources and frequency synthesis, London 1981, pp. 3/1-3/4.

Summary. Dielectric resonators can be used to stabilize the frequency of the output signal of microwave integrated oscillators. Oscillators of this kind will be widely used in the near future in microwave receivers for satellite-television broadcasts. The required high Q-factor, low temperature-dependence and small dimensions of dielectric resonators only became feasible with the availability of mixed ceramics of $Ba_2Ti_9O_{20}$ and $BaTi_4O_9$ or TiO_2. These materials can be evaluated for their usefulness by generating microwave resonances in cylindrical samples and measuring the frequency spectra. In practice, dielectric resonators are discs. They are mounted in a metal case and can be mechanically tuned to the required frequency. The resonators have a small positive temperature coefficient to compensate for the negative temperature coefficients of other elements in the oscillator circuit. A locus for the impedance of coupling line, resonator and load of the active element in the oscillator circuit as a function of oscillation frequency can be drawn on the Smith chart. The intersection of this locus with the line for the input impedance of the active element gives the operating point. The position of the operating point may be stable or unstable. The oscillator circuits are designed for operation with reaction-type, transmission-type, reflection-type or feedback resonators. Stable oscillator circuits have been designed for transponders used in radiosondes. The use of dielectric resonators in oscillators for direct frequency synthesizers has also been investigated.

Scientific publications

These publications are contributed by staff from the laboratories and other establishments that form part of or are associated with the Philips group of companies. Many of the articles originate from the research laboratories named below. The publications are listed alphabetically by journal title.

Philips GmbH Forschungslaboratorium Aachen, Weißhausstraße, 5100 Aachen, Germany — *A*
Philips Research Laboratory Brussels, 2 avenue Van Becelaere, 1170 Brussels, Belgium — *B*
Philips Natuurkundig Laboratorium, Postbus 80 000, 5600 JA Eindhoven, The Netherlands — *E*
Philips GmbH Forschungslaboratorium Hamburg, Vogt-Kölln-Straße 30, 2000 Hamburg 54, Germany — *H*
Laboratoires d'Electronique et de Physique Appliquée, 3 avenue Descartes, 94450 Limeil-Brévannes, France — *L*
Philips Laboratories, N.A.P.C., 345 Scarborough Road, Briarcliff Manor, N.Y. 10510, U.S.A. — *N*
Philips Research Laboratories, Cross Oak Lane, Redhill, Surrey RH1 5HA, England — *R*

H. Boulard, Y. Kamp, H. Ney & C. J. Wellekens *B, H*	Speaker-dependent connected speech recognition via dynamic programming and statistical methods	Biblioth. Phonet. **12**	115-148	1985
J. B. H. Peek *E*	Digitale Signalverarbeitung, ein Fachgebiet mit wachsender Bedeutung	E & M **103**	163-169	1985
L. M. G. Feijs & J. H. Obbink *E*	Process models: methods as programs	ESPRIT '85, Elsevier Science, Amsterdam	577-591	1986
G. F. M. Beenker, T. A. C. M. Claasen & P. J. van Gerwen *E*	Design of smearing filters for data transmission systems	IEEE Trans. **COM-33**	955-963	1985
M. J. H. van de Steeg, H. L. Peek, J.G.C.Bakker, J.A.Pals, B.G.M.H. Dillen & J. M. A. M. Oppers *E*	A frame-transfer CCD color imager with vertical antiblooming	IEEE Trans. **ED-32**	1430-1438	1985
H. D. Hinz & H. Löbl *H*	Electrophoretic recording of electronically stored radiographs	IEEE Trans. **MI-4**	39-43	1985
F. H. P. M. Habraken*, R. H. G. Tijhaar*, W. F. van der Weg* (* *Univ. Utrecht*), A. E. T. Kuiper & M. F. C. Willemsen *E*	Hydrogen in low-pressure chemical-vapor-deposited silicon (oxy)nitride films	J. App. Phys. **59**	447-453	1986
E. F. Stikvoort *E*	Digital dynamic range compressor for audio	J. Audio Eng. Soc. **34**	3-9	1986
P. C. M. Gubbens*, A. M. van der Kraan* (* *Interuniv. Reactor Inst., Delft*) & K. H. J. Buschow *E*	Crystal field in Tm_2Ni_{17}	J. Magn. & Magn. Mater. **54-57**	483-484	1986
P. Haaker, E. Klotz, R. Koppe, R. Linde & H. Möller *H*	A new digital tomosynthesis method with less artifacts for angiography	Med. Phys. **12**	431-436	1985
P. Delsarte, Y. Genin & Y. Kamp *L*	Pseudo-Carathéodory functions and Hermitian Toeplitz matrices	Philips J. Res. **41**	1-54	1986
K. H. J. Buschow & D. B. de Mooij *E*	Structural and magnetic characteristics of several ternary compounds of the type GdX_2Si_2 and UX_2Si_2 (X = 3d, 4d or 5d metal)	Philips J. Res. **41**	55-76	1986
J. Haisma, U. K. P. Biermann, J. Peersman & P. C. Zalm *E*	Resistance modification of indium-oxide layers by laser annealing and ion bombardment respectively	Philips J. Res. **41**	77-81	1986
U. Neitzel (*CHF Müller Med.-Tech. Syst., Hamburg*), J. Kosanetzky & G. Harding *H*	Coherent scatter in radiographic imaging: a Monte Carlo simulation study	Phys. Med. & Biol. **30**	1289-1296	1985
W. Hoving*, P. M. L. O. Scholte*, P. Dorenbos*, G. A. Fokkema*, E. A. G. Weits*, F. van der Woude* (* *Univ. Groningen*), I. Vincze (*Hungarian Acad. Sci., Budapest*) & K. H. J. Buschow *E*	Packing and chemical effects in amorphous Fe-Zr and Fe-B alloys	Phys. Rev. B **32**	8368-8371	1985

G. Duggan, H. I. Ralph & K. J. Moore *R*	Reappraisal of the band-edge discontinuities at the $Al_xGa_{1-x}As$-GaAs heterojunction	Phys. Rev. B **32**	8395-8397	1985
J. Landman*, W. D. Luedtke*, R. N. Barnett*, C. L. Cleveland*, M. W. Ribarsky* (* *Georgia Inst. Technol., Atlanta, GA*), E. Arnold, S. Ramesh, H. Baumgart, A. Martinez & B. Khan *N*	Faceting at the silicon (100) crystal-melt interface theory and experiment	Phys. Rev. Lett. **56**	155-158	1986
A. A. Jafari (*City Univ., New York*), T. N. Saadawi & M. Schwartz *N*	Blocking probability in two-way distributed circuit-switched CATV	Proc. GLOBECOM '85, New Orleans 1985	868-875	1985
A. H. Reader, F. W. Schapink* & S. Radelaar* (* *Univ. Technol. Delft*) *E*	Grain growth in heavily implanted LPCVD polysilicon layers during annealing	Proc. Microsc. Semicond. Mater. Conf., Oxford 1985	151-156	1985
G. Duggan, H. I. Ralph & R. J. Elliot (*Dept. Theor. Phys., Oxford*) *R*	Quantisation effects and interface recombination in GaAs-(AlGa)As quantum wells	Proc. MRS Conf., Strasbourg 1985	37-40	1985
G. Duggan, H. I. Ralph, K. S. Chan* & R. J. Elliott* (* *Dept. Theor. Phys., Oxford*) *R*	Exciton binding energy in quantum wells including the heavy-light hole interaction	Proc. MRS Conf., Strasbourg 1985	47-51	1985
B. A. Joyce, J. H. Neave, P. J. Dobson, K. Woodbridge & J. Zhang (*Imp. College, London*) *R*	RHEED oscillations and surface structure of MBE-grown GaAs-(Al,Ga)As	Proc. MRS Conf., Strasbourg 1985	135-139	1985
H. Dimigen, H. Hübsch, P. Willich & K. Reichelt (*Kernforschungsanlage Jülich*) *H*	Stoichiometry and friction properties of sputtered MoS_x layers	Thin Solid Films **129**	79-91	1985
W. Benecke*, H. Dimigen, P. Eichinger+, H. G. Feller*, U. Jahns+, R. Klinger* (* *Tech. Univ. Berlin*), K. Kobs, R. Leutenecker+, H. Ryssel+, H.-P. Spöhrle+ & K. H. Zeller+ (+ *Fraunhofer-Inst., München*) *H*	Tribologisches Verhalten Stickstoff-implantierter Stähle	Tribologie — Reibung/ Verschleiss/Schmierung, Springer, Berlin	335-365	1985

Contents of Philips Telecommunication Review **44**, No. 1, 1986

Contents of Electronic Components & Applications **7**, No. 4

Volume 43, No. 1/2 pages 1-48 Published 16th December 1986

PHILIPS

PHILIPS

A. J. P. Theuwissen and C. H. L. Weijtens: The accordion imager, a new solid-state image sensor,
Philips Tech. Rev. **43**, No. 1/2, 1-8, Dec. 1986.

Solid-state image sensors are silicon chips in which a charge distribution is generated by incident light. The use of such devices in video cameras for the consumer market will depend greatly on the price of the sensor. As with all chips, this is closely dependent on the chip area. With a new read-out mechanism, in which the charge distribution is stretched out and squeezed shut like an accordion, it is possible to build an image sensor with two electrodes instead of the usual four for each line of the frame. The new sensor can be produced with the same technology as used for the four-phase sensor. The electronic control circuits can be fabricated on the chip with the sensor in a single process.

J. J. G. Willems: Investigation of a new type of rechargeable battery, the nickel-hydride cell,
Philips Tech. Rev. **43**, No. 1/2, 22-34, Dec. 1986.

$LaNi_5$ and related compounds have been investigated for their usefulness as electrode material in hydrogen-based rechargeable batteries. Although $LaNi_6$ and $LaNi_4Cu$ give the required rapid absorption and desorption of large amounts of hydrogen, they are not suitable electrode materials because of the very large decay in their storage capacity with repeated charging and discharging. It was found that this capacity loss is due to the conversion of the active material into $La(OH)_3$, which proceeds more rapidly as the volume changes in the active material caused by repeated charging and discharging become larger. Partial substitution of Co for Ni gives smaller volume changes and hence a more stable electrode material. The stability is further improved by adding small quantities of aluminium or silicon. The capacity of electrodes made from the newly developed $La_{0.8}Nd_{0.2}Ni_{2.5}Co_{2.4}Si_{0.1}$ was found to have decayed by only 30% after 1000 charge and discharge cycles. The experimental — hermetically sealed — nickel-hydride battery made with this material combines a long life with high energy density and power density, and effective protection from overcharging and overdischarging. It also contains no toxic heavy

Name

Initials

Title

Address

stamp
as
postcard

Administration Department
Philips Technical Review

Philips Research Laboratories
Building WBp 42

P.O. Box 80 000

5600 JA Eindhoven
The Netherlands

Supplement to Philips Technical Review
Bijlage van Philips Technisch Tijdschrift
No. 33

October 1986

Recent United States Patents

Abstracts from patents that describe inventions from the following research laboratories, which form part of or cooperate with the Philips group of companies:

Philips GmbH Forschungslaboratorium Aachen, Weißhausstraße, 5100 Aachen, Germany	*A*
Philips Research Laboratory Brussels, 2 avenue Van Becelaere, 1170 Brussels, Belgium	*B*
Philips Natuurkundig Laboratorium, Postbus 80000, 5600 JA Eindhoven, The Netherlands	*E*
Philips GmbH Forschungslaboratorium Hamburg, Vogt-Kölln-Straße 30, 2000 Hamburg 54, Germany	*H*
Laboratoires d'Electronique et de Physique Appliquée, 3 avenue Descartes, 94450 Limeil-Brévannes, France	*L*
Philips Laboratories, N.A.P.C., 345 Scarborough Road, Briarcliff Manor, N.Y. 10510, U.S.A.	*N*
Philips Research Laboratories, Cross Oak Lane, Redhill, Surrey RH1 5HA, England	*R*
Philips Research Laboratories Sunnyvale, P.O. Box 9052, Sunnyvale, CA 94086, U.S.A.	*S*

4 574 329

Multilayer ceramic capacitor

A. J. H. Eijkelenkamp *E*
G. de With
W. R. de Wild

A multilayer ceramic capacitor characterized by a stack of alternate layers of dielectric oxide ceramic material and of electrode layers consisting of a mixture of a metal having a high electric conductivity and ceramic particles of a material having a sintering temperature which is above the sintering temperature of the oxidic ceramic material of the dielectric layers. As a result of this electrode layer composition, the capacitor can be manufactured by means of a uniaxial pressure sintering process in which the stack is sintered while simultaneously applying pressure in the direction transverse to the plane of the layers. This leads to dielectric layers which are substantially free from pores and have a thickness of at most 20 μm.

4 574 445

Method and apparatus for manufacturing a nozzle plate for ink-jet printers

H. Bentin *H*
M. Döring
H. Kronenberg
W. Jeglinski

Nozzles are formed in a plate for an ink-jet printer by holding a metal foil tightly against the side of the plate from which the nozzle is to protrude, and then pressing and punching through the plate and the metal foil together, through an aperture of a pressing die into a cushion of a hard elastic material such as lead. The foil is made of an isotropic material which is harder than that of the nozzle plate, and is preferably an amorphous or microcrystalline metal.

4 574 468

Method of manufacturing a semiconductor device having narrow coplanar silicon electrodes

J. W. Slotboom *E*
H. G. R. Maas
J. A. Appels
F. M. Klaassen

A method of manufacturing a semiconductor device, for example an SPS memory having narrow coplanar silicon electrodes. The electrodes are formed by etching grooves or slots having a width in the submicron range into a polycrystalline silicon layer, the slot width being defined by the oxidized edge of a silicon auxiliary layer. The electrodes are alternately covered by silicon oxide and by a layer comprising silicon nitride. According to the invention, the electrodes formed covered by silicon oxide are first interconnected pairwise, whereupon they are separated from each other in a separate etching step and are provided with self-aligned contact windows. Thus, the very narrow electrodes can be contacted without technological problems and memory cells of very small dimensions can be obtained.

4 574 635

Monitoring of frequency shift of ultrasound pulses in tissue

P. J. 't Hoen *N*

A zero crossing detection circuit for estimating the ultrasonic attenuation in a region of interest in the body from a signal which is representative of pulses of ultrasound energy reflected from said region. The ultrasound attenuation is estimated from the center frequency of the returned energy as measured at various depths in the body.

4 575 462

Method of growing an alloy film by a layer-by-layer process on a substrate, and a method of making a semiconductor device

P. J. Dobson R
C. T. Foxon
J. H. Neave

A method of growing an alloy film by a layer-by-layer process on a substrate is described, together with a method of making a semiconductor device in which an alloy film is grown on a substrate by a layer-by-layer process. The atomic ratio of constituents present in the alloy film is determined during growth of the film from the growth rates of the alloy film and of at least one intermediate film consisting of at least one constituent of the alloy. The intermediate film or films are grown between the alloy film and the substrate. During growth of each film, the growth surface is irradiated with a beam of electrons and measurement is carried out of the period of oscillations in the intensity of the stream of electrons diffracted at the growth surface, or specularly reflected by the growth surface, or emitted from the growth surface, or of the current flowing to ground through the substrate. These periods are equal to the respective times taken to grow on a monolayer of the respective film.

---

4 575 698

Surface acoustic wave device

J. Schofield R

A low insertion loss surface acoustic wave filter in which withdrawal weighted launching and output transducers are acoustically coupled by two high efficiency reflective multistrip couplers. To reduce the insertion loss, the inner bus bars are reduced in width so as to reduce the dead space in the coupler. this makes it impossible to form a reliable wire bond connection to the inner bus bars which are therefore connected via a conducting path across the propagation path at the ends of the transducers. Further reduction in the widths of the inner bus bars and consequent increase in resistive losses are offset by several connections to a further bus via groups of dummy electrodes arranged at null points in the weighting pattern.

---

4 576 046

Device for the examination of objects by means of ultrasound echography

M. A. Fink L
J.-F. Cardoso

A device for scanning objects by means of ultrasound echography, comprising at least one ultrasound transducer which is connected to a transmitter stage and to a receiver stage which comprises an amplifier, a correction circuit for the correction of the gain as a function of time, and a processing circuit for the processing of the results of the echographic examination. The receiver and processing stage also comprise a circuit which is connected to the output of the assembly formed by the amplifier and the gain correction circuit and which comprises means for determining the instantaneous frequency and the instantaneous energy of the echographic signal, means for weighting the instantaneous frequency with the instantaneous energy, and a diffraction correction circuit.

---

4 576 833

Method of forming a luminescent layer on a carrier and low-pressure mercury vapour discharge lamp having a layer applied to a carrier by means of such a method

P. C. Scholten E
R. K. Eijnthoven

A method of forming a luminescent layer on a glass carrier (such as the wall of a discharge vessel of a low-pressure mercury vapour discharge lamp) from a suspension of grains of a luminescent material and a quantity of binder in a suspension medium. According to the invention, the suspension medium preferably consists of water and the binder mainly comprises fibrous crystals of boehmite.

4 577 123

Integrated logic circuit having collector node with pull-up and clamp

J. D. P. van den Crommenacker E
J. Lohstroh

A logic circuit of the I^2L, the ISL or the STL type having a signal input formed by the control electrode of an inverter transistor and plural signal outputs each coupled through a diode to a main electrode of the inverter transistor, this main electrode being connected to a supply line through a pull-up connection. The improvement relates to a further connection path comprising a Schottky diode and a resistor which bridges the main current path of the inverter transistor and which reduces the voltage swing at the main electrode.

---

4 577 129

Electric motor having two co-planar stator sections

L. Bertram H

An electric motor having two stator sections having co-planar central parts extending between first and second co-planar pole pairs. An excitation coil is provided around each stator central part, and the pole shoes forming the pole pairs are spaced from the coil ends. The stators are preferably laminated from iron sheets, corresponding parts of the sheets of the two sections being co-planar.

---

4 578 602

Voltage signal translator

J. A. West S
T. D. Fletcher

A bipolar signal translator contains a pair of transistors arranged as a current mirror with their emitters coupled to a voltage supply by way of a pair of impedance elements that improve stability. Their collectors are coupled through another pair of impedance elements to an input transistor and to a device circuit. The collector of one of the current-mirror transistors is coupled to the base of an output transistor whose collector is preferably coupled through an output impedance element to a current-control transistor that improves power utilization.

---

4 578 613

Diaphragm comprising at least one foil of piezoelectric polymer material

A. Posthuma de Boer E
J. W. Vegt

An electro-acoustic device comprising at least one diaphragm including a foil of a piezo-electric polymer material. In the rest condition the diaphragm is maintained in a curved position under mechanical prestress freely mounted by means of a curved chassis and/or an elastic support with a non-flat supporting surface. The diaphragm is given such a curved shape associated with the rest condition and is provided with electrodes so that changes in surface shape in accordance with the electrical signals and the attendant non-linear conversion into acoustic signals by portions of the diaphragm is combined with similar surface changes of other portions of the diaphragm. The conversion into acoustic signals by the other portions amplifying those of the first-mentioned portions for the fundamental frequency of the signals, whereas the other portions and the first-mentioned portions compensate one another for the even harmonics of the signal. The diaphragm may comprise an assembly of two foils of an anisotropic piezo-electric polymer material which are fixed to each other over the entire surface area with their preferred directions extending at an angle relative to each other. Another preferred construction has a freely mounted diaphragm which consists of at least two oppositely curved parts. The diaphragm is locally provided with electrodes on both sides arranged at the location of maximum curvature of each curved part.

4 578 637

Continuity/leakage tester for electronic circuits

R. J. Allen *S*
R. W. Youden

A device for testing continuity and current leakage at leads of an electronic circuit such as an integrated circuit has a contact structure having test terminals for contacting the leads. A first and a second of the leads are power supply leads respectively contactable with a first and a second of the test terminals. Continuity/leakage detection is done with one or more corresponding detection circuits. Each detection circuit has a channel along which both continuity and leakage are tested. A supply switching circuit appropriately switches voltages between values suitable for continuity testing and values suitable for leakage testing.

---

4 578 651

Magnetooptical modulator

H. Heitmann *H*
W. Tolksdorf
F. Welz
K. Witter

In a magnetic layer of a magnetooptical modulator having fixed magnetic single domain areas, the areas of the layer present between the single domain areas are made electrically conductive by reduction.

---

4 578 777

One step write circuit arrangement for EEPROMs

S. Fang *S*
K. K. Rao

A novel write circuit arrangement for an EEPROM type memory system operable in response to the difference between the information stored in each addressed cell and the information to be stored therein during a writing cycle and writing information into only those addressed cells for which a difference exists regardless of whether the difference indicates to charge or discharge the cell. The arrangement also can simultaneously charge one cell of a byte while discharging another cell of the same byte.

---

4 579 451

Tubular cuvette for atomic absorption spectrometry

B. Lersmacher *A*

A cuvette for atomic absorption spectrometry includes a tube of pyrolytic graphite, electrographite or vitreous carbon with flanges provided at the ends of the tube, or in the proximity thereof, and having a common envelope of pyrolytic graphite. The flanges consist of solid layers of pyrolytic graphite in which the layer planes of the pyrolytic graphite are either directed perpendicularly to the longitudinal axis of the tube, or extend everywhere parallel to the longitudinal axis and the surface of the tube. Cuvettes with flanges having an orientation of the solid layer planes directed perpendicularly to the longitudinal axis of the tube are considered and operate as 'fast', whereas those having an orientation extending everywhere parallel to the longitudinal axis are considered.

---

4 580 154

Insulated-gate field-effect transistors

D. J. Coe *R*

An insulated-gate field-effect transistor which may be of a vertical power D-MOS type includes surface-adjacent source and emitter regions surrounded in a semiconductor body by a surface-adjacent second region of opposite conductivity type. A third region adjoins the second region and has a lower conductivity-type determining doping concentration. At least a part of these second and third regions is located in a main current path from the source region to a drain of the transistor, and an insulated gate, which may be of metal-silicide, capacitively controls a conductive channel at least in this part of the second region. The emitter region is located at a side of the source region remote from the channel part and is separated therefrom by an intermediate part of the second region. The source region is electrically connected to this intermediate part, for example by a short-circuiting metal-silicide layer. A resistive current path in the second region is present below the emitter region and extends from this intermediate part to a further part of the second region, for example by a short-circuiting metal-silicide layer. A source electrode is electrically connected to this further part so as to be electrically connected via the resistive current path to the source region. The emitter region serves to modulate the conductivity of the third region and thus reduce the drain series resistance of the transistor by charge-carrier injection from the intermediate part when the source-drain current along the resistive current path is sufficient to forward-bias the intermediate part with respect to the third region.

---

4 580 237

Digital tone control arrangement

L. D. J. Eggermont *E*
P. J. Berkhout

Digital tone control arrangement for a digital audio signal, comprising a recursive digital filter whose transfer function contains as many poles as there are zeros, the recursive filter also comprising a recursive portion and a non-recursive portion each receiving filter coefficients which are stored in a memory means. So as to limit the total number of filter coefficients the memory means is divided into a first memory field for storing a first sub-group of filter coefficients and into a number of second memory fields in each of which a second sub-group of filter coefficients is stored. By means of a switching device the first sub-group of the filter coefficients is applied either to the non-recursive portion or to the recursive portion and a selected second sub-group of filter coefficients is applied to that portion (recursive and the non-recursive) to which the first sub-group of filter coefficients is not applied.

---

4 580 283

Two-crystal X-ray spectrometer

J. Hornstra *E*

A two-crystal X-ray spectrometer in which hinged radius arms carry respective crystals at equal radii, and a spectrometer wavelength adjustment modifies the angular disposition of the source and detector about the corresponding crystals at half the hinge angle rate. Hitherto the crystals were mounted radially. The improvement consists of displacing the crystals, through opposite angles φ to the radius line, where φ lies in the range of from 50 to 70 degrees. This enables the glancing incidence angle θ to be adjusted from 0 to 75 degrees without obstruction of the beam due to the detector. To reduce the detector background due to scattered radiation, screening blades are moved perpendicularly to the center of the respective crystal surface just clear of the spectrometer beam. This enables the arrangement to be more compact than the prior use of Soller slits.

---

4 581 159

Voltage-dependent resistor and method of manufacturing same

D. Hennings *A*
A. Schnell
H. Schreinemacher

A voltage-dependent resistor having a low operational field strength with a ceramic sintered body on the basis of a polycrystalline alkaline earth metal titanate doped with a small quantity of a metal oxide so as to produce an n-type conductivity, in which the sintered body comprises at its grain boundaries insulating layers formed by in-diffusion of at least a metal oxide or at least a metal oxide compound and comprises of an alkaline earth metal titanate having Perowskite structure of the general formula: $(A_{1-x}Ln_x)TiO_{3-y}TiO_2$ or $A(Ti_{1-x}Me_x)O_{3-y}TiO_2$, wherein A = alkaline earth metal; Ln = rare earth metal and Me = metal having a valency of 5 or more; $0.0005 < x <$ solubility limit in the Perowskite phase; $y = 0.001$ to 0.02. The insulating layers are formed in that the sintered body is covered on its surface with a suspension containing at least a metal oxide having a comparatively low melting-point as compared with the sintered body or at least a metal oxide compound having a comparatively low melting-point with respect to the sintered body and is tempered in an oxidizing atmosphere at a temperature which is above the melting-point of the suspension component(s).

4 581 492

Digital duplex communication system

N. S. Virdee *R*

A digital duplex communication system includes an echo canceller of the look-up table type. The echo canceller has a random access memory (RAM), a digital to analog converter (DAC), a subtractor, adaption means, and an address generator. The echo canceller stores echo replicas for combinations of data bits transmitted by the transmitter and subtracts these echo replicas from a received signal on line before application to the receiver. The capacity required for the RAM is reduced by storing only one echo replica for each of two complementary sets of data. To achieve this the address generator is split into a primary address generator and a complementary address generator so that complementary sets of data present the same address to the RAM. The primary address generator produces a signal to indicate which of the two complementary data sequences is being transmitted and appropriately sets the adaption means over line and a complementing circuit over line. The combination of the signal on line and the output of the subtractor on line causes the echo replica to be updated by the adaption means which may be an adder circuit. The complementing circuit operates on the output of the RAM via the latch circuit to determine the sign of the echo replica applied to the subtractor via the DAC.

---

4 581 750

Transmission system for the transmission of binary data symbols

A. H. Dieleman *E*

Transmission system for bi-phase modulated signals. Generally receiving filters for these signals will have a frequency response up to twice the bit frequency (twice 1/T) passband. For coloured noise whose power increases as the frequency increases this may mean a considerable deterioration of the signal-to-noise ratio compared with the signal-to-noise ratio for unmodulated NRZ-signals. In order to increase the signal-to-noise ratio a receiving filter is used in this case, whose frequency response approximates zero above the bit frequency (1/T) (stopband) and which for lower frequencies is determined such that after filtering a predominantly three-level signal is obtained. The binary data signal can be derived from this signal by rectification and slicing.

---

4 582 535

Invar alloy on the basis of iron having a crystal structure of the cubic $NaZn_{13}$ tye,m an article herefrom

K. H. J. Buschow *E*

An Invar type alloy on the basis of iron is formed by an intermetallic compound having a cubic crystal structure of the $NaZn_{13}$ type having a nominal composition $La(FeCoX)_{13}$, wherein X is Si or Al. By subjecting the present intermetallic compound after melting to a tempering treatment at 800-1000 °C and cooling it in an accelerated manner, a brittle material is obtained which can be ground to form a powder. From this powder, articles having any desired (optionally complicated) shape can be produced by means of powder metallurgy. By mixing powders of two different intermetallic compounds, a material can be obtained having a substantially negligible coefficient of linear thermal expansion in the temperature range of from 0 to 200 °C.

---

4 583 063

Piezo-electric resonator or filter having slots formed which impede undesired vibrational energy

R. F. Milsom *R*

A resonator or filter which comprises a bar of piezoelectric material provided with electrodes which are spaced from the two ends of the bar. In operation, thickness shear vibrations occur between the electrodes and the bar. Width to thickness ratio is such that said vibrations in turn produce Nth harmonic flexure vibrations which propagate across the bar width, N being an even number. In order to accelerate the rate of decay of the vibrations towards the (supported and hence energy-absorbant) ends of the bar, and thus to reduce the distance between the electrodes and the ends of the bar for a given quality factor, (N/2 − 1) slots, some of which may be omitted, are provided in each of these ends so that each end is divided into N/2 prongs of equal width.

---

4 583 087

Matrix display device with diode switching elements

J. L. M. van de Venne *E*

In order to provide a passive electro-optical display medium in a matrix display device with a sufficiently steep threshold with respect to the applied voltage and having a memory, a switching element is placed in series having each picture element. The switching element is provided between a picture electrode of each picture element and a driving electrode. The switching element is formed by a polysilicon island in which n^+-doped regions are provided which are separated by a p-doped region. As a result of this, two series-arranged, oppositely directed p-n junctions are formed of which one is always reverse biased. The width of the p-doped regions is so small that punch-through occurs between the two p-n junctions before one of the p-n junctions breaks down. Due to the occurrence of punch-through, the series resistance of the switching element is negligibly small so that a favourable R_{ON}/R_{OFF} ratio is obtained and the picture elements can be driven with comparatively low voltages.

---

4 583 119

Signal interface circuit

J. A. Roscoe *R*

A synchronizing signal interface circuit for a television monitor comprises two exclusive-NOR gates, which function as controllable inverters. Line and field sync. signals applied at respective input terminals are fed to signal inputs of the gates, and integrated versions of these signals are produced by respective integrators and fed to control inputs. Each of the line and field sync. signals has a duty cycle which results in the logic level (0 or 1) of the sync. pulses of the signal being opposite to the logic level (1 or 0) of the integrated version. Due to the exclusive-NOR function of the gates, the logic level or polarity of the output sync. signal pulses will always be the same (negative), for both negative and positive polarity of the input sync. signal pulses. A gate combines the output sync. signal pulses to produce a composite sync. signal.

---

4 583 243

X-ray tube for generating soft X-rays

W. H. Diemer *E*
P. Hokkeling
H. F. M. Wagemans

In an X-ray tube, particularly for the detection of elements having a low atomic number by X-ray spectral analysis, an anode support is on the target side provided with a layer of scandium. The scandium layer is provided on the support by adhesion via an intermediate layer, preferably of chromium. In a reflection tube, the anode support for the intermediate layer and the scandium layer is preferably made of silver or copper. In a transmission tube, the scandium is provided on a beryllium disc which acts as intermediate layer and as an exit window.

---

4 585 156

Mold and method of manufacturing polyurethane products

J. J. Ponjeé *E*

In order to facilitate the release of polyurethane from a steel or aluminium mould, the metal surface is provided with a mono-layer of an alkylmercaptan. A silver layer may be provided between the mould metal and the alkylmercaptan monolayer. The invention can be advantageously used for manufacturing a luminaire for a tubular discharge lamp.

4 584 205

Method for growing an oxide layer on a silicon surface

T.-Y. J. Chen S
A. Bhattacharyya
W. T. Stacy
C. J. Vorst
A. Schmitz

In an improved method for growing an oxide layer on a silicon surface of a semiconductor body, the semiconductor body is first provided with a silicon surface. A first oxide layer portion is then grown over the silicon surface in a first thermal oxidation process at a temperature of less than about 100 °C. The semiconductor device is then annealed in a nonoxidizing ambient at a temperature above about 1000 °C, and finally a second oxide layer portion is then grown over the first oxide layer portion in a second thermal oxidation process to complete the growth of the oxide layer. The silicon surface may be of either polycrystalline or monocrystalline material. This method avoids both the dopant out-diffusion problems associated with present high-temperature oxidation processes and the stress-related irregularities associated with known low-temperature oxidation processes.

---

4 584 490

Input circuit for providing discharge path to enhance operation of switching transistor circuits

J. A. West S

A bipolar input circuit for regulating the current/voltage level at the base of a switching transistor provides a capacitively-controlled discharge path from the base through a discharge transistor when an input signal makes certain voltage transitions. The base of the switching transistor responds to the voltage at an emitter of an input transistor which has another emitter coupled to the base of the discharge transistor. Its base is further coupled to a capacitor which controls the discharge path.

---

4 584 493

Self referenced sense amplifier

D. T. Y. Lee S

A sense amplifier with two input control stages whose input voltages are equalized during a precharge cycle by a switching means.

---

4 584 507

Motor speed control arrangement

C. R. Taylor R

A variable motor speed control arrangement of the tachogenerator feedback loop type comprises a triac connected in series with the motor. The triac is fired in each half cycle of the ac mains supply. The firing angle of the triac is varied to provide the required control. The arrangement employs a single cycling counter to time the interval between two output pulses of the tachogenerator in order to determine the current motor speed and also to provide a countdown from the beginning of each half cycle to the required firing instant. The control processes are carried out in periods beginning at each counter overflow instant. This breaking up of the processing, together with the use of the single counter allows a microcomputer, which is running other programs to provide the speed control in addition.

---

4 584 567

Digital code detector circuits

J. R. Kinghorn R

A digital code detector circuit for detecting on a priority basis those code combinations of an n-bit binary digital code ($n \geq 3$) which contain only a single bit of a first binary value (e.g. the code combinations 1000, 0100, 0010 and 0001 of a 4-bit binary digital code). The circuit comprises a set of n input leads with associated inverters to supply the inverse of the input code combinations as well as the input code combinations to a logic gating arrangement. The gating arrangement drives m output circuits, where the m is the number of bits of output address code combinations corresponding to each possible input code combination of n-bits. When more than one of the input code combinations containing only a single bit of the fixed binary value are present concurrently on the set of input leads, the gating arrangement is such that only the m-bit address code for the input code combination having the higher binary value is produced by the output circuits.

---

4 584 659

Decimation filter arrangement

E. F. Stikvoort E

A decimation filter arrangement for reducing the sampling frequency of a time-discrete input signal from f_i to f_u, f_u not being a rational portion of f_i. For the generation of the required filter coefficients this arrangement comprises clock pulse generators producing first clock pulses ki(.) at a rate f_i and second clock pulses au(.) at a rate f_u. The arrangement also comprises a coefficients generator in which a deviation component d_n is calculated which indicates the ratio between the time interval located between a clock pulse au(.) and the immediately preceding clock pulse ki(.), and the time interval $1/f_i$ between two consecutive clock pulses ki(.). In response to this deviation component this coefficients generator produces N filter coefficients, the m^{th} filter coefficient, $m = 0, 1, \ldots, N-1$, being equal to $a_n(m) = h[(d_n + m)V_o]$. Herein the function h(v) represents the impulse response of an FIR-filter, v a continuous variable in the interval $-\infty < v < \infty$ and V_o a predetermined constant.

---

4 584 665

Arrangement for protecting against the unauthorized reading of program words stored in a memory

H. Vrielink E

The unauthorized reading of program words stored in a memory of a data processing system is counteracted by supplying the unauthorized reader with nuisance data from a data source instead of program words from the memory. In order to determine whether the memory is being read by an unauthorized reader or by a data processor unit of the system for the execution of the program, use is made of the sequence in which the data processor unit reads the program words from the memory. This sequence deviates from the sequence in which the program words are stored in the memory. Additional information is added to each program word stored in the memory, said additional information containing an indication of a subsequent program word to be read by the data processor unit. On the basis of this additional information it is tested whether the memory is being read in the sequence determined by the data processor, for the execution of the program, or in some other sequence by an unauthorized reader who does not know the sequence determined by the data processor unit.

---

4 584 673

Series/parallel/series shift register memory system

K. E. Kuijk E

A series/parallel/series shift register memory system having storage positions provided on a substrate. In addition to the single parallel-connected storage registers required to achieve the nominal storage capacity, there are provided groups of first and second nominally redundant single storage registers. The first redundant registers are used as substitutes for faulty single storage registers, so that the nominal storage capacity can be maintained. The second redundant registers are used for the transport of redundant code data. Also provided is a multi-state sequencer for indicating, in each state, the information to be carried by a particular group of storage registers and for forming, on the basis of this information, an error-detecting or error correction code which is carried by the second redundant storage registers. Faulty storage registers can thus be pinpointed, after which dummy information is automatically inserted in the input information at locations which are such that it will nominally be carried by the faulty registers, thus effectively substituting a first redundant register for each faulty register. The system is thus self-healing.

4 584 697

Four-phase charge-coupled device having an oversized electrode

T. J. Hazendonk S, E
A. J. Klinkhamer
G. A. Beck
T. F. Smit

In a 4-phase CCD with 90° overlap of the clock voltages, the area below two clock electrodes may be used for the storage of charge packets which thus can be 2 × as large as in conventional modes of operation. By choosing the penultimate electrode before the reading stage to be approximately 2.5 × as large as the other electrodes, this double charge packet can be transferred undivided in time to the output diode, a feature which is particularly advantageous for further signal processing.

---

4 585 307

Compound optical phase grating and switching devices comprising such a grating

H. Dammann H
H. Kurz

The invention relates to a compound blazed optical phase grating. The grating comprises at least two grating sections which are disposed opposite each other in parallel planes. The gratings have grooves which extend parallel to each other. The grating sections have equal grating periods and are movable relative to each other within their planes and perpendicular to the grooves. Over one grating period, the optical path length varies at least substantially parabolically and symmetrically relative to the grating period. The path length varies in such a manner that when both grating sections are symmetrically arranged relative to a common line perpendicular to the grating planes, the optical path length through the compound grating is uniform across the grating. Various optical switches and switching matrices can be formed by using such compound phase gratings.

---

4 586 064

DMOS with high-resistivity gate electrode

L. J. M. Esser E
H. J. H. Wilting
E. F. Stikvoort

By the use of high-resistivity polycrystalline silicon (poly) in MIS elements, a depletion layer can be formed in the poly material which brings about an electric decoupling between the poly (gate) and the underlying semiconductor body. This effect can be utilized advantageously in various circuit elements, such as in CCDs, in order to obtain a favourable potential distribution in the substrate; in MOS transistors in order to reduce the parasitic capacities; and in high-voltage devices in order to increase the breakdown voltage at the edge of the field plate (resurf). It may be applied e.g. in timers as a switch with a very low 'on' resistance and a very small parasitic capacitance in the 'off' position.

---

4 587 443

Auto-zero sample-and-hold circuit

R. J. van de Plassche S

A sample-and-hold circuit contains a pair of differential amplifiers switchably arranged in series. The circuit input signal during sampling is provided to the first amplifier which is coupled to a storage capacitor. The second amplifier provides the circuit output signal during hold. Switching circuitry enables the input and output signals to undergo the same transfer function in the first amplifier. The voltage offset of the first amplifier is thereby cancelled out of the output signal, while the effect of the voltage offset of the second amplifier is reduced drastically so as to provide excellent auto-zeroing.

4 587 478

Temperature-compensated current source having current and voltage stabilizing circuits

W. G. Kasperkovitz E
D. J. Dullemond

A transconductance amplifier includes a differential amplifier, whose collector load is a current mirror having a current output. A current-source transistor arranged in the common emitter line supplies a current having a positive temperature-dependence. This current is obtained from a current-stabilizing circuit. By means of a voltage divider a fraction of a temperature-independent voltage is applied between the control electrodes of the differential amplifier, which voltage is taken from a voltage-stabilizing circuit. Depending on the value of this fraction, the output current is temperature-independent or has a negative temperature-dependence.

---

4 587 557

Field number conversion circuit

L. Doornhein E
J. G. Raven
P. W. G. Welles
M. J. J. C. Annegarn
A. H. H. J. Nillesen

In a field number conversion circuit, the mutual positions of the horizontal and vertical synchronizing signal pattern in a field of the television signal to be converted are measured by means of a measuring circuit and these mutual positions are adequately transferred by means of a coupling circuit to a corresponding field in the converted television signal. Reading the field memories used during the conversion operation is preferably effected at a clock frequency which is not coupled to the clock frequency used during the writing operation.

---

4 587 971

Ultrasonic scanning apparatus

F. R. Stolfi N
R. L. Maresca
P. P. Adamovic

An ultrasonic scanning apparatus includes a rotor, first and second electromagnetic stators, and an ultrasonic transducer mounted on the rotor. Each electromagnetic stator has two curved pole faces arranged opposite pole faces on the rotor. The electromagnetic stators are arranged on opposite sides of the axis of rotation of the rotor. The stator pole faces are tapered such that on rotation of the rotor in one direction, the gaps between the rotor and a first stator decrease while the gaps between the rotor and the other stator increase. On rotation of the rotor in the opposite direction, the gaps between the rotor and the first stator increase and the gaps between the rotor and the second stator decrease. Means are provided for alternately energizing the first and second electromagnetic stators to cause the rotor to oscillate about the axis of rotation.

---

4 588 920

Display tube and an electron beam deflector therefor

J. Smith R

A display tube having an electron gun and an electron beam deflector including first and second electrode arrangements disposed successively along the electron beam path from the electron gun. Each electrode arrangement includes a pair of resistive plates extending transverse to the path of the electron beam and disposed on opposite sides of the path. The plates of each electrode arrangement are joined at their top and bottom ends and a potential difference is applied across the plates to provide electrical fields substantially normal to the electron beam path. The fields provided by the respective electrode arrangements are equal and opposite so that the

angular deflection of the electron beam caused by the first electrode arrangement is cancelled by the second electrode arrangement and the electron beam leaves the electron beam deflector on a path parallel to (or coincident with) the path it entered the deflector. In order to ensure that no additional angular deflection of the electron beam occurs when it crosses the interface between the first and second electrode arrangements, the voltages applied to the second electrode arrangement are varied so that the point of entry of the electron beam is at an equipotential with that of the beam.

---

4 590 093

Method of manufacturing a pattern of conductive material

P. H. Woerlee *E*
J. F. C. M. Verhoeven

A method of providing narrow conductor tracks of metal silicide is provided. According to this technique, a pattern of polycrystalline silicon covered by a protective layer is converted along the edges into the silicide by covering the device with a metal. The edges are then silicidized laterally over a distance of 20 to 500 nm. The remaining silicon is selectively removed, and the tracks obtained can serve as conductor masks, such as, for example, a plate of a capacitor.

---

4 590 506

Charge-coupled buried-channel device with high-resistivity gate electrodes

L. J. M. Esser *E*

By the use of high-ohmic polycrystalline silicon (poly) in MIS elements, a depletion layer can be formed in the poly material which brings about an electric decoupling between the poly (gate) and the underlying semiconductor body. This effect can be utilized advantageously in various circuit elements, such as in CCDs, in order to obtain a favourable potential distribution in the substrate; in MOS transistors in order to reduce the parasitic capacities; in high-voltage devices in order to increase the breakdown voltage at the edge of the field plate (resurf); and as described in this patent.

---

4 590 509

MIS high-voltage element with high-resistivity gate and field-plate

L. J. M. Esser *E*
H. M. J. Vaes
A. W. Ludikhuize

By the use of high-ohmic polycrystalline silicon (poly) in MIS elements, a depletion layer can be formed in the poly material which brings about an electric decoupling between the poly (gate) and the underlying semiconductor body. This effect can be utilized advantageously in various circuit elements, such as in CCD's, in order to obtain a favourable potential distribution in the substrate; in MOS transistors in order to reduce the parasitic capacities; and as described in this patent.

---

4 591 898

Signal-dropout correction circuit for correcting video signals disturbed by signal dropouts

E. de Boer *E*
A. Huijser

A dropout correction circuit is described. It comprises a dropout detector which compares a signal with a reference level and controls a switch which connects an output of the circuit to a line memory, in order to insert a corresponding part of a preceding line during such a dropout. In order to enable the reference level to be selected as high as possible the colour carrier is extracted before the video signal is applied to the dropout detector.

4 592 049

Method of and arrangement for controlling access to a time-division multiplex message transmission path

U. Killat *H*
D. Riekmann
R. Stecher

Method of the transmission of data packets in a TDM transmission loop wherein the frame is subdivided into several groups each having the same number of words, and each group comprises either exclusively narrow-band channels for the transmission of speech data or is associated with the high-rate channel for groups comprising narrow-band channels always comprises an unambiguous bit sample of, for example, the highest priority assigned to each group. When a subscriber station wants access to a word group in the high-rate channel it transmits its own identifying bit sample and possibly priority data in a signaling word. When this bit sample is returned through the loop undisturbed the subscriber station immediately accesses the assigned group of words in the high-rate channel for the transmission of a data packet. Allocation of channel access among individual subscriber stations is prioritized. The bit samples identifying groups comprising narrow-band channels receive the highest priority, so that these channels are automatically protected from access as a high-rate channel. A central control unit can increase the number of narrow-band channels by transmitting a further group of identifying bit samples in the signaling word.

---

4 592 924

Method of manufacturing a reaction vessel for crystal growth purposes

P. D. Kuppers *A, E*
K. H. Schelhas
C. H. J. van den Brekel
G. D. Khoe

In order to prevent impurities, in particular a chlorine impurity, present in the wall of the vessel from diffusing into the interior of the vessel and there disturb the growth process of the crystal, a hollow member, in particular a tube, of quartz is provided on its inside with a coating of silicon dioxide, while argon, gaseous silane and a gaseous oxidant, for example, dinitrogen oxide and/or carbon dioxide are introduced into the hollow member heated at 250 to 350 °C and are converted by means of a microwave resonator into a porous coating of silicon dioxide at a pressure between 20 and 30 mbar, which coating is sintered to form a coating which is preferably at least 50 μm thick.

---

4 593 210

Switching circuit having active pull-off

R. M. Boyer *S*

A bipolar gate has an output transistor that switches in response to the voltage at an emitter of a drive transistor. An active pull-off circuit discharges the base of the output transistor when it turns off. The discharge path is provided through a pull-off transistor whose collector is coupled to the base of the output transistor. The switching of the pull-off transistor is regulated with a control circuit containing a trigger circuit and a bias circuit. The trigger circuit is coupled between the bias circuit and a collector of the drive transistor. A 'kicker' circuit formed with an input transistor and a voltage reference speeds up the switching of the drive transistor.

---

4 593 268

Analog-to-digital converter using absolute-value conversion

R. A. Blauschild *S*

An absolute-value analog-to-digital converter containing a chain of matched main absolute-value differential amplifiers has a gain control for regulating the gain of each main amplifier utilizing an auxiliary absolute-value differential amplifier matched to the main amplifiers. An offset control in the converter drives the offsets of the amplifiers toward zero by using a further absolute-value differential amplifier matched to the other amplifiers. The gain and offset control are implemented with suitable feedback circuitry.

4 593 387

Time division switching system

T. Krol *E*
A. W. M. van den Enden

A time division switching system to which incoming and outgoing transmission channels designed for the transmission of bit streams subdivided into bits are connected. The system has a number N of time division switching stages, a number N of distributors and a number N of collectors, each distributor has N inputs to which an incoming transmission channel is connected, each collector has N outputs to each of which is connected and outgoing transmission channel, each distributor has N outputs, each of the N outputs of a distributor being connected to an input of each of the time division switching stages for a proportionate distribution according to a predetermined pattern of the bit stream of each incoming transmission channel over the N time division switching stages, and each collector has N inputs, each of the N inputs of a collector being connected to an output of each of the time division switching stages for collecting according to a predetermined pattern the bit streams for each outgoing transmission channel.

---

4 594 220

Method of manufacturing a scandate dispenser cathode and dispenser cathode manufactured by means of the method

J. Hasker *E*
P. Hokkeling
J. van Esdonk
J. J. van Lith

A method of manufacturing a scandate dispenser cathode having a matrix at least the top layer of which at the surface consists substantially of tungsten (W) and scandium oxide (Sc_2O_3) and with emitter material in or below said matrix. If said method comprises the following steps: (a) compressing a porous plug of tungsten powder, (b) heating said plug in a non-reactive atmosphere and in contact with scandium to above the melting temperature of scandium, (c) cooling the plug in a hydrogen (H_2) atmosphere, (d) pulverizing the plug to fragments, (e) heating said fragments to approximately 800 °C and firing them at this temperature for a few to a few tens of minutes in a hydrogen atmosphere and slowly cooling in said hydrogen atmosphere, (f) grinding the fragments to scandium hydride-tungsten powder (ScH_2/W), (g) compressing a matrix or a top layer on a matrix of pure tungsten from said ScH_2/W powder or from a mixture of this powder with tungsten powder, (h) sintering and cooling the said matrix, and (i) bringing emissive material into the cathode, a scandate dispenser cathode is obtained the recovery of which after ion bombardment occurs better than in cathodes having Sc_2O_3 grains. The scandium is also distributed more homogeneously in the cathode than in cathodes having Sc_2O_3 grains.

---

4 594 271

Process for coating inorganic particles with condensating polymers

P. C. Scholten *E, N*
F. W. Snijder
H. Sorkin

A first stable suspension of at least one solid monomer, capable of being polymerized to a condensation polymer when heated, is formed in a first organic liquid inert during polymerization and containing a minor amount of a dispersing agent stable during said polymerization. A second stable suspension of finely divided inorganic particles in a second organic liquid inert during said polymerization and miscible with said first organic liquid, is formed and contains a minor amount of a dispersing agent. The first suspension is then added to the second suspension while stirring and heating the second suspension to the polymerization temperature of the monomer.

4 594 531

Circuit arrangement for operating high-pressure gas discharge lamps

H. G. Ganser *A*
R. Schäfer
H. P. Stormberg

A circuit arrangement for operating high-pressure gas discharge lamps with a current of higher frequency comprising a switching mains section including a switching transistor and a control device, in which an upper and a lower reference current level are produced. The switching transistor is switched to the non-conducting state when the lamp current exceeds the upper level and is switched to the conducting state when this current falls below the lower level. The interval between the reference current levels is more than 10% of the average lamp current and a further intermediate reference current level is provided at which the switching transistor is switched each time at a predetermined number of passages of the lamp current through the intermediate reference current level.

---

4 594 564

Frequency detector for use with phase locked loop

J. M. Yarborough *S*

A frequency detector receiving two input frequencies and generating a pump-up/pump-down signal for control of a phase locked loop by matching the frequency of a voltage controlled oscillator to the frequency. The lock is independent of the phase relationship of the signals.

---

4 594 628

Magnetic head having cobalt-containing zinc-ferrous ferrite core

D. Stoppels *E*
P. G. T. Boonen
U. E. Enz
L. A. H. van Hoof

A magnetic head for a magnetic recording and playback device includes a core having two core parts which are spaced from each other and between which a transducing gap is formed. The core consists of a (preferably monocrystalline) zinc-ferrous ferrite. A preferred range of compositions is defined by the formula $Zn_aFe_{1-a}^{II}Fe_2^{III}O_4$, wherein $0.1 \leq a \leq 0.4$. The Zn-ferrous ferrite may further comprise additions of Co^{II}.

---

4 594 725

Combined adaptive equalization and demodulation circuit

L. Desperben *L*
H. Sari
S. Moridi
G. Bonnerot

An adaptive equalizer arrangement for a digital transmission system comprises at the output of the transmission channel a first in-phase path and in parallel with this first path, a second quadrature path, both paths being of the non-recursive transversal filter type having n branches and (n − 1) delay circuits between the inputs of these branches, each of these n branches comprising, arranged in series, a mixer, a low-pass filter, a multiplier, and having their outputs connected to an adder which is followed by a sampling circuit and thereafter by a comparator circuit to decide the symbols to be transmitted from the outputs of these paths. The arrangement also comprises a third control path which comprises two subtracting circuits to determine the differences between the signals before and after decision and a control circuit of a voltage-controlled oscillator, 2n phase shifters and 2n multipliers.

OTHER PHILIPS PUBLICATIONS

Philips Journal of Research

A publication in English on the research work carried out in the various Philips laboratories. Published in annual volumes of six issues each of about 100 pages, size 15½ × 23½ cm.

Philips Telecommunication and Data Systems Review

A publication in English, dealing with the technical aspects of radio, television, radar, telephone and telegraph transmission and automatic exchanges. Published in volumes of four issues, about 40 pages per issue, size 20½ × 28½ cm.

Electronic Components and Applications

A publication in English, containing articles dealing with the theory and practice of electronic components and materials. Four issues per year, about 60 pages per issue, size 21 × 29½ cm.

Medicamundi

A publication in English on diagnostic imaging and radiation therapy. Three issues per volume, about 60 pages per issue, size 21 × 29½ cm.

Forthcoming issues of Philips Technical Review will include articles on:

Silicon cold cathodes

Laser diagnostics for low-pressure mercury discharges

Applications of light guides in process control

Ceramic differential-pressure transducer

Interactive synthesis of MR images

Philips Tech. Rev. Vol. 43, No. 1/2, Dec. 1986

Contents

PHILIPS TECHNICAL REVIEW
Philips Research Laboratories
P.O. Box 80000
5600 JA Eindhoven
The Netherlands

Subscription rate per volume	fl. 80.00 or U.S. $ 35.00
Student's subscription	fl. 32.00 or U.S. $ 14.00
Binder	fl. 10.00 or U.S. $ 4.00

Payment only after invoicing, please.

Printed in the Netherlands